

**“In-depth characterization of the macrophage
response to *Legionella pneumophila* infection”**

Inaugural-Dissertation
to obtain the academic degree
Doctor rerum naturalium (Dr. rer. nat.)

submitted to the Department of Biology, Chemistry, Pharmacy
of Freie Universität Berlin

by

Ann-Brit Johanna Klatt

Berlin, 2023

This thesis was conducted under the supervision of Prof. Bastian Opitz from 1.06.2020 – 30.11.2023 at the Department of Infectious Diseases, Respiratory Medicine and Critical Care, Charité-Universitätsmedizin Berlin.

1st reviewer: Prof. Dr. Bastian Opitz

2nd reviewer: Prof. Dr. Andreas Diefenbach

Date of defense: 16.05.2024

I. Acknowledgement

I would like to express my deepest gratitude to the following persons, who have played a pivotal role in my journey towards completing my dissertation over the past years:

First and foremost, I extend my deepest appreciation to my supervisor, Prof. Bastian Opitz. I am very grateful that I had the opportunity to conduct my dissertation in his laboratory, and his guidance, mentorship, motivation, and unwavering support have been instrumental in shaping my research and academic growth.

I am also immensely thankful to Prof. Andreas Diefenbach, not only for taking on the role of my university supervisor but also for his valuable advice and expertise that enriched my thesis. I would also like to thank the members of my thesis committee, Dr. Olivia Mayer and Dr. Efstathios Stamatiades for their invaluable feedback and contributions to my research project.

Furthermore, I would like to thank all our project partners, Dr. Miha Milek, Dr. Marieluise Kirchner, Prof. Bernd Lepenies, and Christina Diersing, for their collaboration and valuable contributions to the respective projects.

Doing a dissertation is challenging, and it is essential to be surrounded by people who inspire and motivate you and create a nice working environment. Therefore, to my colleagues in the AG Opitz: Facundo, Sandra, Ivo, Patrick, Joshua, Martha, Charlotte, Belen, Benjamin, Lisbeth, and Léa, I owe a debt of gratitude for the collaborative and collegial atmosphere and for so many nice moments shared during or after work and on conferences. I am also very thankful to the members of the AG Witzenrath, AG Sander, and AG Hocke, especially Laura, Lena, Peter, Sophia, and Philipp, for many discussions, nice lunch breaks, and for making the work so much fun.

I would also like to acknowledge the support I received from the IMPRS-IDI Graduate School by funding and enabling me to participate in many interesting courses, seminars and conferences. I am very thankful to Dr. Franziska Stressmann and Sybille Kim for their advice and cooperation at any time.

Finally, I would like to thank many people outside of the lab: To my parents for their unconditional support and encouragement at every step. To my friends, who never failed to distract me from work and would celebrate every accomplishment with me over the past 4.5 years. And, of course, to my partner, Bernard, for all his support, love, and inspiration.

This accomplishment would not have been possible without the support of each of you. I am extremely grateful for your contributions to my academic and personal growth.

II. Declaration of Independence

Herewith I certify that I have prepared and written my thesis independently and that I have not used any sources and aids other than those indicated by me. I also declare that this thesis has not been submitted in any other examination process and/or to any other institution.

III. Content

I.	Acknowledgement	I
II.	Declaration of Independence.....	III
IV.	List of abbreviations.....	VII
V.	List of Figures	X
VI.	List of Tables.....	XII
VII.	Zusammenfassung.....	XIII
VIII.	Summary	XV
1.	Introduction	1
1.1.	<i>Legionella pneumophila</i>	1
1.1.1.	Infection mechanism of <i>L. pneumophila</i>	2
1.1.2.	Bacterial effectors of <i>L. pneumophila</i> – many ways to manipulate the host cell.....	3
1.2.	The immune system	7
1.2.1.	The innate immune response in the lung.....	8
1.2.2.	Detection of PAMPs by different classes of PRRs	9
1.2.2.1.	The C-type lectin receptor CLEC12A.....	14
1.2.3.	The early cellular innate immune response in the lung.....	15
1.2.3.1.	Alveolar macrophages.....	16
1.2.3.2.	Neutrophils, dendritic cells & inflammatory monocytes	19
1.3.	The innate immune response against <i>L. pneumophila</i>	20
1.3.1.	A possible role for CLEC12A in <i>L. pneumophila</i> recognition?.....	24
1.4.	The limited view of current cell culture models into mechanisms of host-pathogen interaction during <i>L. pneumophila</i> infection.	25
1.5.	Aim of study.....	26
2.	Material & Methods.....	27
2.1.	Bacteria.....	27
2.2.	Mice.....	27
2.3.	<i>In vivo</i> methods	28
2.3.1.	Murine <i>L. pneumophila</i> infection model.....	28
2.3.2.	Determination of bacterial counts in lung	28
2.3.3.	Lung digestion for subsequent analysis of cell populations by fluorescence cytometry.....	28
2.3.4.	Preparation of lung lysates for cytokine quantification.....	29
2.3.5.	Preparation of lung lysates for evaluation of mRNA-expression.....	29

2.3.6.	Isolation of infected and non-infected bystander leucocytes and AMs from BALF samples of B6 WT mice.....	30
2.4.	Immunofluorescence microscopy	31
2.5.	Cell culture	31
2.5.1.	BMDM isolation, differentiation, and cultivation.....	31
2.5.2.	Human AM isolation and cultivation.....	32
2.5.3.	Cultivation and differentiation of human BLaER1 cell line	32
2.5.4.	Short-term infection of cells.....	33
2.5.5.	<i>In vitro</i> intracellular replication assays	33
2.6.	Immunological Methods	34
2.6.1.	Enzyme-linked immunosorbent assay.....	34
2.6.2.	Flow cytometry analysis	34
2.7.	Molecular Biology Methods	35
2.7.1.	Preparation and processing of samples for bulk RNA-seq analysis of <i>in vivo</i> infected and uninfected AMs	35
2.7.2.	Preparation and processing of samples for mass spectrometry analysis of <i>in vivo</i> infected and uninfected AMs	36
2.7.3.	Preparation and processing of samples for sc RNA-seq analysis of <i>in vivo</i> infected and uninfected leucocytes	37
2.7.4.	Generation of a BLaER1 <i>CLEC12A</i> ^{-/-} cell line.....	37
2.7.5.	Screening for BLaER1 <i>CLEC12A</i> ^{-/-} clones	37
2.7.6.	Isolation of total RNA and cDNA synthesis	38
2.7.7.	Quantitative real-time PCR.....	38
2.8.	Statistical analysis	39
2.9.	Materials.....	40
3.	Results	44
3.1.	The role of CLEC12A in the immune response to <i>L. pneumophila</i> infection	44
3.1.1.	The CLR CLEC12A has no significant role during pulmonary <i>L. pneumophila</i> infection <i>in vivo</i>	44
3.1.2.	CLEC12A does neither affect <i>L. pneumophila</i> replication, nor infection-induced cytokine response in murine macrophages	47
3.1.3.	Infection with <i>L. pneumophila</i> in BLaER1-derived macrophages indicates no role of CLEC12A in the immune response in human macrophages	48
3.2.	Investigating the innate immune response of AMs to <i>L. pneumophila</i> infection	51
3.2.1.	GFP-expressing <i>L. pneumophila</i> allow discrimination of infected and non-infected bystander AMs from BALF samples	53

3.2.2.	<i>L. pneumophila</i> Δ <i>flaA</i> -infected, and to a slightly lesser extent Δ <i>dotA</i> -infected AMs, show a robust upregulation of proinflammatory genes.....	54
3.2.3.	The DEGs in Δ <i>flaA</i> -infected vs. bystander AMs are similar to the DEGs in AMs from Δ <i>flaA</i> -infected mice vs. PBS-treated animals.....	57
3.2.4.	<i>L. pneumophila</i> -infected AMs show a significant upregulation of proteins that are not consistently regulated on mRNA level.....	58
3.2.5.	Concordantly regulated molecules in Δ <i>flaA</i> -infected AMs are related proinflammatory pathways and cholesterol biosynthesis.....	60
3.2.6.	Comparison of mRNA and protein expression allows identification of molecules that appear to be exclusively up- and downregulated in AMs from Δ <i>flaA</i> -infected mice, as well as of genes whose translation seems to be T4SS-dependently impaired.....	63
3.2.7.	A single cell RNA sequencing analysis demonstrated upregulation of potential targets for further investigation of their role in the immune response to <i>L. pneumophila</i> in AMs <i>in vivo</i>	67
4.	Discussion	72
4.1.	Summary – Investigating the potential role of the CLR CLEC12A during <i>L. pneumophila</i> infection.....	72
4.1.1.	The hemITIM-containing receptor CLEC12A has no critical function in the response to <i>L. pneumophila</i> infection <i>in vitro</i> and <i>in vivo</i>	73
4.2.	Summary - A global view on the transcriptomic and proteomic response in <i>L. pneumophila</i> infected AMs	76
4.2.1.	A slightly stronger proinflammatory gene transcription was observed in AMs infected with <i>L. pneumophila</i> Δ <i>flaA</i> as compared to cells infected with Δ <i>dotA</i>	78
4.2.2.	Many proinflammatory transcripts induced upon Δ <i>flaA</i> infection in AMs seem not to be translated into proteins	80
4.2.3.	Molecules that were upregulated on mRNA and protein levels in Δ <i>flaA</i> -infected AMs might have relevance for the immune response to <i>L. pneumophila</i> infection....	83
4.2.4.	Bystander AMs in lungs of <i>L. pneumophila</i> infected mice might only be activated at the end of the bacterial replication cycle <i>in vivo</i>	87
4.2.5.	The downregulation of the cholesterol biosynthesis in Δ <i>flaA</i> -infected AMs – an interplay between bacterial effectors and the antibacterial defense?	88
5.	Conclusion & Outlook	92
6.	References	94
	Appendix	120

IV. List of Abbreviations

AECs	alveolar epithelial cells	DEP	differential expressed protein
AIM2	absent in melanoma 2	DISCO	differential concordance
AM	alveolar macrophages	dsDNA	double-stranded DNA
AP-1	activator protein 1	dsRNA	double-stranded RNA
APC	antigen-presenting cell	eEF1A/By	elongation factor 1A/1By
ASC	apoptosis-associated speck-like protein containing a carboxy-terminal CARD	ELISA	enzyme linked immunosorbent assay
AT1/2	alveolar type I/II cell	ER	endoplasmatic reticulum
ATF3	activating transcription factor 3	eIF4E	Eukaryotic initiation factor 4E
AYE	ACES-buffered yeast extract	FACS	fluorescence activated cell sorting
BALF	bronchoalveolar lavage fluid	FC	fold change
BCYE	buffered charcoal yeast extract	FcRγ	fragment crystallizable receptor γ
BMDM	bone marrow-derived macrophage	FCS	fetal calf serum
bulk RNA-seq	bulk RNA sequencing	FDR	False discovery rate
CARD	caspase activation and recruitment domain	GDF15	Growth differentiation factor 15
cDNA	complementary DNA	GFP	green fluorescence protein
CFU	colony forming unit	GFRAL	GDNF Family Receptor Alpha Like
cGAS	cGAMP synthase	GM-CSF	granulocyte macrophage coloy-stimulating factor
CLR	C-type lectin receptor	GSEA	Gene set enrichment analysis
CTLD	C-type lectin-like domain	HBSS	Hanks' Balanced Salt Solution
DAMP	damage-associated molecular pattern	Hsp70	Heat shock protein 70
DC	dendritic cell	i.p.	intraperitoneal
ddH₂O	double-distilled H ₂ O		
DEG	differential expressed gene		

IFN	interferon	MOI	multiplicity of infection
IL-	interleukin-	mRNA	messenger RNA
iM	interstitial macrophage	MSU	monosodium urate
iMono	inflammatory monocyte	mTOR	mechanistic target of rapamycin kinase
InDel	insertion and deletion	mTORC1	mechanistic target of rapamycin complex 1
IRF3	Interferon Regulatory Factor 3	mTORC1	mechanistic target of rapamycin complex 1
ISGs	IFN-stimulated genes	MyD88	myeloid differentiation primary response
ITAM	immunoreceptor tyrosine-based activating motif	NaCl	sodium chlorid
ITIM	immunoreceptor tyrosine-based inhibitory motif	NF-κB	nuclear factor kappa-light-chain-enhancer of activated B-cells
KO	knock-out	NFAT	nuclear factor of activated T-cells
<i>L. pneumophila</i>	<i>Legionella pneumophila</i>	NK	natural killer cells
LCV	Legionella-containing vacuole	NKT	natural killer T cell
LD	Legionnaires disease	NLR	Nod-like receptor
LDL	low-density lipoprotein	OD	optical density
LDLR	low-density lipoprotein receptor	OXPPOS	oxidative phosphorylation
log₂ FC	fold change [log ₂]	p(-value)	p value
LPS	lipopolysaccharide	PCR	polymerase chain reaction
M-CSF	macrophage colony-stimulating factor	p.i.	Post infection
MALT1	Mucosa-associated lymphoid tissue lymphoma translocation protein 1	p_{adj}(-value)	adjusted p value
MAPK	mitogen activated protein kinase	PAMP	pathogen-associated molecular pattern
MAVS	molecule mitochondrial antiviral signaling	PAP	pulmonary alveolar proteinosis
MHC	major histocompatibility complex	PBMCs	peripheral blood monocyte-derived macrophages
		PBS	phosphate buffered saline

PCR	polymerase chain reaction	STING	sensor molecule stimulator of interferon genes
Pen/Strep	penicillin/streptomycin	SYK	spleen tyrosine kinase
PMN	polymorphonuclear neutrophil	T4SS	type IV secretion system
PO₂	partial oxygen pressure	TBK1	TANK-binding kinase 1
PPAR-γ	peroxisome proliferator-activated receptor gamma	TGFβ	transforming growth factor β
PRR	pathogen recognition receptor	TJ	tight junction
qPCR	quantitative real-time PCR	TLR	Toll-like receptor
RIG-I	retinoic acid-inducible gene I	TNFα	tumor necrosis factor alpha
RLR	RIG-I-like receptor	TNFR	tumor necrosis factor receptor
ROS	reactive oxygen species	TRIF	TIR-domain-containing adapter-inducing interferon β
RQ	relative quantity	Ube2N	ubiquitin-conjugation enzyme E2 N
sc RNA-seq	single cell RNA sequencing	UMAP	uniform manifold approximation and projection
SD	standard deviation	UPR	unfolded protein response
SHP-1/2	Src homology region 1 domain-containing phosphatase	wt	wild-type
SP	surfactant protein		

V. List of Figures

Figure 1) The intracellular life cycle of <i>L. pneumophila</i> in infected host cells.	2
Figure 2) <i>L. pneumophila</i> effectors modulate a broad variety of host cell pathways.	6
Figure 3) The four functional classes of myeloid CLRs and their downstream signaling events to modulate the immune response upon ligand binding.	14
Figure 4) Schematic overview of the immune response in macrophages to infection with <i>L. pneumophila</i>	22
Figure 5) The CLR CLEC12A recognizes and binds <i>L. pneumophila</i>	25
Figure 6) CLEC12A plays a limited role in <i>L. pneumophila</i> lung infection in mice.	45
Figure 7) Cell composition of immune cell population does not differ between <i>L. pneumophila</i> -infected WT and <i>Clec12a</i> ^{-/-} animals 24 h p.i.	46
Figure 8) <i>L. pneumophila</i> replication in murine BMDMs as well as type I IFN response and TNF α production are not influenced by CLEC12A.	47
Figure 9) BLaER1-derived macrophages allow intracellular replication of <i>L. pneumophila</i> and express CLEC12A to a similar extent as <i>ex vivo</i> cultivated human AMs.	49
Figure 10) CLEC12A does not impact replication of <i>L. pneumophila</i> nor immune response in human BLaER1-derived macrophages.	50
Figure 11) The immune response of AMs to infection with <i>L. pneumophila</i> was investigated on the transcriptional and proteome level.	52
Figure 12) Infection with GFP-expressing <i>L. pneumophila</i> allowed discrimination of infected and non-infected bystander AMs from murine BALF samples by FACS-sort.	53
Figure 13) DEGs in AMs of mice infected with <i>L. pneumophila</i> Δ <i>flaA</i> or Δ <i>dotA</i> and of animals treated with PBS.	55
Figure 14) <i>L. pneumophila</i> -infected AMs show enrichment and upregulation of proinflammatory and cell cycle pathways in AMs 12-14 h p.i. <i>in vivo</i>	56
Figure 15) DEGs in Δ <i>flaA</i> -infected vs. bystander AMs are similar to DEGs in AMs from Δ <i>flaA</i> -infected mice vs. PBS-treated mice.	58
Figure 16) The proteome analysis revealed that some top-upregulated proteins in <i>L. pneumophila</i> -infected AMs are not consistently regulated on mRNA level.	59

Figure 17) Numbers of molecules identified in AMs from <i>ΔflaA</i> -infected or <i>ΔdotA</i> -infected mice and PBS-treated animals on protein and mRNA levels by bulk RNA-seq and proteome analysis, respectively.	60
Figure 18) <i>L. pneumophila ΔflaA</i> -infected AMs upregulate transcripts involved in TNFα signaling and to a lesser extent the corresponding proteins, whereas transcripts and proteins related to cholesterol biosynthesis are simultaneously downregulated.	61
Figure 19) Assignment of proteins detected in AMs of <i>L. pneumophila</i> -infected mice to classes based on their transcriptional and translational regulation.....	64
Figure 20) Molecules that were exclusively up- and downregulated in <i>L. pneumophila ΔflaA</i> -infected AMs, as well as proteins that were identified to be potentially impaired in their translation in a T4SS-dependent manner.	65
Figure 21) Bacterial-derived GFP signal allowed FACS-sort of <i>L. pneumophila</i> -infected and non-infected leucocytes from murine BALF samples at 6 and 20 h p.i..	68
Figure 22) AMs and PMNs were the two main leukocyte populations in BALF samples of <i>L. pneumophila</i> -infected mice at 6 and 20 h p.i..	69
Figure 23) AMs isolated from mice infected with <i>L. pneumophila ΔflaA</i> upregulate gene expression of inflammatory genes at 6 and 20 h p.i.....	70

VI. List of Tables

Table 1) Lysis buffer for protein isolation from whole lung samples.....	29
Table 2) Hashtags for leukocytes	31
Table 3) Antibodies for FACS-Sort of leukocytes and AMs from BALF samples	31
Table 4) Cultivation and differentiation medium for BMDMs.....	32
Table 5) Cultivation and differentiation medium for BLaER1 cells.....	33
Table 6) Commercial ELISA Kits.....	34
Table 7) Antibodies for flow cytometry analysis.....	35
Table 8) Protein lysis buffer for protein isolation from AMs	36
Table 9) TaqMan assays.....	38
Table 10) Chemicals.....	40
Table 11) Enzymes.....	41
Table 12) Commercial Kits	41
Table 13) Consumables	42
Table 14) Instruments.....	42

VII. Zusammenfassung

Legionella pneumophila (*L. pneumophila*), ein intrazelluläres Bakterium und häufiger Erreger von ambulant erworbenen Lungenentzündungen, besitzt ausgefeilte Strategien zur Infektion und Vermehrung in Alveolarmakrophagen (AM). Diese Strategien umfassen die Translokation von mehr als 300 bakteriellen Effektorproteinen in das Zytoplasma der Wirtszelle, wo sie verschiedene zelluläre Signalwege manipulieren. Infizierte Zellen haben jedoch ebenfalls diverse Strategien entwickelt, um eine Infektion zu erkennen und ihr entgegenzuwirken. Das Ergebnis der Wechselwirkung zwischen Wirt und Pathogen, ob es zur Eliminierung der Bakterien oder zu einer schwerwiegenden Infektion führt, hängt von der Balance zwischen den Virulenzstrategien des Erregers und den Abwehrmechanismen des Wirts ab. Eine Vielzahl von Studien haben die Wechselwirkung zwischen Wirt und Pathogen *in vitro* untersucht, hauptsächlich unter Verwendung von murinen und humanen hämatopoetischen Zellkultursystemen. Allerdings sind die genauen Mechanismen der bakteriellen Erkennung und der ausgelösten Immun-Signalwege in infizierten Zellen nicht vollständig verstanden, und bisher ist wenig darüber bekannt, wie gewebständige AMs auf eine Infektion reagieren.

Im ersten Teil dieser Studie wurde die Rolle des C-Typ-Lektin-Rezeptors CLEC12A, der *L. pneumophila* bindet, in der Immunantwort gegen den Erreger untersucht. Die Ergebnisse von Infektionsexperimenten in einem murinen *in vivo*-Modell sowie in murinen und humanen Makrophagen *in vitro* deuten darauf hin, dass der Rezeptor keinen signifikanten Einfluss auf das Ergebnis einer Infektion mit *L. pneumophila* hat. Der zweite Teil der Studie untersuchte die Reaktion von *in vivo* mit *L. pneumophila* infizierten AMs und nicht infizierten (so genannten "Bystander") AMs. Transkriptom- und Proteomanalysen zeigen eine robuste Hochregulierung vieler proinflammatorischer und immunregulatorischer Gene in infizierten AMs, während nicht infizierte Bystander-Zellen erst gegen Ende des ersten Replikationszyklus von *L. pneumophila* (20 h nach Infektion) aktiviert zu werden scheinen. Viele proinflammatorische Proteine scheinen in ihrer Translation in virulent infizierten AMs inhibiert zu sein (z.B. IL-1 β , CCL6, CCL9), wohingegen einige andere Proteine, wie z.B. IL-1 α , ATF3, GDF15 und A20 in ihrer Expression nicht gehemmt sind. Darüber hinaus liefern die Ergebnisse dieser Studie Hinweise darauf, dass die Infektion die Cholesterin-Homöostase von AMs *in vivo* beeinflusst.

Zusammenfassend ermöglichen die Ergebnisse dieser Studie ein tieferes Verständnis der an der Immunantwort gegen den Erreger beteiligten Proteine, und bieten einen einzigartigen Einblick in die Gesamtzellreaktion von gewebsständigen AMs auf eine Infektion mit *L. pneumophila in vivo*.

VIII. Summary

Legionella pneumophila, an intracellular pathogen and a common cause of community-acquired pneumonia, employs sophisticated strategies to infect and replicate in alveolar macrophages (AMs). These strategies include translocating over 300 bacterial effector proteins into the host cytosol, where they manipulate various cellular pathways. However, infected cells have developed numerous strategies to detect and counteract the infection. The outcome of the host-pathogen interaction, whether it results in bacterial clearance or an extensive infection, depends on the balance between the pathogen's virulence strategies and the host's defense mechanisms. Several studies have investigated the host-pathogen interaction *in vitro*, mainly using murine and human hematopoietic cell culture systems. However, the exact mechanisms of bacterial detection by the innate immune system are incompletely explored, and little is known about how tissue-resident AMs respond to the infection.

Within the first part of this study, the role of the C-type-lectin receptor CLEC12A, which binds to *L. pneumophila*, in the immune response was examined. The findings from infection experiments in a murine *in vivo* model and in murine and human macrophages *in vitro* indicate that the receptor has no significant impact on the outcome of the infection with *L. pneumophila*. The second part of the study investigated the response of *in vivo* *L. pneumophila*-infected and uninfected bystander AMs. Transcriptome analysis revealed a robust upregulation of various proinflammatory and immunoregulatory genes in infected AMs, while uninfected bystander cells seem to be only activated towards the end of the first replication cycle of *L. pneumophila* (20 h post infection). Proteome analyses further indicate that several proinflammatory proteins are impaired in their translation in virulent infected AMs (e.g., IL-1 β , CCL6, CCL9) and that only a limited number of proteins including IL-1 α , ATF3, GDF15, and A20 were found to be expressed on protein level in infected AMs. Furthermore, *L. pneumophila* seems to affect the cholesterol homeostasis of AMs *in vivo*.

In conclusion, this study enables a deeper understanding of the immune response against *L. pneumophila* and provides a unique view of the overall cellular response in tissue-resident AMs towards the infection *in vivo*.

1. Introduction

1.1. *Legionella pneumophila*

In the summer of 1976, it was reported that several American veterans fell ill after attending the annual American Legion convention at the Bellevue-Stratford Hotel in Philadelphia, Pennsylvania ¹. Most patients developed a range of mild flu-like symptoms, but cases of severe pneumonia also occurred, ultimately leading to a fatal outcome for 29 individuals ². The cause of the illness, referring to its victims named Legionnaires disease (LD), could not be determined until later that same year, when the American microbiologist Joseph E. McDade at the Centers for Disease Control, Atlanta, Georgia, isolated and identified a gram-negative bacterium from lungs of patients. The bacterium was named *Legionella pneumophila* (*L. pneumophila*) and has since been acknowledged as an important causative agent for community-acquired and nosocomial pneumonia worldwide ³⁻⁵. *L. pneumophila* inhabits various freshwater environments and manmade water systems, such as cooling towers, whirlpools, or decorative fountains ⁶⁻⁸. In those environments, the bacterium grows mostly in a biofilm structure or parasitizes free-living protozoan, e.g., amoebae of the genera *Acanthamoeba* ^{9,10}. Indeed, *L. pneumophila* can adapt and replicate within a diverse range of protozoan hosts ¹¹. The ability to establish a replicative niche in hosts with an evolutionary distance from each other has been suggested to be attributed to the acquisition of foreign genes ^{12,13}. This evolutionary-driven adaptation to different hosts has endowed *L. pneumophila* with the ability to infect humans, with serogroup 1 being the dominant serotype isolated from patients and accounts for approximately 84% of infections ¹⁴. Person-to-person transmission has only been reported once, suggesting that human infection causes a non-communicable disease and supports consideration of *L. pneumophila* as an accidental pathogen ^{13,15}. The outcome of the infection depends on the bacterial virulence factors and the host immunity. Typically, *L. pneumophila* infections are asymptomatic or cause a mild respiratory illness known as Pontiac fever ¹. However, elderly individuals and people with weakened immune systems or chronic lung diseases are more susceptible to developing LD, a severe form of pneumonia with potentially fatal outcomes. Risk factors for developing LD besides age include smoking, steroid therapy and other immunosuppressive treatments, diabetes mellitus, and may confer substantial morbidity and mortality ¹⁶. It has been reported that LD constitutes about 2–9% of total community-acquired pneumonia cases worldwide; however, due to underdiagnosis, variation in diagnostics method, awareness, and reporting

and documentation standards in different countries, the actual dispersal is difficult to determine¹⁷.

1.1.1. Infection mechanism of *L. pneumophila*

L. pneumophila typically enters the lung via inhalation of contaminated aerosols¹⁸. In humans, alveolar macrophages (AMs) are the primary cell type infected by *L. pneumophila* and provide a niche for intracellular replication of the bacterium. AMs are usually able to detect and canonically phagocytize many types of invading pathogens in the alveoli to prevent and clear infection¹⁹. However, *L. pneumophila* is able to survive in these cells in a modified vacuole, the so-called *Legionella-containing vacuole* (LCV) (see Figure 1)^{20,21}.

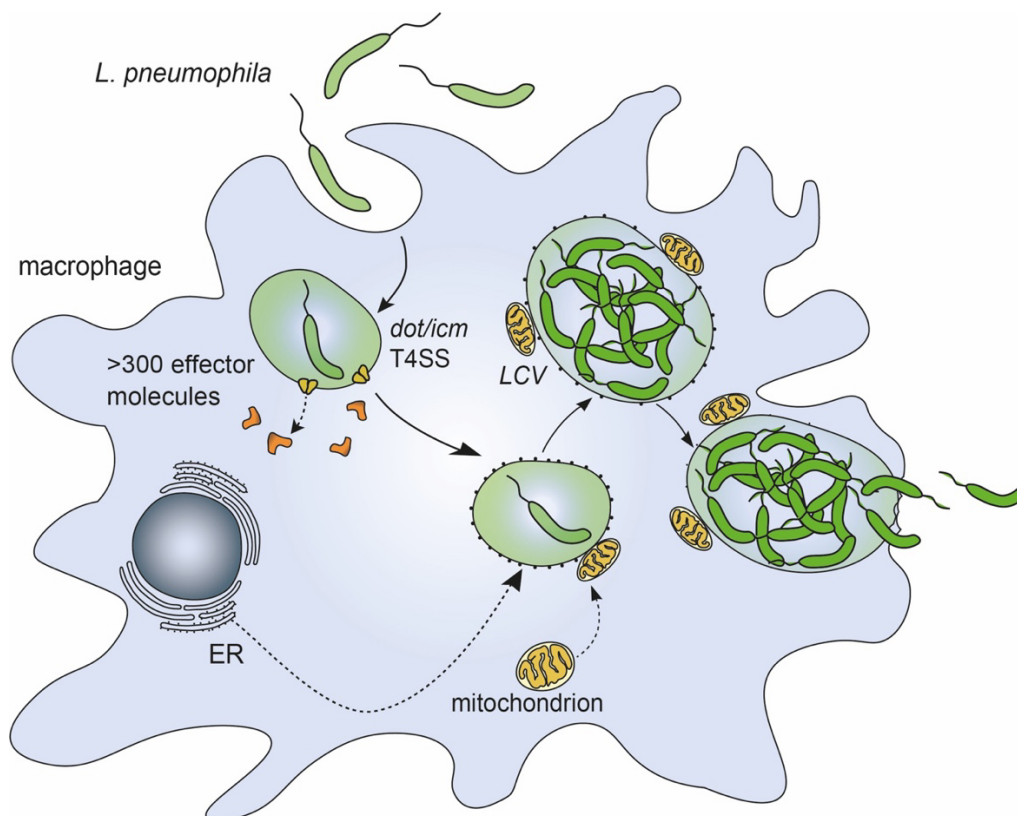


Figure 1) The intracellular life cycle of *L. pneumophila* in infected host cells. Upon phagocytosis by macrophages, *L. pneumophila* resides in a modified vacuole (LCV), from which it translocates more than 300 effector molecules into the host cytosol via a type IV secretion system (T4SS). The modification of various cellular processes by the bacterial effector proteins allows the replication of *L. pneumophila* in the LCV, from which the bacteria finally egress to start a new infection cycle.

The fate and appearance of the LCV differ from vacuoles harboring canonically phagocytized bacteria in macrophages in multiple ways²²: Thus, the established LCV exhibits no classical markers of the endocytic pathway, such as the proteins Rab5, which localizes to early endosomes, Rab7, typically found at late endosomes, and LAMP-1, a

lysosomal transmembrane protein^{23,24}. Additionally, no acidification of the LCV occurs, but a stable pH of about 6.1 is maintained²⁵. Thus, the LCV bypasses the endocytic pathway and transforms into a replication-supporting environment for *L. pneumophila*. Microscopy studies revealed that the outer membrane of the LCV is decorated with smooth vesicles and ribosomes, which are actively recruited from the endoplasmic reticulum (ER) to the LCV, creating a unique ER-like compartment^{20,26,27}. Additionally, mitochondria localize at the LCV, and even though the function of this re-localization remains not fully understood, it seems to result in a metabolic shift in *L. pneumophila* infected cells, which likely favors bacterial replication^{28–30}. *L. pneumophila* persists in the modified phagosome for 4 to 10 h before starting to replicate³¹. The complete replication cycle in the LCV lasts roughly until 24 h after bacterial uptake in the host cell^{27,32}. One of the key virulence factors essential for *L. pneumophila* to establish a successful infection is the type IV secretion system (T4SS), encoded by the *dot/icm* genes^{33,34}. The T4SS is a multi-protein complex composed of 27 proteins, whose expression is activated by *L. pneumophila* shortly after successful invasion³³. It could be demonstrated that *L. pneumophila* strains deficient for Dot/Icm T4SS components, such as *ΔdotA*, are unable to replicate and quickly enter the endocytic pathway, which is characterized by the fusion of the phagosome with the lysosome, acidification, and finally degradation of the vacuolar trapped microorganism^{24,35,36}. In addition to the T4SS, *L. pneumophila* exhibits other secretion systems required for pathogenicity and successful infection establishment, as they complement the function of the Dot/Icm system. Those include a T2SS system (*Lsp*), a T1SS system (*Lss*), and a second T4SS (*Lvh*). It was demonstrated that mutations in one of these systems significantly limit the range of potential hosts for *L. pneumophila* and impede cell invasion, replication, survival, and biofilm formation^{37–39}. The functional Dot/Icm T4SS allows the translocation of more than 300 effector molecules into the host cytosol²⁶. These effectors act on the host cell in many different ways and consequently enable the establishment of a replication-permissive environment in the LCV, from which *L. pneumophila* finally egresses into the alveolar space after successful multiplication, thereby lysing its former host cell and starting a new infection cycle⁴⁰.

1.1.2. Bacterial effectors of *L. pneumophila* – many ways to manipulate the host cell

Intracellular pathogens have evolved sophisticated strategies to manipulate their host cells into niches that enable their survival and persistence⁴¹. In this context, effector proteins have

been proven to be a successful strategy for many different bacteria, such as *Salmonella enterica*, *Shigella flexneri*, or *Chlamydia trachomatis*^{41,42}. Often, these bacterial effectors target the structural organization and alter cellular functions of organelles, such as endosomes, the ER, Golgi apparatus, and mitochondria, or they modulate various cellular processes⁴¹. In the case of *L. pneumophila*, bacterial effectors are temporal-hierarchically translocated from the LCV into the host cytosol via the T4SS, depending on the bacterial growth phase and on their cellular targets and effects, to create an optimal replication niche for the pathogen⁴⁰. The full range of *L. pneumophila*-secreted effector molecules and their mechanism of action has not been completely characterized yet; however, various studies examining the function of single effector proteins alone or in combination have found that *L. pneumophila* affects the host cell in multiple ways. Effector-mediated manipulation of the host cell thereby impacts and remodels diverse host cell processes, including its metabolism, phagosome maturation, small GTPase signaling, ubiquitination, apoptosis, autophagy, cell cycle, cytoskeletal and mitochondrial dynamics, as well as mRNA transcription, and protein synthesis (see Figure 2)^{36,40,41,43,44}.

Impairment of the host protein synthesis

Up to date, several *L. pneumophila* effectors have been identified to collectively contribute to translation impairment in infected cells, including Lgt1-3, SidI, SidL, LegK4, and RavX⁴⁵. Targets of these effectors were found to be the eukaryotic GTPase elongation factor 1A and 1By (eEF1A and eEF1By), as well as the phosphorylation of the cytosolic chaperon heat shock protein 70 (Hsp70), attenuating its protein-refolding capacity on translating polysomes and thereby impairing translation⁴⁵⁻⁴⁷. Additionally, it was found that wild-type (wt) *L. pneumophila* can impair the cap-dependent translation initiation by suppression of eukaryotic initiation factor 4E (eIF4E)⁴⁸. The full range of host proteins that are impaired in translation due to the action of *L. pneumophila* effector proteins has not been discovered yet. However, *in vitro* studies indicate that infection with *L. pneumophila* led to a dramatic reduction of global protein translation in bone marrow-derived macrophages (BMDMs) and attenuated production of proinflammatory cytokines such as tumor necrosis factor alpha (TNF α), interleukin 6 (IL-6) and interleukin 12 (IL-12)⁴⁹⁻⁵¹. Furthermore, translational impairment also seems to affect the unfolded protein response (UPR), a cellular response induced by sensing ER stress, which includes signaling cascades that mediate downstream events to limit cellular stress and restore cellular homeostasis⁵²⁻⁵⁴.

Modulation of host ubiquitination pathways

Several effectors of *L. pneumophila* have also been found to be involved in the subversion of cellular ubiquitin pathways and are critical for successful bacterial replication^{55,56}. Modulation of ubiquitination by the enzymatic activity of bacterial effectors from the SidE family has been shown to facilitate and ensure LCV biogenesis as well as to regulate the activity of the mechanistic target of rapamycin (mTOR) kinase, which is important for nutrient acquisition by *L. pneumophila* (see below)⁵⁷⁻⁵⁹. Additionally, the antagonistic activity of the two effectors MavC and MvcA has been found to regulate the ubiquitination and, thereby, activation of the host protein ubiquitin-conjugating enzyme E2 N (Ube2N), which in turn regulates levels and activity of the nuclear factor 'kappa-light-chain-enhancer' of activated B-cells (NF- κ B) inhibitor I κ B α , thereby directly impacting inflammatory host gene transcription^{60,61}.

Nutrient acquisition and manipulation of host-metabolism

L. pneumophila is auxotrophic for several host-derived amino acids for intracellular replication⁶². One of the essential bacterial effectors involved in facilitating the acquisition of amino acids from the host is AnkB, which acts to recruit polyubiquitinated proteins to the LCV, where they attach in an effector-mediated manner and are subsequently proteolyzed by the host 26S proteasome^{63,64}. Deletion of *ankB* and chemical inhibition of 26S proteasome impedes bacterial replication in the LCV. However, supplementation of cell culture with free amino acids rescues the growth of intracellular *L. pneumophila* lacking *ankB*⁶³. Another important target of *L. pneumophila* effectors is mTORC1, a conserved complex in eucaryotic cells and a core component of the mTOR kinase. Activation of the complex is partly regulated by amino acids and nutrient availability, and its activation controls many cellular processes, such as the repression of autophagy, translation initiation, and lysosome biosynthesis⁶⁵. The Lgt and SidE effector families modulate the activity of mTORC1: the translation-inhibitory activity of Lgt activates mTORC1, whereas SidE family effectors are negative regulators of the complex, thereby facilitating the availability of free host amino acids for bacterial intake⁵⁷. Finally, *L. pneumophila* also directly affects the host-metabolism, partly in an effector-dependent manner: Infected human macrophages show a shift towards a Warburg-like metabolism, characterized by upregulation of glycolysis and a reduction of oxidative phosphorylation (OXPHOS)²⁹. It is assumed that these changes in metabolism also enable nutrient acquisition and optimal replication conditions in the LCV⁶⁶.

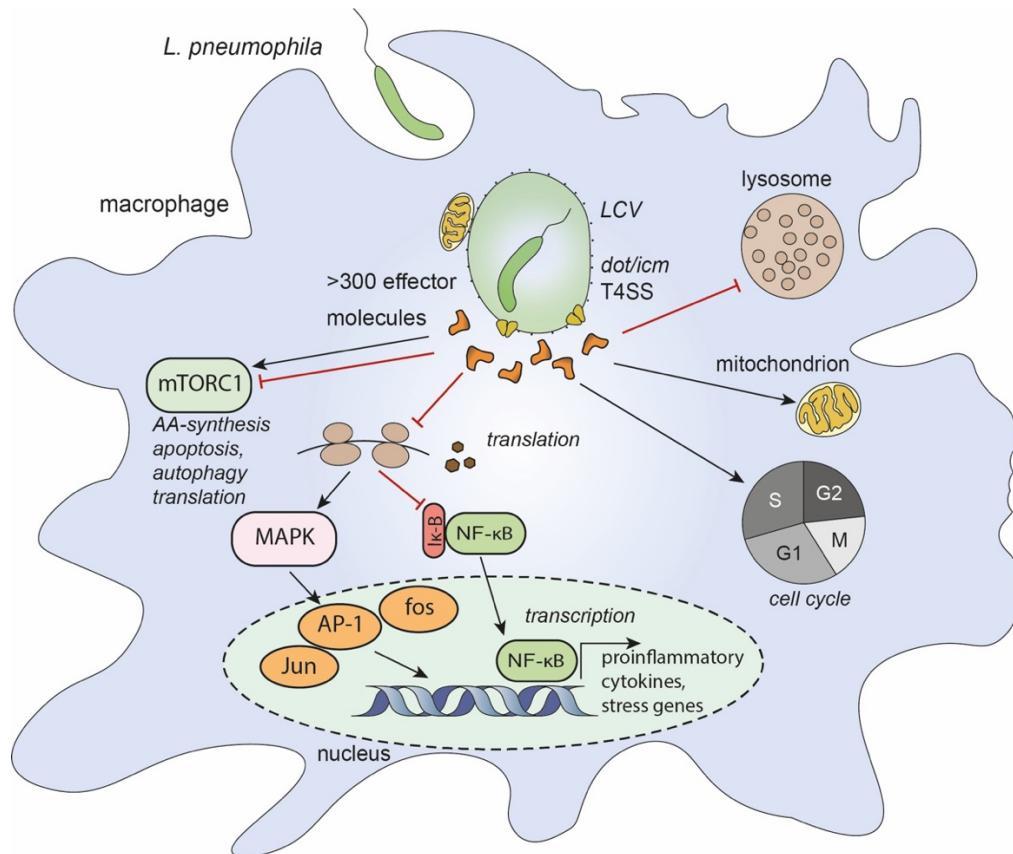


Figure 2) *L. pneumophila* effectors modulate a broad variety of host cell pathways. Effector-mediated manipulation of the host cell impacts and remodels diverse host cell processes, including, among others, its metabolism, phagosome-lysosome-fusion, apoptosis, amino acid (AA) synthesis, cell cycle, mitochondrial dynamics, as well as protein synthesis. Effector activity results in a unique transcriptomic response, which is characterized by prolonged MAPK- and NF- κ B-signaling.

Overall, most of the effector-driven mechanisms of cellular manipulation aim to facilitate bacterial survival and dampen the inflammatory response in infected cells to some extent. However, at the same time, it was observed that the effector activity induces a so-called “effector-triggered response” of the host cell, characterized by a unique transcriptional profile. Blockage of translation initiation and elongation, as well as the effector-mediated ubiquitinylation activity, affects the synthesis and activation of various transcriptional regulators, e.g., NF- κ B inhibitor I κ B^{48,67}. This leads to a prolonged expression of NF- κ B-regulated transcripts as well as an enhanced mitogen-activated protein kinase (MAPK)-signaling activity. Among those mRNAs are stress response genes and proinflammatory cytokines and chemokines, such as *Il1a*, *Il1b*, *Tnfa*, *Il23a*, *Csf1*, and *Csf2*^{67–70}. Most of these transcripts fail to be translated in the presence of bacterial effectors. However, a subset of these genes, including IL-1 α , have been found to be translated in *L. pneumophila*-infected cells and drive the proinflammatory response and antibacterial defense⁷¹. Translational bypassing was thereby found to be largely dependent on TLR-signaling via the adaptor

protein myeloid differentiation primary response 88 (MyD88), as well as on high ribosome loading on a specific sequence structure in the 5' untranslated mRNA regions of low-abundance transcripts^{49,72}.

The outcome of an infection with *L. pneumophila*, whether it is the elimination of the bacterium or the establishment of LD, is eventually determined by the balance between the bacterial virulence and the host defense strategies.

1.2. The immune system

In the surrounding environment, humans and other multicellular organisms are exposed to microorganisms such as viruses and bacteria, which may be inhaled, swallowed, or enter the body due to disruptions of physiological barriers. Additionally, various microbes inhabit the body as part of the commensal microbiota, many of them providing some essential or beneficial functions for their host. However, in some cases, contact with microorganisms might be harmful and lead to illness. Whether the encounter causes a disease relies on the balance between the pathogenicity of the respective microorganism on the one hand and the capacity of the host defense mechanisms, the immune system, on the other hand. The mammalian immune system is traditionally categorized into two main components, based on the pace and specificity of their reactions: innate and adaptive immunity. Despite this categorical division, much interplay was found between the individual mechanisms driving both innate and adaptive immunity, making the immune system a complex network orchestrating the immune response to exogenous and endogenous stimuli. Innate immunity encompasses physical, chemical, and microbiological barriers but primarily involves defined cellular elements (e.g., neutrophils, monocytes, macrophages), signaling molecules (e.g., cytokines, complement system), and proteins (e.g., acute phase proteins) that provide immediate defense against pathogens. While the innate immune response is highly conserved across various species, adaptive immunity is a hallmark of the immune system in vertebrates and involves antigen-specific reactions driven by T and B lymphocytes. Furthermore, while the innate response is rapid but less specific, the adaptive response is usually more precise but takes several days or weeks to develop fully. Moreover, the adaptive response exhibits memory; subsequent exposure to the same pathogen triggers a more vigorous and rapid immune response^{73,74}.

1.2.1. The innate immune response in the lung

Inhalation for respiration not only provides oxygen to the lungs but also exposes land-living vertebrates to the risk of potentially inhaling infectious agents, hazardous pollutants, and toxic particles. This makes the respiratory tract one of the most common routes of infections, causing diseases associated with high morbidity and mortality rates⁷⁵. Maintaining a healthy state of the lungs depends, among others, on the innate immune system. The pulmonary epithelium acts as the front line of defense against infections, forming a protective physical barrier between the respiratory lumen and the vasculature. The barrier function of the pulmonary epithelium thereby depends on the formation of tight junctions (TJ), which are heteromeric protein complexes, forming the sealing interface between adjacent epithelial cells^{76,77}. An intact epithelial layer in the lungs and the alveolar space prevents infectious agents from colonizing and disseminating from the lungs. However, the integrity of the barrier might be disrupted by bacterial or viral infections, which mostly lead to an alteration of TJ formation^{78,79}. The damage of the epithelial integrity can lead to unfavorable outcomes, permitting infectious agents to spread into the bloodstream and causing fluid accumulation in the lungs, which, in turn, impairs gas exchange⁸⁰. To prevent epithelial barrier disruption, constant monitoring of the pulmonary epithelium by innate immune cells to detect and discriminate self and non-self agents is crucial. Therefore, a central element of innate immunity is the expression of pathogen recognition receptors (PRRs). PRRs are expressed by immune cells and allow them to detect molecular structures that originate from microorganisms, so-called pathogen-associated molecular patterns (PAMPs), which are also expressed by non-virulent microbes. Further, PRRs may also recognize some danger-associated molecular patterns (DAMPs), which are endogenous molecules released from damaged and dying cells during sterile or pathogen-induced infection^{74,81}. PAMPs exhibit three primary characteristics: First, they display invariability across microorganisms within a specific class, facilitating the recognition of a diverse array of microbes. Second, they do not always but often arise from pathways mostly exclusive to microorganisms, making them particularly suited for distinguishing self- from non-self-entities. Third, they play a critical role in microbial physiology and are indispensable for their survival, which restricts the capacity to alter or modify these attributes to evade detection by the innate immune system⁷⁴. Classical PRR-activating PAMPs are, e.g., bacterial cell wall components like lipopolysaccharide (LPS), peptidoglycan, mycolic acids, and bacterial flagellin⁸²⁻⁸⁵. Additionally, nucleic acids serve as viral and bacterial PAMPs. At this juncture, the self vs.

non-self-discrimination is based on specific chemical modifications within microbial-derived acids or their non-physiological localization, e.g., within the cytosol of infected cells⁸⁶⁻⁸⁸. Recognition of microbial PAMPs often leads to the activation of different signaling cascades that initiate and modulate the innate immune response and induce the production of, e.g., proinflammatory cytokines and chemokines or production of antimicrobial proteins that act to directly clear the infection or recruit other immune cell populations to the site of infection^{89,90}.

1.2.2. Detection of PAMPs by different classes of PRRs

In 1989, Charles Janeway Jr. introduced the idea of a group of receptors being expressed in innate immune cells responsible for recognizing conserved microbial structures⁷⁴. His revolutionary concept was a strong fundament for today's understanding of innate immunity. After extensive years of study, it is indeed known that establishing a rapid and effective response to pathogens relies on the expression of germline-encoded PRRs, which can sense a broad range of microbial PAMPs and induce different antimicrobial-defense signaling cascades¹⁸⁹. PRRs are categorized into at least five structurally and functionally different families or groups: (i) Toll-like receptors (TLRs), (ii) NOD-like receptors (NLRs), (iii) RIG-I-like receptors (RLRs), (iv) cytosolic DNA receptors, and (v) C-type lectin receptors (CLRs).

Toll-like receptors

The first discovered and most extensively characterized family of PRRs are the TLRs. TLRs have been named after the Toll proteins discovered in *Drosophila* fruit flies, which were found to be pivotal in embryonic development and immune responses to fungi^{91,92}. In vertebrates, this receptor family is, as far as known, solely implicated in innate immune defenses, and several TLRs have been characterized. In humans, 10 TLR family members (TLR1-10) have been identified so far, whereas 12 have been discovered in mice (TLR1-9 and TLR11-13; the murine TLR10 gene contains a stop codon, therefore it is not expressed in mice)⁹³. TLRs are considered the primary sensors of many invading pathogens, as they are membrane-bound PRRs localized within the plasma or endosomal membrane and, therefore, monitor the cell surface and the phagocytized content for PAMP signatures. Among the receptors primarily expressed on the cell surface are TLR1, 2, 4, 5, and 6, which recognize PAMPs derived primarily from bacteria, such as LPS (TLR4) or flagellin (TLR5).

TLR3, 7, 8, and 9 are membrane-bound to endocytic compartments and primarily sense nucleic acid derived from various viruses and/or bacteria^{93–95}. The recognition and binding of the respective PAMP via the extracellular binding domain leads to a structural change of the cytoplasmatic domain and allows binding of the adaptor proteins MyD88 or TIR-domain-containing adapter-inducing interferon β (TRIF)⁹³. This triggers the signaling of downstream events, which result in the expression of proinflammatory cytokines and type I IFNs via the transcription factors NF- κ B or Interferon Regulatory Factor 3 (IRF3)⁹⁶.

NOD-like receptors

NLRs are a PRR family that senses a wide range of ligands in the cytosol of host cells. To date, 23 NLRs have been identified in humans, whereas about 34 NLRs were found in mice⁹⁷. Structurally, NLRs are composed of three main domains: First, the C-terminal LRR domain recognizes microbial PAMPs and endogenous host molecules. Second, an intermediate NOD domain is required to induce the conformational change for activation of downstream signaling upon ligand binding. Third, the N-terminal protein-interaction domain, of which four structural variants are known, further dividing NLRs into four subfamilies: (i) NLRA (with an acidic transcriptional activation domain), (ii) NLRB (exhibits a baculoviral inhibition of apoptosis repeat (BIR) domain), (iii) NLRC (with a caspase activation and recruitment domain [CARD]) and (iv) NLRP (with a pyrin domain [PYD])⁹⁸. Two of the most studied NLRCs-members are NOD1 and NOD2. Both receptors recognize conserved structures of peptidoglycans from bacterial cell walls⁹⁹. Recognition of the respective PAMP has been shown to induce oligomerization of the receptors, which induces recruitment of the adaptor protein RIP2 to the CARD domain, activation of NF- κ B and MAPK-signaling, and subsequent inflammatory cytokine transcription. Moreover, some studies have implicated that NOD1 and NOD2 are involved in the activation of type I IFNs via the activation of transcription factors IRF7 and IRF3^{89,97}.

Some NLRs have also been involved in activating an inflammatory multiprotein complex known as the “inflammasome” upon activation by PAMPs and/or other activators. Inflammasomes are composed of an NLR protein (e.g., NLRP3, NLRC4, NLRP1), an adaptor protein (e.g., apoptosis-associated speck-like protein containing a carboxy-terminal CARD [ASC]), and a downstream effector caspase (e.g., caspase-1)¹⁰⁰. A well-studied NLR that has been demonstrated to form an inflammasome is NLRP3. The receptor has a broad spectrum of activators, including microbial nucleic acids, pore-forming toxins,

peptidoglycans, ATP, uric acid, and silica crystals^{81,89,101}. Canonical inflammasome activation induces caspase-1-dependent proteolytic cleavage of proIL-1 β and proIL-18 into their mature cytokine forms, critical for their subsequent secretion and proinflammatory effect. Furthermore, caspase-1 activation has also been demonstrated to induce pyroptosis, a highly inflammatory form of regulated cell death^{100,101}. Another inflammasome-inducing NLR is NLRC4. NLRC4 recognizes bacterial flagellin, which leads to heterodimerization with another NLR protein of the NAIP subfamily, NAIP5. The subsequent binding of ASC by the NLRC4/NAIP5 inflammasome also leads to IL-1 β and IL-18 maturation and release, as well as to pyroptosis^{98,102}.

RIG-I-like receptors

A small class of PRRs is RLRs, which only contain three members: retinoic acid-inducible gene I (RIG-I), melanoma differentiation-associated gene-5 (MDA-5), and laboratory of genetics and physiology 2 (LGP2), with all of them being cytosolic RNA-sensing receptors^{103,104}. MDA-5 and RIG-I both recognize long double-stranded (ds) RNA or shorter dsRNA, which exhibit 5'-triphosphate ends and that are specific to viruses and not present in host RNA^{88,105}. It has been found that upon nucleic acid binding, RIG-I and MDA5 activate the adaptor molecule mitochondrial antiviral signaling (MAVS) via their CARD domain, which leads to the downstream activation of the transcription factors IRF3 and 7, which regulate type I IFN expression, as well as activation of NF- κ B, leading to proinflammatory cytokine expression. RIG-I has further been demonstrated to become indirectly activated by cytosolic AT-rich DNA that is converted into 5'-triphosphate RNA in an RNA polymerase III-dependent manner¹⁰⁶. The third protein of the RLR family, LGP2, is supposed to act as a regulator of the other two RLR proteins, as it lacks the CARD domain, which prevents direct downstream signaling¹⁰⁷.

Cytosolic DNA receptors

Sensing foreign cytosolic DNA by cytosolic DNA sensors is an integral and critical component of the innate immune system. Most PRRs involved in dsDNA sensing have only been discovered in recent years, and these receptors belong to different protein families, thus exhibiting structural differences. However, a common feature among some of these receptors is the induction of type I IFNs by the adaptor and sensor molecule stimulator of interferon genes (STING), the TANK-binding kinase 1 (TBK1), and, subsequently, the transcription

factor IRF3^{108,109}. In addition, the activation of STING has also been shown to induce proinflammatory cytokine expression through NF- κ B in a TBK1-dependent manner¹¹⁰. In mammalian cells, the DNA sensor cGAMP synthase (cGAS) is an important activator for STING^{111,112}. The binding of intracellular DNA in the cytosol induces the cyclic dinucleotide GMP-AMP (cGAMP) production by cGAS. cGAMP is a second messenger molecule and an agonist of STING and activates downstream signaling^{112,113}. To date, cytosolic DNA detection has been found to activate various signaling pathways besides STING-mediated type I IFN and proinflammatory cytokine induction. For example, the cytoplasmic sensor absent in melanoma 2 (AIM2) recruits ASC upon dsDNA binding, as well as caspase-1 to form the AIM2 inflammasome, which modulated the inflammatory response via cytokine maturation of IL-1 β and IL-18, as well as induction of pyroptosis¹¹⁴⁻¹¹⁶.

C-type lectin receptors

The fifth family of PRRs is the CLR, which comprise more than 1,000 proteins. In mammals, C-type lectins are either found as secreted or transmembrane proteins, harboring a characteristic C-type lectin-like domain (CTLD). Based on the phylogeny and structural organization of their CTLDs, they have been further divided into 17 subfamilies, of which three are mainly expressed on myeloid cells (myeloid CLR)^{117,118}. Their name is initially derived from their binding activity, as many C-type lectins exhibit Ca²⁺-dependent recognition of carbohydrates via a sequence motif within their CTLD¹¹⁹. Conversely, other members of this family lacking this sequence were found to bind a broader repertoire of ligands, such as proteins or lipid-derived ligands and even inorganic molecules. Their ability to recognize endogenous (self) and exogenous (non-self) ligands implicates a broad range of physiological functions. Transmembrane CLR can induce various intracellular signaling pathways upon binding microbial molecules. Examples are the CLR Dectin-1 and Dectin-2, which recognize β -1,3-glucans and α -mannans found in fungi, as well as the receptor Mincle, which binds α -mannose from *Malassezia* spp., as well as glycolipids like Glucosyl-Diacylglycerol and Trehalose-6,6'-Dimycolate (TDM) from pneumococci and mycobacteria, respectively¹²⁰⁻¹²⁵. CLR that interact with endogenous ligands are, for instance, DNGR-1/CLEC9A, which recognizes F-actin, or Mincle, which senses the protein SAPI30 and β -Glucosylceramide¹²⁶⁻¹²⁸. Myeloid CLR are single-pass transmembrane proteins further categorized into type I and type II CLR with an extracellular N-terminus

and intracellular N-terminus, respectively ¹²⁹. Structurally, they are composed of the extracellular domain (ECD), formed by one or multiple CTLDs and a neck (stalk) region, the transmembrane domain, anchoring the receptor to the cytoplasmatic membrane, and the intracellular tail. The intracellular domain often has an immune signaling function and categorizes myeloid CLRs into four functional classes based on the nature of the signaling motif in the cytoplasmatic tail (see Figure 3). The first class is immunoreceptor tyrosine-based activating motif (ITAM)-coupled CLRs, which recruit intracellular adapter molecules expressing ITAM, such as fragment crystallizable receptor γ (FcR γ) or DNAX-activation protein 12 (DAP12) ^{127,130–132}. The second class is hemITAM-containing CLRs, directly containing an LxxY tandem motif in their cytoplasmatic tail ¹³³. These two receptor classes are activating CLRs. The third class is the ITIM immunoreceptor tyrosine-based inhibitory motif (ITIM)-containing CLRs and are considered to act as inhibitory receptors. Finally, a fourth class of receptors signals independently of ITAMs/ITIMs ¹³⁴.

ITAM-coupled and hemITAM-containing CLRs recruit the spleen tyrosine kinase (SYK) upon binding their respective ligand. Following the binding to the cytoplasmatic tail, SYK activates itself by auto-phosphorylation. Examples of hemITAM-containing CLRs are Dectin-1 or CLEC2, whereas Dectin-2 or MDL-1 are CLRs acting in an ITAM-coupled manner ^{127,131–133,135,136}. Activated SYK then triggers the NF- κ B- and nuclear factor of activated T-cells (NFAT)-dependent proinflammatory gene expression in a signaling pathway involving a protein complex composed of caspase-recruitment domain protein 9 (CARD9), B cell lymphoma/leukemia 10 (BCL10), and mucosa-associated lymphoid tissue lymphoma translocation protein 1 (MALT1) ¹³⁷. Other immune-modulating mechanisms induced by hemITAM-containing CLRs include the production of reactive oxygen species (ROS) ¹³⁴. In contrary, ITIM-containing CLRs, such as DCIR or CLEC12A (also referred to as MICL), associate with the tyrosine phosphatase like Src homology region 1 domain-containing phosphatase (SHP-1) or SHP-2 ^{138–140}. Activated SHP1 and -2 have been shown to impair intracellular signaling cascades and confer the negative regulation of proinflammatory pathways ¹⁴¹.

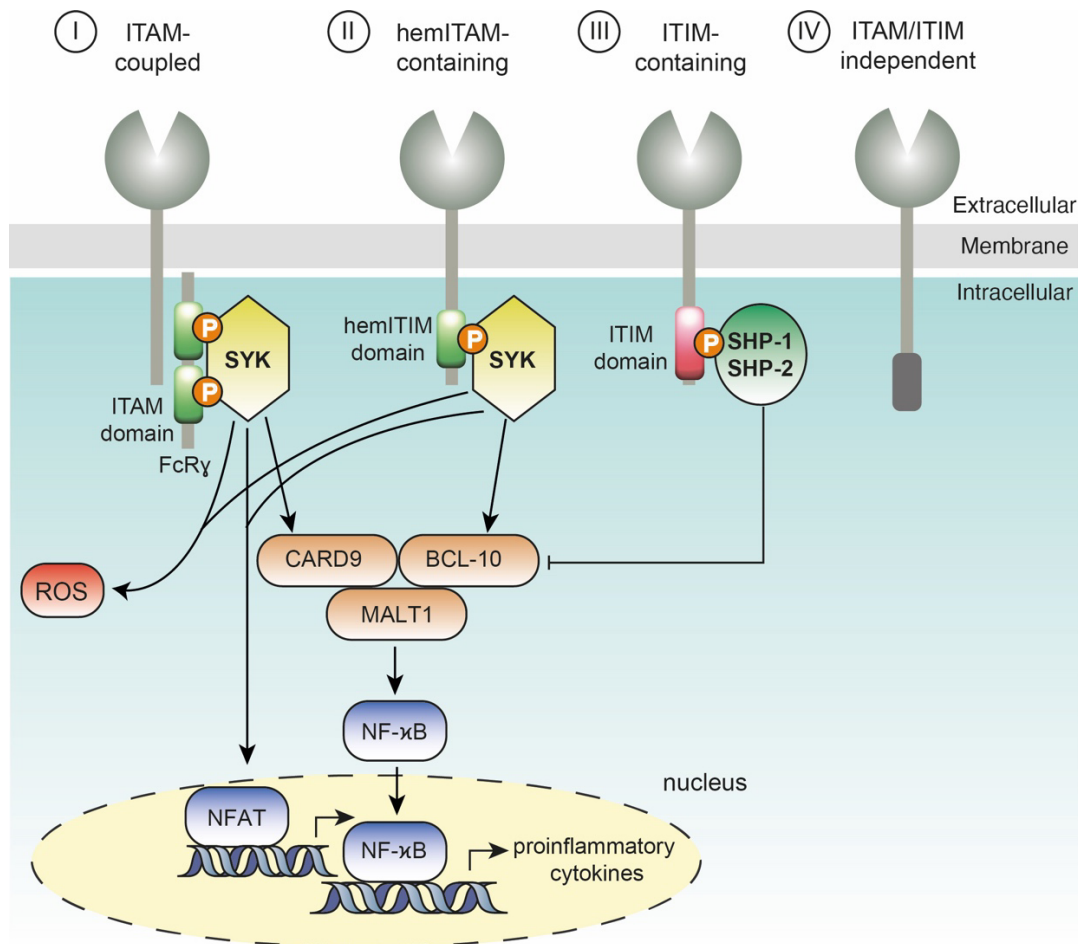


Figure 3) The four functional classes of myeloid CLR and their downstream signaling events to modulate the immune response upon ligand binding. ITAM-coupled as well as hemITAM-containing CLR recruit SYK and signal to activate transcription of proinflammatory cytokines and production of ROS. ITIM-containing CLR recruit SHP-1 and SHP-2 and have an anti-inflammatory signaling function. A fourth class of CLR signals ITAM/ITIM-independent.

1.2.2.1. The C-type lectin receptor CLEC12A

The CLR CLEC12A, also known as MICL, belongs to the C-type lectin domain family 12 and is a type II transmembrane protein, which is predominantly expressed on myeloid cells, such as granulocytes, macrophages, dendritic cells, and monocytes¹⁴². Human and murine CLEC12A share structural and functional similarities. However, they differ in glycosylation patterns, with human CLEC12A being heavily glycosylated as a monomer and murine CLEC12A as a less glycosylated dimer¹⁴³. Harboring an ITIM motif in its cytoplasmic tail, the receptor negatively regulates various inflammatory signaling cascades¹¹⁸. Prior research has attributed significant roles to CLEC12A in maintaining homeostasis and regulating inflammation, particularly in conditions like rheumatoid arthritis and experimental autoimmune encephalomyelitis^{144,145}.

CLEC12A has been identified as a receptor responsible for detecting uric acid crystals (monosodium urate, MSU). MSU is considered a critical danger signal, released from dying cells and inducing a robust immune response¹⁴⁶. Recently, another crystalline ligand of CLEC12A was identified, namely plasmodial hemozoin. In this context, it was shown that CLEC12A deficiency in mice protects the animals from developing experimental cerebral malaria upon infection with *Plasmodium berghei*¹⁴⁰. The involvement of CLEC12A in the context of bacterial infections is marginally studied. Studies performed in a murine model investigating *Salmonella* infection in *Clec12a*^{-/-} mice found that the loss of the receptor made mice more susceptible to the infection. The study further indicated that CLEC12A contributes to antibacterial autophagy during *Salmonella* infection: CLEC12A was found to be recruited to bacteria-autophagosome complexes and to interact with the E3-ubiquitin ligase complex, thereby influencing autophagic responses¹⁴⁷. Moreover, murine CLEC12A was reported to bind mycolic acids from various mycobacterial species. This binding was observed to be even stronger by human CLEC12A¹⁴⁸. Additionally, CLEC12A-deficient mice exhibited augmented innate immune responses upon *M. tuberculosis* infection, suggesting that mycobacteria exploit CLEC12A via their mycolic acids to subvert the host immune defenses¹⁴⁸. Conclusively, the inhibitory receptor CLEC12A seems to have a role in microbial infections. The receptor's potential role in the immune response against *L. pneumophila* will be discussed below (see 1.3.1.).

1.2.3. The early cellular innate immune response in the lung

The innate pulmonary immune response is a temporally orchestrated process whose first steps are initiated by PAMP-PRR interaction on sensing immune cells, followed by the involvement of a series of partially interdependent effector cells. Many innate immune cell populations are involved in lung inflammation caused by invading pathogens. These cells either contribute to pathogen elimination directly after PAMP sensing, without further intermediates, or upon recruitment to the site of infection in a signaling molecule-dependent manner. Phagocytic leucocytes, such as AMs, neutrophils, inflammatory monocytes, and dendritic cells, are important in the early innate immune response.

1.2.3.1. Alveolar macrophages

In the lung, interstitial macrophages (IMs) and AMs are the two main types of macrophages residing in different anatomical compartments of the lung, with AMs being considered the most abundant pulmonary macrophage population. Their location on the luminal surface of the alveoli predestinates them to be among the first cells of the innate immune system to encounter inhaled pathogens or pollutants. AMs play crucial roles in inflammation and tissue repair, but also in clearing surfactant in the lung to maintain lung homeostasis^{19,149,150}. The specific microenvironment of the lung, characterized by strong fluctuation in partial oxygen pressure (PO₂), abundant surfactant, and influences of alveolar type I and II (AT1 and AT2) cells, contributes to the distinct phenotype of AMs. Like other murine tissue-resident macrophages, they show expression of MerTK, CD54, CD68, CD206, and F4/80 but lack fractalkine receptor CX3CR1 or integrin CD11b expression. Additionally, AMs can be identified in flow cytometry investigation by expression of integrin CD11c and sialic acid-binding lectin Siglec-F^{151–153}. The expression of CD206, CD169, CD11b, and HLA-DR characterizes human AMs in a normal healthy state^{149,153}. Due to their high granularity, both human and murine AMs exhibit high levels of autofluorescence^{154,155}.

Identifying the exact origin of AMs has been an important research topic for many years. During embryogenesis, several waves of macrophages populate the lung and, for a long time, were assumed to be the precursors of AMs^{156,157}. As the alveolar niche does not exist until birth and is established after the newborn's first breath, it is now understood that circulating fetal monocytes populate the alveolar space during the first days after birth and mature into AMs^{149,158,159}. While AMs possess the ability to self-renew and maintain in the alveolar niche in the lung at a steady state, factors like infections, environmental stress, and aging may decrease their numbers in the lung. These factors are assumed to lead to infiltration of circulating hematopoietic stem cell-derived monocytes that may feed into the pool of lung-resident macrophages in adults^{160–162}. The differentiation of fetal monocytes and engraftment in the alveolar niche was found to depend on the cytokine granulocyte-macrophage colony-stimulating factor (GM-CSF), which is produced by AT2 cells¹⁶³. GM-CSF signaling is required for expression of the peroxisome proliferator-activated receptor gamma (PPAR- γ), a key regulator of lipid metabolism and transcription factor essential for activating the transcriptional program driving the macrophage adaptation to the lung environment¹⁵⁹. In support of this, it was found that mice lacking the common α (*Csf2ra*^{-/-}) or β (*Csf2rb*^{-/-}) chain of the GM-CSF receptor do not show endogenous populations of

AMs in their lung ^{159,164,165}. Besides GM-CSF, the cytokine transforming growth factor β (TGF β) is crucial for the development and maintenance of AMs. TGF- β is produced by AMs in an autocrine manner and, like GM-CSF, was found to impact PPAR- γ -driven gene expression for AM development ¹⁶⁶. Other factors, which were found to essentially confer to AM development and maintenance, were the transcription factors BACH2 and C/EBP β ^{167,168}. Finally, the actin-bundling protein L-plastin, which has an important role in regulating the actin cytoskeleton, was found to be crucial for the transmigration and retention of AMs precursors into the alveolar niche ¹⁶⁹.

The role of AMs at steady state

In the unperturbed lung, AMs are primarily responsible for the clearance of excess surfactant in the airways, which is produced and secreted by AT2 cells and essential for normal lung function. The pulmonary surfactant forms a surface-active monolayer at the air-water interface of the alveoli. It functions in increasing pulmonary compliance as well as reducing the surface tension to prevent a pulmonary collapse at low lung volumes and enabling better gas exchange in the alveoli ^{170,171}. Chemically, the pulmonary surfactant is composed of phospholipids (mainly dipalmitoylphosphatidylcholine [DPPC]), neutral lipids (mainly cholesterol), and surfactant proteins, with an approximate ratio of 10:1:1 ^{170,172,173}. The surfactant-associated proteins are the hydrophobic surfactant protein B (SP-B) and SP-C, which accelerate surfactant adsorption and promote its low surface tension function. Additionally, the hydrophilic glycoproteins SP-A and SP-D have been shown to interact with the lipids-fraction of the surfactant and affect its structure and composition ^{174–176}. Dysfunction in the pulmonary surfactant homeostasis drastically increases the risk of developing pulmonary alveolar proteinosis (PAP), which is characterized by the accumulation of surfactant in the alveolar space. It is often the result of impaired GM-CSF signaling, mainly due to mutations in the GM-CSF receptor genes, which leads to defective surfactant clearance by AMs in the lung ¹⁷⁷.

Besides their function in surfactant homeostasis, AMs have a crucial immunoregulatory role in a non-inflammatory state in the lung. Central to this is the process of “efferocytosis”, which is the ingestion of apoptotic cells. Removal of cell debris and dying cells by macrophages is critical to prevent a strong proinflammatory response to released cell contents and inflammation-stimulating factors and to obviate subsequent tissue damage. Efferocytosis further induces the production of anti-inflammatory mediators in AMs, such as TGF- β , prostaglandin E2 (PGE3), and platelet-activating factor (PAF) by AMs, which

contribute to maintaining an immunosuppressive state in the lung at steady state^{178–181}. Additionally, *in vitro* co-cultivation studies showed that AMs promote the generation of regulatory T cells (Tregs) by stimulating FOXP3 expression in CD4⁺ T cells in a retinoic acid- and TGF- β 1-dependent manner^{182,183}. The lung epithelium fosters the anti-inflammatory phenotype of AMs under steady-state conditions: AMs are constantly exposed to negative regulatory signals from alveolar epithelial cells (AECs), including CD200 stimulation, as well as interleukin 10 (IL-10) and TGF- β 1 signaling that impairs with their proinflammatory activation^{150,184–186}.

The role of AMs in inflammation

Besides their anti-inflammatory and homeostasis-maintaining function at a steady state, AMs also have a significant role in the inflammatory response in the alveolar environment, operating as sentinels. Macrophages are often separated into two subpopulations referring to the functional programs they adopt, so-called macrophage polarization, in response to signals from their environment: Macrophages in the ground state M0 can be driven to either classically activated M1 macrophages and alternatively activated M2 macrophages. While M1 macrophages are defined as oriented towards inflammation and antimicrobial defense, M2 macrophages contribute to immune tolerance and tissue repair¹⁸⁷. Recent studies have challenged this classification, especially *in vivo*, where classical M1 and M2 markers are expressed in the same macrophage population, and the phenotype is strongly dependent on the respective microenvironment as well as on other factors, e.g., the respective mouse strain used. Therefore, macrophage phenotypes in response to microbial infections *in vivo* are assumed to reflect a great diversity that has not been fully characterized yet^{187–191}.

In the lung, the proinflammatory activation of AMs can be induced by PAMP detection and internalization of inhaled pathogens, as well as by destruction of airway epithelia in acute inflammation, the resulting loss of immunosuppressive ligand-signaling by AECs, and release of DAMPs¹⁵⁰. The switch to the proinflammatory state is therefore accompanied by inhibition of immunosuppressive signaling, e.g., impairment of IL10-receptor signal transduction through TLR2, TLR4, and TLR9 activation¹⁹². Activated AMs produce proinflammatory cytokines, such as TNF α , IL-1 β , IL-6, and type I IFNs. Furthermore, they have a greater phagocytotic capacity and an increased release of the oxygen metabolites superoxide and H₂O₂ (also referred to as “oxidative burst”)^{193–195}. The proinflammatory activity of AMs further activates adjacent epithelial cells and recruits other leucocytes, such as neutrophils, to the site of infection, thereby initiating the subsequent steps of the innate

immune response^{184,193,196,197}. Proinflammatory mediators produced by other immune cell populations, such as type II IFNs produced by lymphocytes, can, in turn, further enhance the proinflammatory phenotype of AMs, overall characterized by transcriptomic and metabolic changes, as well as increased production of proinflammatory molecules and antimicrobial peptides^{28,198,199}.

1.2.3.2. Neutrophils, dendritic cells & inflammatory monocytes

Polymorphonuclear neutrophils (PMNs) are the most abundant leukocyte population in the human circulation system²⁰⁰. Phenotypically, they can be identified by expression of surface markers CD11b and lymphocyte antigen 6 complex locus G6D (Ly6G). Upon pathogen recognition by sentinel cells, they are quickly recruited and activated at the side of infection²⁰¹. Infiltration into the lung tissue takes place within a few hours and is mainly orchestrated by the production and secretion of chemokines with a chemoattractant activity such as CXCL1, CXCL2, and CXCL5 by AMs or AECs observed, e.g., during *L. pneumophila* infection^{202,203}. Activated PMNs contribute to the elimination of the pathogenic source by phagocytosis and intracellular degradation, degranulation, which is the release of antibacterial molecules with bactericidal activity, and the generation of so-called neutrophil extracellular traps (NETs), which contribute to immobilization of bacteria^{204–206}. Furthermore, they produce a variety of chemokines with leucocyte-recruiting activity, e.g., CXCL1, CXCL8, or CXCL10, as well as the proinflammatory proteins S100A8/A9^{207,208}. To prevent tissue damage due to PMN stimulation and action on the side of infection, the activity and lifespan of PMNs are restricted, e.g., by apoptosis. Apoptotic PMNs are removed by other phagocytes, such as AMs or dendritic cells (DCs)^{178,201,209}.

DCs are antigen-presenting cells (APCs), which operate at the interface of innate and adaptive immunity²¹⁰. These cells are located throughout the pulmonary tissue, underlying the epithelial layer, which predestines them to encounter pathogens, PAMPs, DAMPs, pollutants, or allergens in the lung. Their main function is to recognize, internalize, process, and present antigen material via major histocompatibility complex (MHC) molecules on their surface, which activates other immune cell populations, such as T cells, thereby aiding the initiation of the adaptive immune response^{211,212}. Furthermore, ligand binding to their PRRs can also induce the secretion of proinflammatory cytokines, such as IL-1 β or IL-12. Thereby, DCs contribute to inducing and fostering the inflammatory immune response at the early stages of pulmonary infection¹⁸⁴.

A third group of phagocytes is inflammatory monocytes (iMonos), which are characterized by high expression of the surface marker Ly6C^{71,213,214}. They are recruited mainly via CCL2 and CCL7 from the bone marrow into the lung during infection, where they can differentiate into macrophages with high phagocytosis capacity or antigen-presenting DCs^{214–218}. Additionally, iMonos are an important source of proinflammatory cytokines such as IL-1 β , TNF α , and IL-12^{71,213}.

1.3. The innate immune response against *L. pneumophila*

Following the inhalation of contaminated aerosols, *L. pneumophila* is recognized and phagocytosed by AMs, which serve as a replication niche for the bacterium, as *L. pneumophila* is able to evade the endocytic pathway and phagolysosomal degradation in those cells. However, the mammalian immune system has co-evolved a strong defense against the intracellular infection, including macrophage-intrinsic antimicrobial defense strategies, as well as an innate and adaptive immune response orchestrated by other pulmonary immune cell populations, including PMNs, iMonos, DCs, natural killer (NK) cells, natural killer T (NKT) cells, B and T cells. The network of the immune detection signaling and various defense cascades usually results in bacterial clearance and resolution of the infected site in immunocompetent individuals^{51,219}. In this chapter, the recognition of the pathogen and subsequent specific immune signaling cascades in macrophages will be described in more detail (see Figure 4 for a schematic overview).

The role of TLRs

Detection of *L. pneumophila* in infected macrophages occurs via a diverse range of PRRs on the cell's surface or PRRs that sense intracellular bacterial compounds and cooperatively activate the antibacterial defense. The membrane-bound TLRs TLR2 and TLR5 are involved in *L. pneumophila* detection at the cell surface. Thus, TLR2 recognizes lipoproteins in the pathogen's cell wall, whereas TLR5 senses *L. pneumophila*-derived flagellin^{220,221}. TLR2 critically impacts the immune response to *L. pneumophila* infection, as *TLR2*^{-/-} mice exhibited higher bacterial burdens and impaired production of proinflammatory mediators in their lungs compared to infected WT mice^{222–224}. In contrast, *TLR5*^{-/-} mice exhibit no increased colony forming unit (CFU) levels in their lungs upon *L. pneumophila* infection but impairment in neutrophil recruitment. Simultaneously, the production of several proinflammatory cytokines was found to be enhanced in a TLR5-dependent manner in this

model, as well as prolonged pulmonary inflammation, indicating that receptor signaling is involved in the resolution of the inflammatory response. Furthermore, an association was found between a stop codon polymorphism in TLR5 in humans and LD development^{221,225,226}. A third TLR receptor that recognizes *L. pneumophila* is TLR9, which senses bacterial DNA in *L. pneumophila*-containing endosomes but seems to play a rather redundant role in restricting the infection^{225,227}. Activation of TLRs results in stimulation of NF- κ B-dependent gene expression via Myd88 as well as MAPK-signaling to induce the expression of various proinflammatory cytokines, such as IL-1 β and TNF α ^{221,222,225}.

The role of NLRs and inflammasomes

Besides TLRs, NLRs also play a role in the immune response against *L. pneumophila*. NOD1 and NOD2 localize in the cytosol of, e.g., macrophages, where they sense bacterial peptidoglycan secreted from the LCV via the T4SS. The absence of these receptors or their downstream signaling protein RIP2 was shown to impact bacterial clearance in mice as well as to diminish the recruitment of neutrophils, underlining the importance of this signaling pathway during infection^{68,228}. The NAIP5/NLRC4 inflammasome recognizes cytosolic flagellin, which is delivered through the T4SS from the LCV. Recognition of flagellin subsequently contributes to bacterial clearance by promoting LCV-lysosome fusion, cytokine production, and induction of pyroptosis by caspase 1 activation^{229–231}. Flagellin-deficient (*ΔflaA*) *L. pneumophila* mutants, as well as non-flagellated *Legionella* species, such as *L. longbeachae*, do neither induce pyroptosis nor cytokine maturation of IL-1 β and IL-18 mediated by the NAIP5/NLRC4 inflammasome^{232,233}. Another cytosolic inflammasome involved in the immune response against *L. pneumophila* is the NLRP3, ASC, and caspase-1 inflammasome, which seems to compensate for the production of IL-1 β and IL-18 when NAIP5/NLRC4 activation fails. However, it was found to be somewhat redundant during *L. pneumophila* infection *in vivo*^{234,235}. Finally, the non-canonical caspase 11 inflammasome was found to take part in the immune response towards *L. pneumophila*, as it binds LPS in the cytosol, thereby activating pyroptosis, phagosome-lysosome fusion, LCV lysis as well as NLRP3-inflammasome activation^{236,237}.

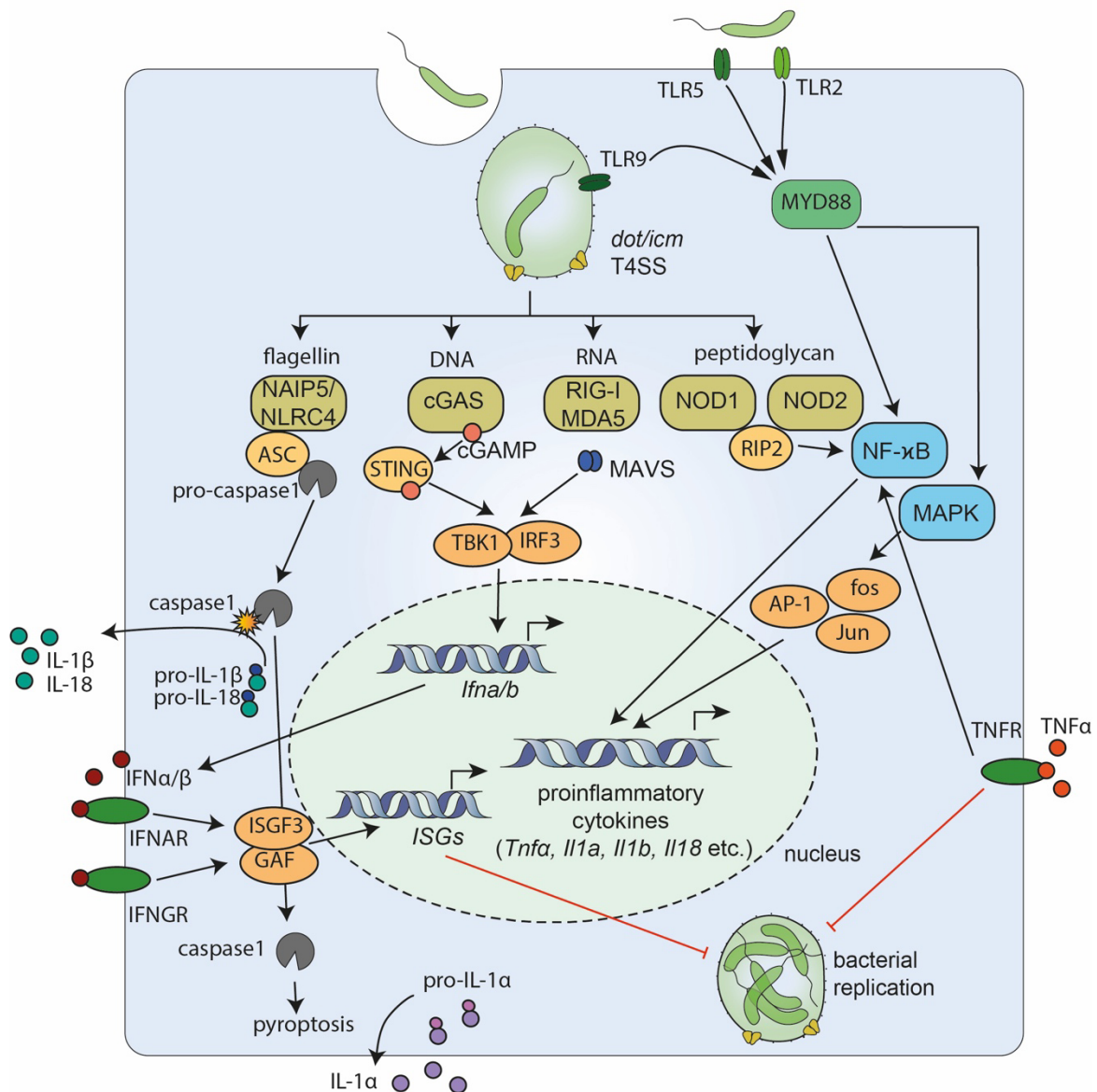


Figure 4) Schematic overview of the immune response in macrophages to infection with *L. pneumophila*. Various PRRs are involved in the recognition of *L. pneumophila* on the cell surface (e.g., by TLR2 and TLR5) and of bacterial components in the cytosol (e.g., by NOD1/NOD2 or cGAS) and activate different intracellular signaling cascades, which mediate the antibacterial defense. See the text for a detailed explanation.

The role of cytosolic nucleic acid detection

The detection of bacterial nucleic acid in the host cytosol is essential for activating the full range of antibacterial defense strategies. *L. pneumophila* DNA is sensed by the cytosolic DNA receptor cGAS, thereby activating the STING-dependent type I IFN response in infected cells via the transcription factor IRF3^{238–241}. It was found that the hypomorphic allelic variation HAQ of the gene *TMEM173* encoding STING leads to an impairment of type I IFN production in *L. pneumophila*-infected human macrophages and is associated

with susceptibility to LD in humans ²⁴¹. Additionally, one study described an involvement of the RNA-binding receptors RIG-I and MDA5 together with their adapter molecule MAVS in the *L. pneumophila*-induced production of type I IFNs ²⁴².

The role of IL-1 family cytokines

The inflammasome-dependent production of IL-1 α and IL-1 β was found to be essential for the control of *L. pneumophila* infection. These cytokines activate non-infected bystander macrophages and recruit and activate PMNs, monocytes, DCs, and non-hematopoietic cells by binding to the IL-1R receptor. Binding to IL-1R enhances the production of proinflammatory cytokines, such as TNF α or IL-12, or of chemokines produced by AECs, such as CXCL1 and CXCL2, which promotes PMN recruitment ^{70,71,235,243,244}. It was found that even though IL-1 α and IL-1 β signal through the same receptor, IL-1 β seems to be less important than IL-1 α for PMN recruitment and bacterial defense *in vivo* ^{70,235}. Furthermore, the inflammasome-dependent release of IL-18 was found to be required for stimulating the production of IFN- γ by NK cells and for bacterial clearance in pulmonary as well as systemic mouse models of *L. pneumophila* infection ^{234,244–246}.

The role of type I and II IFN production

Both type I and II IFNs critically regulate gene expression and induction of cell-intrinsic defense mechanisms in macrophages during infection with *L. pneumophila*. Different studies have shown that defects in type I and II IFN signaling affect the immune response against the pathogen *in vivo* ^{28,238,247}. IFN α and β (type I IFNs) are produced by AMs and bind to the IFN α/β (IFNAR) receptor. The binding of type I IFNs to IFNAR results in the activation of the transcription factor complexes ISGF3 and GAF, which subsequently translocate into the nucleus and induce transcription of a broad variety of IFN-stimulated genes (ISGs) that contribute to bacterial clearance ^{248,249}. On the contrary, IFN γ is not produced by AMs but mainly by resident lymphoid cells. IFN γ binds to the IFN γ receptor (IFNGR) of AMs and stimulates ISG expression in a similar but not the same manner as type I IFNs. ^{214,250–253} Some ISGs encode antimicrobial molecules, e.g., the immune-responsive gene 1 (IRG1), which localizes around the LCV to control the infection. IRG1 catalyzed the production of itaconic acid, a side product of the TCA cycle, which restricts the replication of *L. pneumophila* inside the LCV ^{28,254}.

The role of TNF α

Another cytokine that has been found to play a significant role in the defense against *L. pneumophila* infection in macrophages is TNF α . It was found that patients who receive anti-TNF α therapy have a higher risk of developing LD²⁵⁵⁻²⁵⁷. TNF α is mainly produced by PMNs and monocytes and signals via two receptors on AMs, tumor necrosis factor receptor 1 and 2 (TNFR1/TNFR2), which are suggested to activate different signaling cascades during *L. pneumophila* infection. Whereas TNFR1 signaling seemingly contributes to bacterial clearance in AMs *in vitro* and PMN recruitment, IL-12 production, and bacterial clearance *in vivo*, TNFR2 was found to have a role in restraining excessive inflammation during *L. pneumophila* infection^{255,258}. The detailed mechanism of how TNF α interferes with bacterial replication in infected macrophages is not fully understood, but studies indicate that it contributes to the NAIP5-mediated antibacterial defense^{255,258,259}. Alternatively, it was found that TNF α -induced restriction of *L. pneumophila* via TNFR1 is independent of NLRC4, caspases-1 and 11, and the production of reactive ROS in BMDMs *in vitro*. Instead, *L. pneumophila* clearance seems to be dependent on NF- κ B signaling, the triggering of lysosome acidification and fusion with the LCV, and other caspases^{255,259,260}.

1.3.1. A possible role for CLEC12A in *L. pneumophila* recognition?

Currently, the role of CLEC12A in the recognition of *L. pneumophila* and the induction of innate immune responses during an intracellular infection in macrophages is unknown. Prior to this project, preliminary studies from my lab in collaboration with the group of Prof. Bernd Lepenies (Tierärztliche Hochschule Hannover) investigated the binding of a broad set of various CLRs to *L. pneumophila* wt. As shown in Figure 5, a specific binding of CLEC12A to heat-killed *L. pneumophila* was observed, which was not found for other CLRs tested in this screening assay. The results from this flow cytometry binding assay were the starting point for this project, as they indicate a potential involvement of CLEC12A in the innate immune response to *L. pneumophila* infection. Therefore, this study aimed to investigate further the receptor's role during *L. pneumophila* infection *in vitro* and *in vivo*.

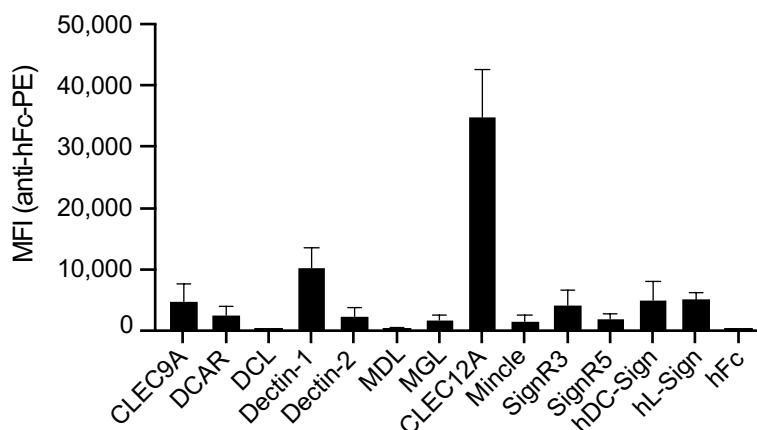


Figure 5) The CLR CLEC12A recognizes and binds *L. pneumophila*. Flow cytometry-based binding study of a comprehensive CLR-Fc fusion protein library to *L. pneumophila* wt strain JR32. A PE-conjugated anti-hFc antibody was used for CLR detection. The results are presented as the mean fluorescence intensities (MFI) (This figure and figure description were adapted and modified from Klatt *et al.* 2023, IJMS ²⁶¹).

1.4. The limited view of current cell culture models into mechanisms of host-pathogen interaction during *L. pneumophila* infection.

AMs have been reported to be the primary host cell type of *L. pneumophila* and serve as niches for intracellular replication for the bacterium ⁵¹. It has been observed that the number of detectable AMs decreases quickly upon infection, potentially due to lysis and egress upon successful replication of the bacterium, as well as to inflammasome-induced pyroptosis ^{50,51}. However, up to date, there is limited knowledge about how tissue-resident AMs respond to an infection with *L. pneumophila*, as it is difficult to isolate these cells in high yield and to maintain a consistent phenotype during *in vitro* cultivation ²⁶². Most studies investigating the *L. pneumophila*–macrophage interaction *in vitro* have been conducted by using culture systems of hematopoietic macrophages, such as murine BMDMs or human peripheral blood monocyte-derived macrophages (PBMCs). The advantage of these cell models is that they are easier to obtain in sufficient numbers for experimental procedures ^{262–264}. Still, these cell-culture systems do not fully reflect the actual situation *in vivo*, as they lack the specific factors provided by the microenvironment within the organism that shapes the phenotype of tissue-resident AMs ^{151,191,265}. Additionally, the embryotic origin of AMs differs from monocyte-derived macrophages that develop from hematopoietic stem cells during adulthood. These differences likely lead to differences in their transcriptome, proteome, and metabolome response to infection ^{187,262,266}. Recently, the cultivation of murine AMs *ex vivo* has been successfully established by various different research groups ^{267,268}, and data

collected in our lab indicate that these cells support replication of *L. pneumophila* (master thesis of L. Hasler, master thesis of L. Boillot, unpublished). However, although these cells exhibit an AM-like transcription profile and are, upon transfer into the lungs of B6 mice, able to efficiently engraft into the pulmonary niche, they differ in some aspects of their metabolomic profile compared to primary AMs^{267,268}. To better understand the mechanisms of how AMs respond to an infection with *L. pneumophila*, it is advisable to investigate the immune response in a suitable *in vivo* model, as done in the presented study.

1.5. Aim of study

The aim of the presented study was to investigate the interaction of *L. pneumophila* with macrophages, its primary host cells, in more depth. While the function of various PRRs, such as TLRs and NLRs, in the innate immune response to *L. pneumophila* has been thoroughly characterized in recent years, the role of CLRs was largely unknown. Based on preliminary data from a screening experiment that indicated specific binding of the CLR CLEC12A to *L. pneumophila*, the first part of the study, therefore, explores the role of this PRR in the interaction of macrophages with the bacterium. The second part focuses on the interaction of *L. pneumophila* with AMs, which differ from hematopoietic macrophages in various aspects such as ontogeny, life cycle, and function. Most studies so far have used hematopoietic macrophages as a cellular model to investigate *Legionella* interaction with host cells, while very little is known about how tissue-resident AMs respond to the infection. The study investigates the transcriptomic and proteomic profile of infected and non-infected AMs isolated from *L. pneumophila*-infected mice using bulk as well as single-cell (sc) RNA sequencing (-seq) and mass spectrometry analysis. The comparative analyses of transcriptome and proteome are of interest not only to understand how AMs respond to *L. pneumophila* infection but also to systematically characterize how the bacterium might interfere with the translation of host proteins as a virulence strategy.

2. Material & Methods

2.1. Bacteria

The bacterial strains used in this study were stored in N-(2-acetamido)-2-aminoethanesulfonic acid (ACES)-buffered yeast extract (AYE) broth (10 g/l ACES buffer, 10 g/l yeast extract, 0.4 g/l cysteine, 0.135 g/l ferric nitrate, pH 6.9) with 50% glycerol at -80°C. The *L. pneumophila* serogroup type I strain JR32 WT, the isogenic mutants *ΔflaA* and *ΔdotA*, and their corresponding strains expressing eGFP from a plasmid were used in this study^{233,269,270}. Bacteria were cultured on buffered charcoal yeast extract (BCYE) agar (AYE broth, 2 g/l activated charcoal, 15 g/l agar) for 3 d. For maintenance of the green fluorescence protein (GFP)-containing plasmid, 5 μg/ml chloramphenicol was added to the cultivation medium. Bacteria from the first streak outs were again plated on BYCE agar and cultivated for 2 d at 37°C and 5% CO₂ before the respective multiplicity of infection (MOI) for each *in vitro* experiment was adjusted in PBS or the respective infection medium. For *in vivo* infection experiments, bacteria from the second plating were inoculated in AYE broth at an optical density (OD)₆₀₀ of 0.01 and grown for 16 h until the culture reached an OD₆₀₀ of 1 (corresponding to 10⁹ CFU/ml). Bacteria cultures were then washed by centrifugation for 10 min at 6,000 x g, and the resulting pellet was adjusted in PBS to the final infection dose indicated in the respective experiments.

2.2. Mice

All animal experiments were approved by the institutional and governmental animal welfare committees. All mice used for infection experiments were on a C57BL/6J background and were 8 to 16 weeks old when included in the *in vivo* infection experiments. *Clec12a*^{-/-} and the corresponding WT control animals were provided by Dr. Bernd Lepenies (Tierärztliche Hochschule Hannover). For infection experiments only including female WT mice, animals were obtained from breeding facilities at Charité or purchased from Charles River Laboratories. Animals of both sexes between the ages of 8 and 35 weeks were used for cell isolation. Upon transfer to the institute's animal unit, mice were kept in ventilated cages at a room temperature of 22°C +/- 2°C and humidity at 55% +/- 5%. A dark/light cycle of 12 h/12 h was maintained. All experiments were approved by the LaGeSo (Landesamt für Gesundheit und Soziales, G0334/17, G0115/21) Berlin.

2.3. *In vivo* methods

2.3.1. Murine *L. pneumophila* infection model

All mice were anesthetized by intraperitoneal (i.p.) injection of narcosis (80 mg/kg ketamine, 25 mg/kg xylazine). Narcotized animals were intranasally infected with a dose of either 1×10^6 , 1×10^7 , or 1×10^8 CFU bacteria suspended in 40 μ l phosphate-buffered saline (PBS). Control mice were equally anesthetized and treated with 40 μ l PBS. At indicated time points, mice were anesthetized (160 mg/kg ketamine, 75 mg/kg xylazine) and sacrificed by final blood withdrawal from the *vena cava*. Blood was collected, and after exsanguination, lungs were either flushed with sterile 0.9% NaCl via the pulmonary artery and removed for further analysis, or bronchoalveolar lavage fluid (BALF) samples were collected. The weight and temperature of all animals were recorded directly before the infection and monitored every 12 or 24 h until the end of the experiment.

2.3.2. Determination of bacterial counts in lung

Lungs were dissected and homogenized using a cell strainer (100 μ m, BD Bioscience). Homogenized lungs were collected in reaction tubes containing 5 or 10 ml RPMI. One ml of the homogenates was lysed with 0.2% Triton X-100 for 10 min to determine bacterial counts, and serial dilutions were plated on BCYE agar plates. Plates were incubated for 3 d at 37°C, 5% CO₂, before assessment of colonies and calculation of the corresponding bacterial load per lung.

2.3.3. Lung digestion for subsequent analysis of cell populations by fluorescence cytometry

Total lungs were dissected and cut into small pieces to investigate cell populations in 24 h infected lungs of WT and *Clec12a*^{-/-} mice. Shredded lungs were weighted, equally split into two parts, and half of the lung was used for flow cytometry analysis, whereas the other half was kept on ice for later analyses of CFU load, protein, and mRNA levels. The shredded lung suspensions were digested by transferring them into a fresh tube containing 5 ml RPMI, supplemented with 2% fetal calf serum (FCS), 0.4 mg/ml DNase, and 1 mg/ml collagenase, and incubated for 40 minutes in a water bath heated to 37°C while shaking. Afterward, digested lungs were vortexed for about 20 sec until they appeared cloudy and were then transferred through a 70 μ m strainer into a fresh tube. The old tube was flushed with 20 to

30 ml of RPMI collected in the new tube. Cell suspensions were then washed by centrifugation for 5 min at 300 x g and 4°C, and the obtained pellet was resuspended in 1 ml of red blood cell lysis buffer (BD Bioscience), quickly vortexed, and incubated at room temperature. After two minutes, lysis was stopped by adding 10 ml of ice-cold PBS, and cells were again washed by centrifugation for 5 min at 300 x g and 4°C. The remaining pellet was resuspended in 1 ml of fluorescence activated cell sorting (FACS) buffer (PBS + 2% FCS) and further processed for fluorescence analysis (see 2.6.2.).

2.3.4. Preparation of lung lysates for cytokine quantification

Proteins from *L. pneumophila*-infected murine lungs were isolated as follows: The second half of the shredded lungs mentioned above (see 2.3.3.) was transferred through a cell strainer into new tubes in 5 ml PBS each. Two ml of each lung suspension were then further processed for protein isolation, and the rest was kept for mRNA isolation (see 2.3.5.) and evaluation of CFU levels (see 2.3.2.). The lung suspensions were centrifuged at 300 g and 4°C for 5 min, and supernatants were discarded. Pellets were resuspended in 150 µl of lysis buffer (see Table 1) and centrifuged at 300 x g, 4°C for 5 min. After centrifugation, supernatants were transferred into new reaction tubes (Eppendorf) and snap-frozen in N₂. Protein samples were stored at -80°C until further analysis (see 2.6.1.).

Table 1) Lysis buffer for protein isolation from whole lung samples

Buffer	Composition
phosphoprotein washing buffer	5 ml sodium orthovanadate 98% (200 mM) 50 ml sodium pyrophosphate (150 mM) 50 ml sodium fluoride 99% (1 M) add 395 ml ddH ₂ O
lysis buffer	810 µl phosphoprotein washing buffer 100 µl Tris-HCL, pH 7.4 (500 mM) 50 µl NP40 (20%) 40 µl complete proteinase inhibitor cocktail (25-fold)

2.3.5. Preparation of lung lysates for evaluation of mRNA-expression

Isolation of mRNA was conducted by centrifuging 2 ml of the homogenized lung suspensions at 300 x g and 4°C for 5 min. Supernatants were discarded, and pellets were resuspended and lysed in 500 µl of TRIzol™ Reagent (Thermo Fisher) under a chemical

hood. The lung lysates were then snap-frozen in N₂ and stored at -80°C until further processing (see 2.7.6.).

2.3.6. Isolation of infected and non-infected bystander leucocytes and AMs from BALF samples of B6 WT mice

BALF samples were collected from mice that were infected with GFP-expressing *L. pneumophila* or treated with PBS after 6 h, 12h, 14 h, and 20 h. After injection of narcosis and exsanguination by cutting the *vena cava*, a cannula was inserted into the trachea of the animals 1 ml of BAL buffer was instilled into the lungs and directly collected. Lungs were flushed 3 more times, and collected cells were pooled for the mice of the same infection groups. Cells were centrifuged for 5 min at 300 x g and 4°C. The resulting pellet was suspended in red blood cell lysis buffer and incubated at room temperature for 2 min. Lysis was stopped with ice-cold PBS, the cells were washed by centrifugation, and pellets were resuspended in 100 µl of FACS buffer. Samples that were subsequently analyzed by bulk RNA sequencing or mass spectrometry were stained with an anti-mouse CD45, anti-mouse Siglec-F, and anti-mouse CD11c antibody as well as Fc-Block (anti-CD16/32) as well as Fixable Viability Dye eFlour® 780 (eBioscience) for 20 min at 4°C in the dark (see Table 3). For samples included in the single-cell RNA sequencing analysis, cells of the same group were hashtagged with TotalSeq™ anti-mouse Hashtags (Biolegend) with an individual barcode sequence that allowed assignment of the cells to the respective infection group after sequencing. Following this, cells were incubated at 4°C for 20 min with the hashtags (see Table 2). After incubation, cells were washed by centrifugation at 300 g, 4°C and 5 min three times and then resuspended in 100 µl of FACS buffer containing an anti-CD45 antibody as well as an Fc-Block (anti-CD16/32) and Fixable Viability Dye eFlour® 780 (eBioscience) and stained for additional 20 min at 4°C in the dark. After staining, all samples were washed with FACS buffer, transferred into fresh 15 ml tubes, and FACS-sorted at a FACS Aria™ II SORP flow cytometer cell sorter (Becton Dickinson) gating for either live AMs (CD45+, Siglec-F+, CD11c+) or live leukocytes (CD45+). GFP positive (GFP+) and GFP negative (GFP-) cells were sorted from these populations. Cell suspension derived from PBS-treated mice, which only contained GFP- cells, were used to define the gate thresholds for GFP+ and GFP- cell fraction. Cells were collected in 0.2% BSA-coated FACS tubes in RPMI containing 20% FCS and directly processed after FACS-Sort for subsequent bulk RNA-seq (see 2.7.1.), mass spectrometry (see 2.7.2.) and sc RNA-seq (see 2.7.3.) analysis.

Table 2) Hashtags for leukocytes

Hashtag	Clone	Barcode
C0301-anti-mouse-hashtag1	M1/42; 30-F11	ACCCACCAGTAAGAC
C0302-anti-mouse-hashtag2	M1/42; 30-F11	GGTCGAGAGCATTCA
C0303-anti-mouse-hashtag3	M1/42; 30-F11	CTTGCCGCATGTCAT
C0304-anti-mouse-hashtag4	M1/42; 30-F11	AAAGCATTCTTCACG
C0306-anti-mouse-hashtag6	M1/42; 30-F11	TATGCTGCCACGGTA

Table 3) Antibodies for FACS-Sort of leukocytes and AMs from BALF samples

Antigen	Marker	Clone	Manufacturer	Dilution Factor
anti-mouse CD45	PE	104	eBioscience	0.2 mg/ml
anti-mouse CD45	PerCP	30-F11	BD Bioscience	0.2 mg/ml
anti-mouse Siglec-F	PE	E50-2440	BD Bioscience	0.2 mg/ml
anti-mouse CD11c	APC	N418	BioLegend	0.2 mg/ml

2.4. Immunofluorescence microscopy

Fluorescence-sorted infected and non-infected murine leukocytes and AMs were washed once by centrifugation at 300 x g, 4°C, and 5 min. Supernatants were discarded, and cells were resuspended in 100 µl RPMI medium + 10% FCS. The total cell suspension was then transferred into an 18-well microscopy slide (Ibidi) and incubated for 3 h at 37°C, 5% CO₂ to allow attachment of the cells. Samples were examined with an LSM 780 microscope (objectives: Plan Apochromat 40×/1.40 oil DIC M27). Images were processed using ZEN 2010 (Zeiss) and ImageJ software (<http://imagej.nih.gov/ij/>).

2.5. Cell culture

2.5.1. BMDM isolation, differentiation, and cultivation

Bone marrow cells from WT and *Clec12a*^{-/-} mice were isolated from the tibia and femur of 8 to 16 week-old mice of both sexes. Bones were washed in 70% ethanol and flushed with IMDM + 10% FCS + 2mM L-Glutamine + 100 U/ml Pen/Strep. The collected cell suspension was passed through a 40 µm cell strainer and centrifuged at 300 x g for 5 min. Red blood cell lysis was performed and bone marrow cells were washed and stored at -150°C

in 10% DMSO. For differentiation into BMDMs, cells were cultivated in BMM growth medium (see Table 4) for 10 days, and fresh medium was added on day 4 of cultivation. Differentiated cells were replated in BMDM replating medium (see Table 4), and 4×10^5 cells/ml were seeded in 48-well plates one day before the experiment.

Table 4) Cultivation and differentiation medium for BMDMs

Medium	Component
BMDM growth medium	RPMI 1640 + 20% FCS + 30% L929 fibroblast supernatant + 4.5 mM L-glutamine + 100 µg/ml Pen/Strep
BMDM differentiation medium	RPMI 1640 + 20% FCS + 30% L929 fibroblast supernatant + 4.5 mM L-glutamine + 100 µg/ml Pen/Strep

2.5.2. Human AM isolation and cultivation

Primary human AMs were kindly provided by the group of Prof. Andreas Hocke (Charité-Universitätsmedizin Berlin). Cells were isolated by repeated perfusion of the human lung tissue (ethics approval Charité EA2/079/13) with Hanks' Balanced Salt Solution (HBSS) as described before ²⁷¹. After isolation, cells were washed by centrifugation for 10 min at room temperature and 200 x g. Supernatants were discarded, and the pellet was resuspended in 5 ml RPMI. Cells were counted with a counting chamber (NanoEntek) and seeded at a density of 1×10^6 cells per well in a 6-well plate format. After 2 h of incubation at 37°C, 5% CO₂, cells were washed with HBSS by centrifugation and seeded in the desired well plate format in RPMI supplemented with 2% FCS, 1% Glutamine, and 1% Pen/Strep. Cells were incubated overnight at 37°C, 5% CO₂, before used for infection experiments.

2.5.3. Cultivation and differentiation of human BLaER1 cell line

Human BLaER1 B-cells were grown in BLaER1 cultivation medium (see Table 5) in a cell culture flask (BD Bioscience), and cells were passaged every 4 days when they reached a confluency of 70 to 80%. Passages between 5 and 30 were used for all experiments. For trans-differentiation into BLaER1-derived macrophages, cells were seeded at a density of 2×10^5 cells into a 48-well plate in BLaER1 differentiation medium (see Table 5) and incubated for 6 days at 37°C, 5% CO₂. After incubation, cells were washed and detached by trypsinization, and the differentiation stage was confirmed via flow cytometry by evaluating

the expression of surface markers CD11b and CD19 (see 2.6.2.). For infection experiments, cells were washed twice with warm PBS and directly infected at the desired MOI.

Table 5) Cultivation and differentiation medium for BLaER1 cells

Medium	Component
BLaER1 cultivation medium	RPMI 1640 + 10% FCS + 100 µg/ml Pen/Strep
BLaER1 differentiation medium	RPMI 1640 + 10% FCS + 100 µg/ml Pen/Strep + 10 ng/ml IL-3 + 10 ng/ml M-CSF + 100 nM β-estradiol

2.5.4. Short-term infection of cells

Murine BMMs, human BLaER1 cells, and human AMs were seeded in 48-well plates and infected with *L. pneumophila* at a MOI of 10. For each *in vitro* infection experiment, an uninfected control was included. Infected cells were centrifuged at 200 x g for 5 min and then incubated for 8 h (gene expression), 12 h, or 18 h (cytokine production) at 37 °C and 5% CO₂, respectively. For the evaluation of gene expression of infected and uninfected cells, supernatants were discarded after incubation, and cells were lysed with RLT lysis buffer (Qiagen). Lysed cells were stored at -20°C, or RNA was directly isolated (see 2.7.6.) to evaluate mRNA expression. To quantify proinflammatory cytokine production, supernatants of infected and uninfected cells were taken off and either stored at -20°C or directly evaluated by ELISA (see 2.6.1).

2.5.5. *In vitro* intracellular replication assays

Murine BMMs, human BLaER1 cells, and human AMs were infected with an MOI 0.1. Bacterial infection suspensions adjusted in infection medium (RPMI + 10% FCS) were added to cells seeded in a well-plate format, centrifuged at 200 x g for 5 min and subsequently incubated at 37°C, 5% CO₂. After 30 min, cells were washed with pre-warmed PBS, and medium supplemented with 50 µg/ml gentamycin was added. After 1 h, cells were again washed twice with pre-warmed PBS, and fresh medium was added, and cells were continuously incubated at 37°C and 5% CO₂. Cell lysis for evaluation of CFU at 2 h, 24 h, 48 h, and 72 h *post infection* (p.i.) was performed by taking of supernatants and adding a 0.1% saponin solution to each well. Cells were incubated at 37°C for 10 min with

the saponine solution and then detached and lysed by vigorous pipetting. Combined CFUs of cell lysate and supernatants were evaluated by plating a defined volume of different serial dilutions on buffered charcoal yeast extract (BCYE) agar.

2.6. Immunological Methods

2.6.1. Enzyme-linked immunosorbent assay

Cytokine levels from homogenized lung lysates of B6 WT and *Clec12a*^{-/-} mice (see 2.3.4.) were measured with LEGENDplex™ Mouse Anti-Virus Response Panel Multi-Analyte Flow Assay Kit (BioLegend). Samples were investigated using a fluorescence cytometer instrument (BD FACS Canto™), and LegendPlex™ software (BioLegend) was used for evaluation.

For quantification of cytokine concentration in supernatants of *in vitro* infected cells (see 2.5.4.), commercially available sandwich ELISA kits were used, according to the manufacturer's instructions. Protein concentrations were determined in a FilterMax F5 Multi-Mode Microplate Reader (Molecular Devices) at 450 nm.

Table 6) Commercial ELISA Kits

Kit	Manufacturer
TNF α Mouse Uncoated ELISA Kit	Thermo Fisher
ELISA MAX™ Deluxe Set Human CXCL10 (IP-10)	BioLegend
IL-1 β Human Uncoated ELISA Kit	Thermo Fisher
TNF α Human Uncoated ELISA Kit	Thermo Fisher

2.6.2. Flow cytometry analysis

For flow cytometry analysis of cell populations in lungs of WT and *Clec12a*^{-/-} mice (see 2.3.3.), cells were collected after lung tissue digestion and red blood cell lysis and resuspended in 1 ml of FACS buffer (PBS + 2% FCS). Cells were counted and adjusted to stain a total number 2×10^6 cells with staining-master-mix, containing the respective antibodies and including a Fc-Block (anti-CD16/32) as well as Fixable Viability Dye eFlour® 780 (eBioscience 1:1000).

To analyze the differentiation stage of cultivated human BLaER1 cells (see 2.5.3.), cells were resuspended in master-mix containing antibodies for human surface marker CD19, as

well as CD11b as well as a Fc-Block (anti-CD16/32). For evaluation of CLEC12A expression in BLaER1-derived monocytes (see 2.7.5.), cells were stained with a human anti-CLEC12A marker.

Staining was performed at 4°C for 20 min in the dark. After staining, cells were washed in FACS buffer three times and resuspended in 150 µl of FACS. Subsequent sample analysis was performed using a fluorescence cytometer instrument (BD FACS Canto™). Data were evaluated with FACS Diva and FlowJo software (version 7.6.5.).

Table 7) Antibodies for flow cytometry analysis

Antigen	Marker	Clone	Manufacturer	Dilution Factor
anti-mouse CD45	FITC	30-F11	BioLegend	0.5 mg/ml
anti-mouse CD11c	APC	N418	BioLegend	0.2 mg/ml
anti-mouse CD11b	BV421	M1/70	BioLegend	0.4 mg/ml
anti-mouse Siglec-F	PE	E50-2440	BD Bioscience	0.2 mg/ml
anti-mouse Ly6C	PerCp	HK1.4	BioLegend	0.2 mg/ml
anti-mouse Ly6G	BV510	1A8	BioLegend	0.2 mg/ml
anti-human CD19	BV421	REA675	Milteny	0.2 mg/ml
anti-human CD11b	APC	REA713	Milteny	0.2 mg/ml
anti-human CLEC12A	PE	REA431	Milteny	0.2 mg/ml

2.7. Molecular Biology Methods

2.7.1. Preparation and processing of samples for bulk RNA-seq analysis of *in vivo* infected and uninfected AMs

Fluorescence-sorted infected and non-infected murine AMs, as well as AMs isolated from PBS-treated mice, were washed by centrifugation at 300 x g, 4°C, and 5 min. Supernatants were discarded, cell pellets were resuspended in 100 µl PBS, and cell number was evaluated for each FACS sorted sample group. Cell numbers were adjusted to correspond to 20,000 cells per group, centrifuged again, and resuspended in 100 µl Trizol. Samples were stored at -80°C until further procession. RNA isolation from samples was performed using the Direct-zol RNA Microprep Kit (Zymo Research), following the manufacturer's instructions. Further procession of samples, including evaluation of RNA concentration by Qubit™, quality checks via TapeStation (Agilent), and sequencing of RNA libraries on a NovaSeq

6000 S4 flowcell type with 100 cycles targeting 400 million reads, was performed by the MDC-BIMSB | BIH Genomics facility. The bioinformatic data quality assessment and analysis were performed in collaboration with Dr. Miha Milek from the Core Unit Bioinformatics, Berlin Institute of Health at Charité, Berlin, Germany.

2.7.2. Preparation and processing of samples for mass spectrometry analysis of *in vivo* infected and uninfected AMs

For downstream proteomic analysis, infected and non-infected AMs and AMs isolated from PBS-treated mice were FACS-sorted in PBS with 2% FCS. Directly after the sort, cells were washed by centrifugation at 300 x g, 4°C, and 5 min twice, and pellets were resuspended in 100 µl PBS and counted in a Neubauer Chamber. Cell numbers were adjusted for 50,000 cells per replicon and resuspended in protein lysis buffer (see Table 8). Additionally, proteins were extracted from a murine BMDM sample, comprised of 1 million cells (referred to as “booster reference”), to increase the coverage of protein identification and quantification during subsequential mass-spectrometry analysis. Downstream processing of the samples and mass-spectrometry analysis was performed by Dr. Marieluse Kirchner from the BIH Core Unit Proteomics. The bioinformatics data quality assessment and analysis were performed in collaboration with Dr. Marieluse Kirchner and Dr. Miha Milek from the Core Unit Bioinformatics, Berlin Institute of Health at Charité, Berlin, Germany.

Table 8) Protein lysis buffer for protein isolation from AMs

Buffer	Components
protein lysis buffer	1% SDC (sodium deoxycholate) in 100 mM Tris pH 8 + 1mM EDTA + 150 mM NaCl + 10 mM DTT (Dithiothreitol) + 40 mM iodoacetamide + phosphatase Inhibitors (Sigma Phosphatase Inhibitor Cocktail 2 and 3, 1:100)

2.7.3. Preparation and processing of samples for sc RNA-seq analysis of *in vivo* infected and uninfected leucocytes

Hashtagged and FACS-sorted single-cell suspensions were counted and pooled to 50,000 cells per group. Libraries for each experimental group were generated using the Chromium Single Cell 5' (v2) Reagent Kit (10x Genomics), following the manufacturer's instructions. The generated libraries were sequenced on a NovaSeq 6000 S4 flowcell type with 200 cycles and 30,000 cells per lane and 2 lanes in total, targeting 750 million reads/lane. Quality control, as well as bioinformatical analysis of data were performed by Ivo Röwekamp (Charité-Universitätsmedizin Berlin).

2.7.4. Generation of a BLaER1 *CLEC12A*^{-/-} cell line

A BLaER1 *CLEC12A*^{-/-} cell line was generated using the P3 Primary Cell 4D-Nucleofector™ x Kit S (Lonza). 2.0 x 10⁶ BLaER1 WT cells were used for nucleofection and resuspended in nucleofection buffer P3. The CAS9 enzyme and the specific guide RNA (GCTGGACGCCATACATGAGA) (IDT, IA, USA) were assembled *in vitro* following the instructions of the manufacturer, and the ribonucleoprotein was mixed with the cells followed by electroporation in a 4-D nucleofector (Lonza) in program EH-140. Electroporated cells were collected in prewarmed BLaER1 cell cultivation medium and incubated at 37°C and 5 % CO₂ for 72 h. Single cells were sorted by flow cytometry and expanded in a 96-well plate.

2.7.5. Screening for BLaER1 *CLEC12A*^{-/-} clones

Screening for Insertion and Deletion (InDel) mutations was done by extracting DNA from 10⁵ cells of each clone and performing PCR, followed by Sanger sequencing. The sequence of the primers used for PCR and subsequent Sanger sequencing were as follows: TGACATGCCACAATTGTCTACTCA (forward-primer) and TTGCCAAGACTCCCAATCCAA (reverse-primer). Sanger sequences of the respective clones were analyzed via the TIDE sequencing analyzer tool (<https://tide.nki.nl>). Cells were transdifferentiated (see 2.5.3.) to confirm the loss-of-function mutation in BLaER1 clones via flow cytometry (see 2.6.2.). Undifferentiated BLaER1 cells of positive clones were further cultivated and expanded for infection experiments.

2.7.6. Isolation of total RNA and cDNA synthesis

Total RNA was isolated from murine lung homogenates using Trizol, followed by phenol-chloroform extraction. For murine as well as human *in vitro* and *ex vivo* cultivated cells, the RNeasy Kit from QIAGEN was used according to the manufacturer's protocol. Isolated RNA was evaluated via Nano-Drop and reverse-transcribed into cDNA, following the instructions of the high-capacity reverse transcription (HCRT) kit (Applied Biosystems).

2.7.7. Quantitative real-time PCR

Quantitative gene expression from cDNA was evaluated by quantitative real-time PCR (qPCR). Upon RNA isolation and cDNA synthesis (see 2.7.6.), 10-100 ng of template were added to the master mix containing Taq buffer and specific TaqMan assays (Thermo Fisher; see Table 9). Measurements were performed on a qTOWER³ G instrument (Analytic Jena AG). The input was normalized to the average expression of murine and human GAPDH, and the relative expression (relative quantity, RQ) of the respective gene in untreated cells or PBS-treated mice was set as 1.

Table 9) TaqMan assays

Assay	ID	Manufacturer
<i>mIfnb1</i>	Mm00439552_s1	Thermo Fisher
<i>mGAPDH</i>	Mm00439552_s1	Thermo Fisher
<i>mATF3</i>	Mm00476033_m1	Thermo Fisher
<i>mGDF15</i>	Mm00442228_m1	Thermo Fisher
<i>mTnf</i>	Mm00443258_m1	Thermo Fisher
<i>mIl1b</i>	Mm00434228_m1	Thermo Fisher
<i>mCdkn1b</i>	Mm00438168_m1	Thermo Fisher
<i>mIrf1</i>	Mm01288580_m1	Thermo Fisher
<i>mFdft1</i>	Mm01598574_g1	Thermo Fisher
<i>hCLEC12A</i>	Hs00370621_m1	Thermo Fisher
<i>hIFNB1</i>	Hs01077958_s1	Thermo Fisher
<i>hIL1B</i>	Hs01555410_m1	Thermo Fisher
<i>hTNFA</i>	Hs00174128_m1	Thermo Fisher
<i>hGAPDH</i>	Hs02786624_g1	Thermo Fisher

2.8. Statistical analysis

All experiments were performed without randomization and conducted in an unblinded fashion. Statistical analysis of the data was performed using GraphPad Prism software or R-Studio. Data points were, if not specified otherwise, presented as mean \pm SD. A two-way ANOVA followed by a Bonferroni posttest and a Man-Whitney U test, or a multiple paired t-test was used to compare and evaluate significant differences between groups. Thresholds for significance were defined as $p_{\text{adj}} \leq 0.05$. Bioinformatic analysis of sequencing and proteome data was conducted by Dr. Miha Milek, Dr. Marieluise Kirchner, and Ivo Röwekamp. Thresholds for significance of sequencing and mass spectrometry data were defined as $p_{\text{adj}} \leq 0.05$.

2.9. Materials

Table 10) Chemicals

Chemicals	Company
ACES	Sigma-Aldrich
activated charcoal	Roth
agar	NeoFroxx
Ampuwa® (RNase-free H ₂ O)	Fresenius Kabi
BSA	Sigma-Aldrich
chloramphenicol	Sigma-Aldrich
chloroform	Merck
complete proteinase inhibitor cocktail tablets	Roche Diagnostics GmbH
cystein	Sigma
DMSO	Sigma-Aldrich
dithiothreitol	Thermo Fisher Scientific
EDTA	Roth
EGTA	Sigma-Aldrich
ethanol	Merck
FCS	CAPRICORN Scientific
ferric nitrate	Sigma-Aldrich
gentamycin	Cytogen GmbH
glutamine	Gibco
glycerol	Merck
HBSS	Gibco
iodoacetamid	Thermo Fisher Scientific
isopropanol	Sigma-Aldrich
IL-3	PreproTech
ketamine	Sigma-Aldrich
M-CSF	PreproTech
NaCl (0.9%)	B. Braun
NP40	Roth
PBS	Gibco
penicillin/streptomycin	PAA
RLT lysis buffer	Qiagen
RPMI 1640	Gibco

saponine	Sigma-Aldrich
sodium deoxycholate	Thermo Fisher Scientific
sigma phosphatase inhibitor cocktail 2 and 3	Sigma-Aldrich
sodium fluoride	Sigma
sodium orthovanadate	Sigma
sodium pyrophosphate	Sigma
Thilo Tears® Gel	Novartis Pharma GmbH
tris-HCL	Roth
Triton X-100	Sigma-Aldrich
TRIzol™	Thermo Fisher Scientific
trypsin-EDTA	Gibco
xylazine	Bayer
yeast extract	BD Bioscience
β-estradiol	PeptoTech
β-mercaptoethanol	Sigma

Table 11) Enzymes

Enzyme	Company
Cas9	IDT
collagenase type III	Worthington-Biochemical
DNase	Sigma
reverse transkriptase	New England Biolabs
Taq-B DNA polymerase	New England Biolabs

Table 12) Commercial Kits

Kit	Company
Chromium Single Cell 5' (v2) Reagent Kit	10x Genomics
Direct-zol RNA Microprep Kit	Zymo Research
High Capacity Reverse Transcriptio Kit (HCRT)	Applied Biosystems
LEGENDplex™ Mouse Anti-Virus Response Panel	BioLegend
Multi-Analyte Flow Assay Kit	
P3 Primary Cell 4D-Nucleofector™ x Kit S	Lonza
RNeasy Mini Kit	Qiagen

Table 13) Consumables

Consumable	Company
0.2 µm filters	BD Bioscience
cell culture flasks	BD Bioscience
cell culture plates (6-well, 24-well, 48-well, 96-well)	Falcon
cell culture tubes (15 ml, 50 ml)	Falcon
cell strainers (40 µm, 70 µm, 100 µm)	Greiner Bio-One
cuvettes	Sarstedt
ELISA-plates (96-well)	Corning
FACS-tube	Sarstedt
inoculation loops	Sarstedt
C-Chip neubauer chamber	NanoEntek
petri dish	BD Bioscience
reaction tubes (0.5 ml, 1.5 ml, 2 ml)	Eppendorf
serological pipets	Thermo Scientific
Sterican® canula	B. Braun
syringes (1 ml, 5 ml, 10 ml)	BD Bioscience
µ-slide 18-well	Ibidi

Table 14) Instruments

Instrument	Company
4-D nucleofector	Lonza
BD FACS Canto™	BD Bioscience
FACS Aria™ II SORP flow cytometer cell sorter	Becton Dickinson
FilterMax F5 Multi-Mode Microplate Reader	Molecular Devices
Haereus Typ BB 6220 CO ₂ Incubator	Thermo Scientific
Heraeus Biofuge Fresco	Thermo Scientific
Heraeus Typ HS 18 safety bench	Thermo Scientific
Heraeus Typ HS 9 safety bench	Thermo Scientific
Herasafe™ KS safety bench	Thermo Scientific
LSM 780 microscope	Zeiss
Mastercycler Gradient	Eppendorf
NanoDrop 2000	Thermo Scientific

photometer	Eppendorf
pipetboy	Integra Biosciences AG
pipets (10 μ l, 20 μ l, 100 μ l, 200 μ l, 1000 μ l)	Eppendorf
qTOWER ³ G	Analytic Jena
Qubit TM Tapestation	Agilent
Rotanta 460 R	Hettich
SW23 water bath	Julabo GmbH

3. Results

3.1. The role of CLEC12A in the immune response to *L. pneumophila* infection

The first part of the thesis aimed to investigate the potential role of the CLR CLEC12A in the context of infection with the intracellular pathogen *L. pneumophila*. By using a murine *in vivo* model, as well as examining the immune response in murine and human WT and CLEC12A-deficient macrophages, the impact of the receptor on *L. pneumophila*-induced inflammation was examined more in-depth. The results from this study were published in Klatt *et al.*, (2023), IJMS ²⁶¹.

3.1.1. The CLR CLEC12A has no significant role during pulmonary *L. pneumophila* infection *in vivo*

Preliminary flow cytometry-based binding studies have shown that the murine receptor CLEC12A binds specifically to *L. pneumophila*, indicating its possible role in the immune response to *L. pneumophila* infection (see 1.3.1). Therefore, I first investigated if the receptor CLEC12A impacts the immune response against *L. pneumophila in vivo*. B6 WT and *Clec12a*^{-/-} mice were intranasally infected with 10⁶ CFU *L. pneumophila* for 24 h, 48 h, and 96 h. During the infection, the body weight and temperature of mice were monitored every 12 h. After sacrificing mice at the indicated endpoints of the experiment, the bacterial burden from whole lungs was assessed. As shown in Figure 6A, no significant differences in CFUs were observed, but a trend towards lower bacterial loads in the lungs of CLEC12A-deficient animals at both 48 h ($p_{\text{adj-value}} = 0.063$) and 96 h ($p_{\text{adj-value}} = 0.096$) after infection. Likewise, the body weight and temperature did not differ significantly between WT and *Clec12a*^{-/-} mice throughout the experiment (see Figure 6B, C).

In addition to CFU loads, gene expression and proinflammatory cytokine levels in the lungs were evaluated 24 h p.i. with *L. pneumophila*. A qPCR analysis was performed to measure mRNA levels of *Ifnb1*, whereas the results suggest no difference in expression levels in the lungs of WT and *Clec12a*^{-/-} mice (see Figure 6D). Further, ELISA assays were conducted to quantify IFN γ , TNF α , and IL-6 (see Figure 6E, F, G). None of these cytokines were found to be significantly influenced by CLEC12A deficiency in the lungs of mice.

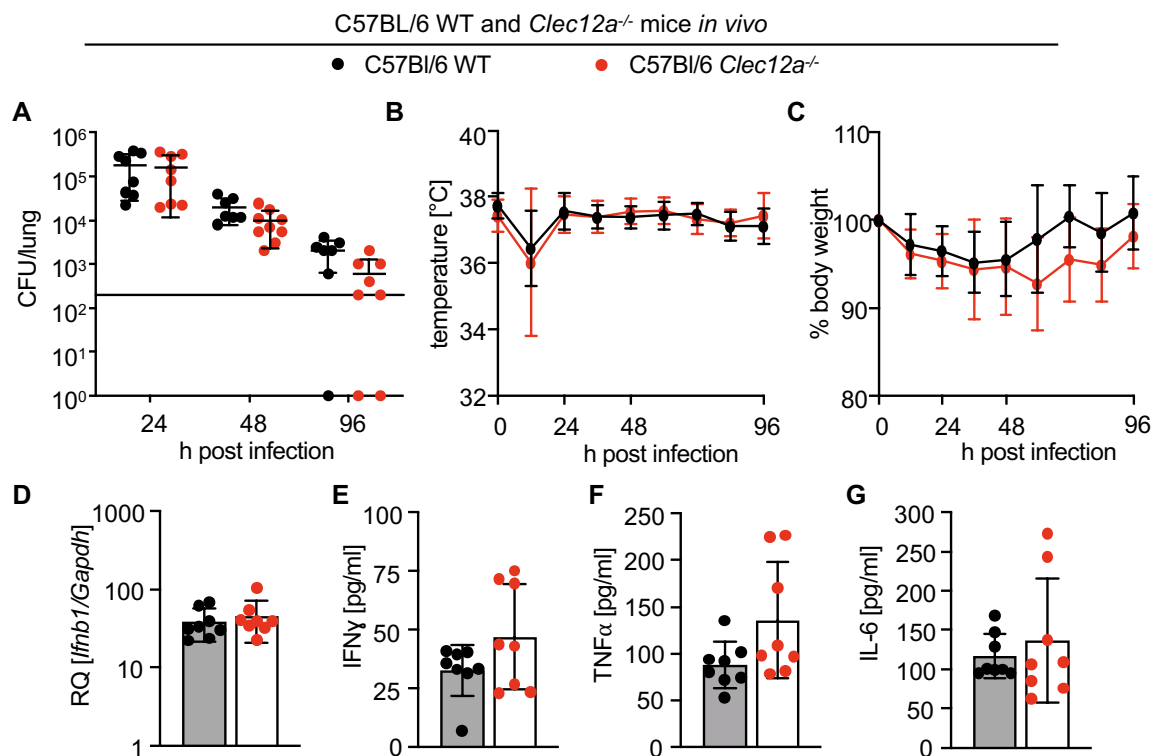


Figure 6) CLEC12A plays a limited role in *L. pneumophila* lung infection in mice. WT and *Clec12a*^{-/-} C57BL/6 mice (8 mice per group and time point respectively) were infected with *L. pneumophila* at a dose of 10^6 CFU / mouse and (A) bacterial loads from their lungs were assessed at 24, 48 and 96 h post infection by plating serial dilutions of homogenized lungs on BYCE agar. (B, C) Infected WT and *Clec12a*^{-/-} C57BL/6 mice were monitored for their temperature and body weight over the course of the respective infection experiment. (D) *Ifnb1* expression in homogenized murine lungs 24 h after infection were assessed by qPCR and normalized to lungs of PBS-treated WT mice. (E, F, G) Levels of IFN γ , TNF α and IL-6 in mouse lungs were measured 24 h after infection. All data represent means \pm SD of 2 independent experiments with 4 mice per experiment. Differences were assessed using a two-way ANOVA and the Mann-Whitney U Test. Comparisons with a $p_{adj} < 0.05$ were considered significant. This figure and figure description were similarly published and taken from Klatt *et al.* (2023), IJMS ²⁶¹ with permission of MDPI.

Finally, the composition of cell populations, known to be involved in the immune response against *L. pneumophila*, was investigated for the lungs of 24 h infected WT and *Clec12a*^{-/-} animals ^{50,51}. A flow cytometry analysis of single-cell suspensions of lung homogenates was conducted (see Figure 7A), and the ratio (see Figure 7B, C, D) and the number (see Figure 7E, F, G) of AMs, iMonos, and PMNs were calculated. As in the previous experiments, no differences between WT and *Clec12a*^{-/-} animals were found. Overall, the results obtained from the *in vivo* study suggest that CLEC12A does not substantially impact pulmonary *L. pneumophila* infection in mice.

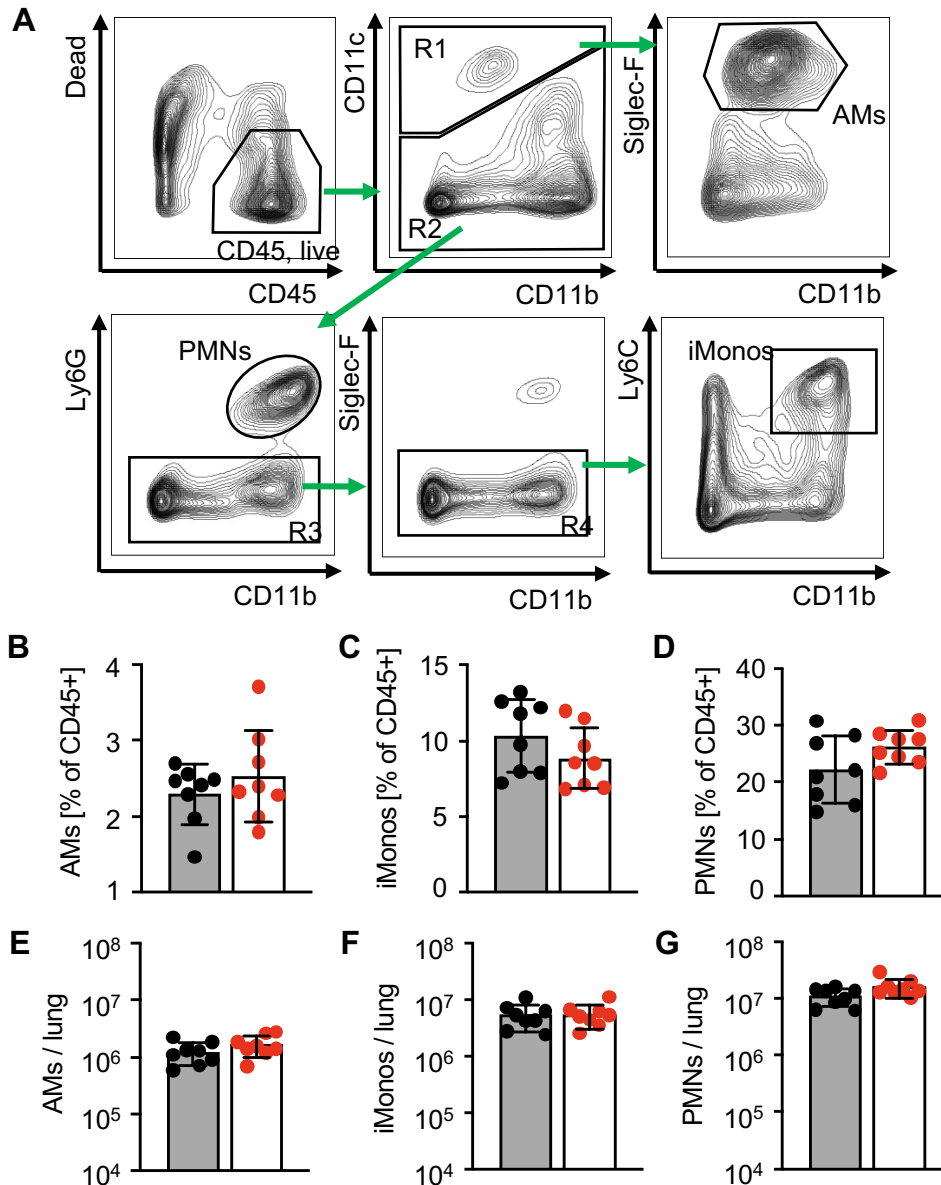
C57BL/6 WT and *Clec12a*^{-/-} mice *in vivo*● C57BL/6 WT ● C57BL/6 *Clec12a*^{-/-}

Figure 7) Cell composition of immune cell population does not differ between *L. pneumophila*-infected WT and *Clec12a*^{-/-} animals 24 h p.i. (A) Representative flow cytometric analyses of AMs (CD45⁺, CD11c⁺, CD11b⁻, Siglec-F⁺), iMonos (CD45⁺, CD11c⁻, CD11b⁺, Ly6C⁺) and PMNs (CD45⁺, CD11c⁻, CD11b⁺, Ly6G⁺). (B - G) Percentages and numbers of AMs, iMonos and PMNs in the lungs of WT and *Clec12a*^{-/-} mice 24 h after infection. All data represent means \pm SD of 2 independent experiments with 4 mice per experiment. Differences were assessed using a Mann-Whitney U Test. Comparisons with a $p < 0.05$ were considered significant. This figure and figure description was similarly published and taken from Klatt *et al.* (2023), IJMS²⁶¹ with permission of MDPI.

3.1.2. CLEC12A does neither affect *L. pneumophila* replication, nor infection-induced cytokine response in murine macrophages

Next, BMs were isolated from B6 WT and CLEC12A-deficient mice, differentiated into BMDMs, and subsequently infected with *L. pneumophila* at different MOIs. The *L. pneumophila* JR32 WT strain, as well as the flagellin-deficient mutant $\Delta flaA$, were used in this study. While it has been demonstrated that the NAIP5/NLRC4 inflammasome usually restricts the growth of the WT strain due to recognition and activation of bacterial flagellin secreted from the LCV, the $\Delta flaA$ mutant is supposed to replicate stronger and cause a substantial infection in cells^{229,272}. BMDMs were first infected with an MOI of 0.1, and intracellular replication of $\Delta flaA$ was assessed over 72h.

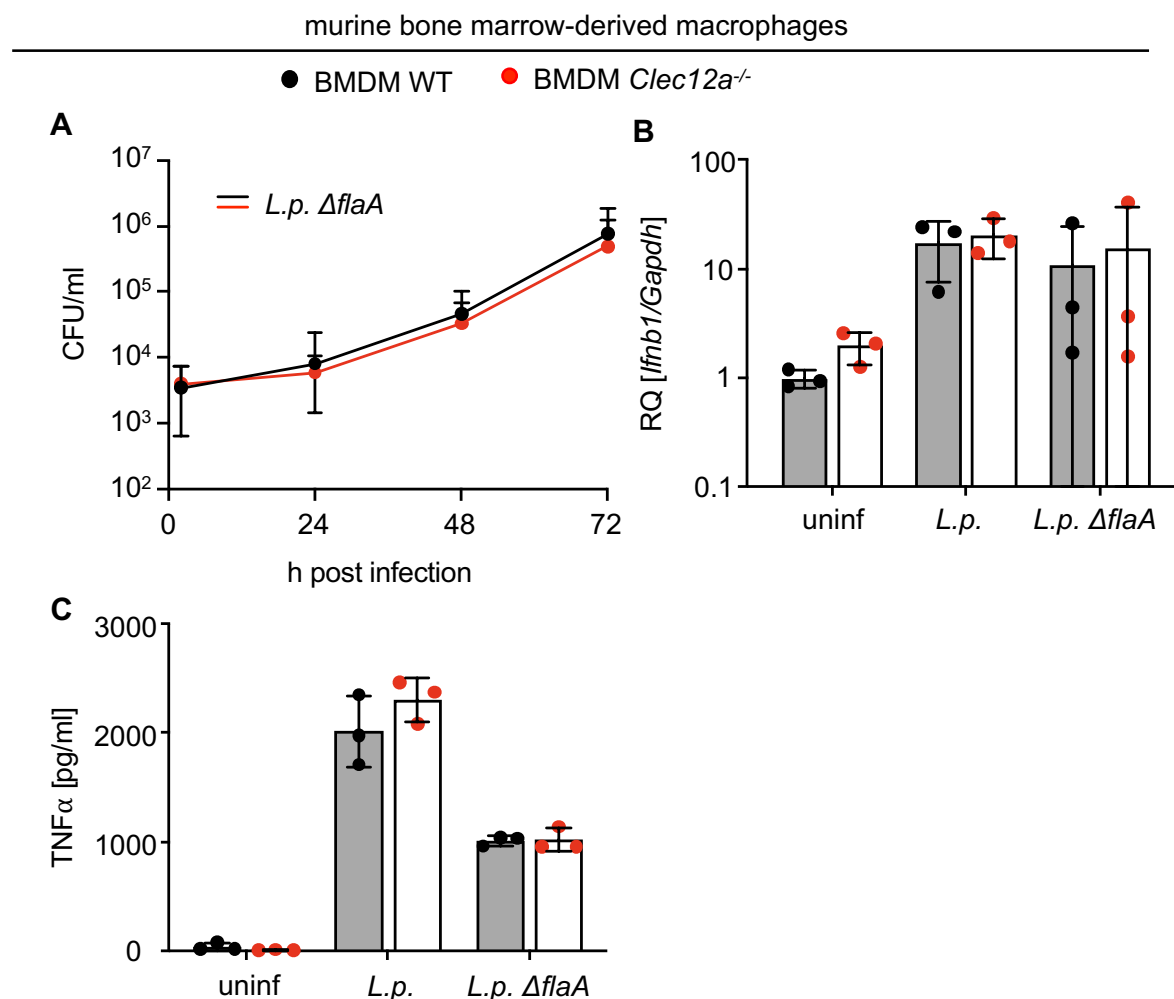


Figure 8) *L. pneumophila* replication in murine BMDMs as well as type I IFN response and TNFα production are not influenced by CLEC12A. (A) WT and *Clec12a*^{-/-} BMDMs were infected with *L. pneumophila ΔflaA* at MOI 0.1 and replication was assessed by evaluating CFUs in cells and supernatants after 2, 24, 48 and 72 h. (B, C) WT and *Clec12a*^{-/-} BMDMs were infected with *L. pneumophila* JR32 (*L.p.*) or $\Delta flaA$ at MOI 10, and *Ifnb1* expression was evaluated 8 h post infection by qPCR, or TNFα levels were quantified from supernatants after 18 h. All data represent mean ±

SD of 3 independent experiments carried out in triplicates. Differences were assessed using a multiple paired t-test. Comparisons with a $p < 0.05$ were considered significant. This figure and figure description were published and taken from Klatt *et al* (2023), IJMS ²⁶¹ with permission of MDPI.

3.1.3. Infection with *L. pneumophila* in BLaER1-derived macrophages indicates no role of CLEC12A in the immune response in human macrophages

Finally, the role of the receptor CLEC12A during *L. pneumophila* infection in human cells was evaluated. To this end, BLaER1-derived macrophage-like cells were first investigated for their suitability as a human cell culture model to study *L. pneumophila* infection. Cells of the immortalized B cell line BLaER1 can transdifferentiate into BLaER1-derived macrophages by inducing overexpression of the myeloid transcription factor C/EBP α (see Figure 9A) ²⁷³. This overexpression is achieved by stimulating cells in culture with the steroid hormone β -estradiol and the cytokines IL-3 and M-CSF for five to seven days ²⁷⁴. Transdifferentiated BLaER1 macrophages show similar traits as primary macrophages, as they are adherent and non-proliferative while maintaining a highly phagocytotic activity and a macrophage-like transcriptional profile ²⁷⁴. Additionally, they resemble multiple innate immune signaling pathways regarding their sensitivity and outcome to a greater extent than other commonly used cell lines such as THP1 and U937 ^{274,275}.

BLaER1-derived macrophages were first infected with a MOI of 0.1, and bacteria replication was compared to human AMs. The results demonstrated that *L. pneumophila* replicates equally in BLaER1-derived macrophages and human *ex vivo* AMs (see Figure 9B). It was further shown that BLaER1-derived macrophages and human AMs express *CLEC12A* similarly (see Figure 9C). It was concluded that BLaER1-derived macrophages serve as a suitable cell line culture model to study the immune response against *L. pneumophila* and the role of the receptor CLEC12A in this context more in-depth.

To this end, a BLaER1 *CLEC12A*^{-/-} cell line was constructed using the CRISPR/Cas9 technology that allowed the introduction of a frameshift of 1 bp in *CLEC12A* (see Figure 9D). Loss of the receptor was confirmed by flow cytometry analysis with a PE-labelled antibody for human CLEC12A (see Figure 9E).

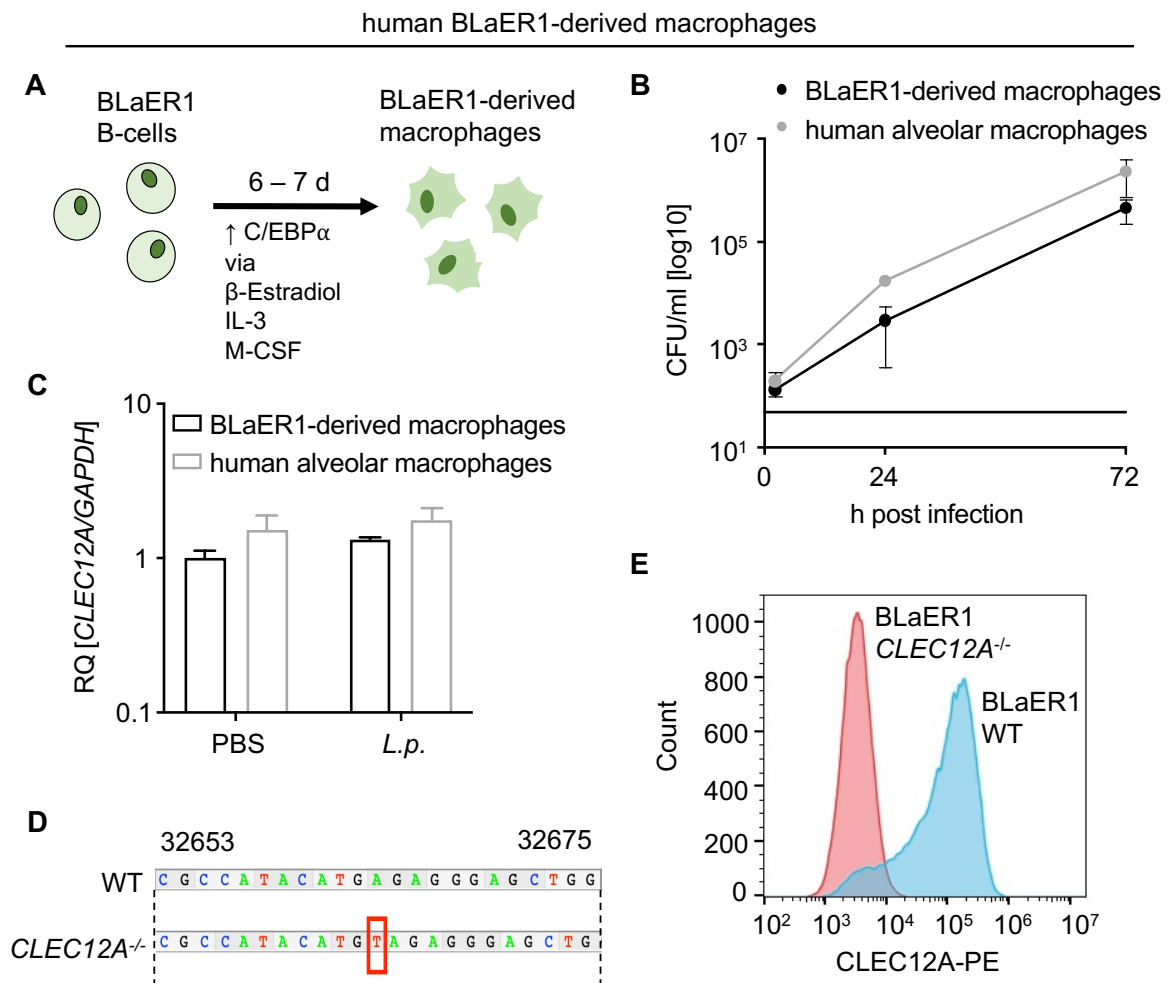


Figure 9) BLaER1-derived macrophages allow intracellular replication of *L. pneumophila* and express CLEC12A to a similar extent as *ex vivo* cultivated human AMs. (A) BLaER1 cells were transdifferentiated into BLaER1-derived macrophages by stimulation of the transcription factor C/EBP α with β -estradiol, IL-3, and M-CSF for 6 to 7 days. (B) *L. pneumophila* shows similar replication in BLaER1-derived macrophages and human AMs and (C) similar relative expression levels of *CLEC12A* in BLaER1-derived macrophages and human AMs was measured upon *L. pneumophila* infection. Data represent the mean \pm SD of 2–3 independent experiments carried out in triplicates. Differences were assessed using a multiple paired t-test. Comparisons with a $p < 0.05$ were considered significant. (D) BLaER1 *CLEC12A*^{-/-} cells were generated by introducing a frameshift of one base into *CLEC12A* (see red box) by CRISPR/Cas9. (E) The loss of CLEC12A in BLaER1 cells was confirmed by flow cytometry, using an anti-CLEC12A-PE labelled antibody. This figure and figure description were similarly published and taken from Klatt *et al.* (2023), IJMS²⁶¹ with permission of MDPI.

Next, bacterial replication of *L. pneumophila* and cytokine production in response to infection was assessed in BLaER1 WT and *CLEC12A*^{-/-} cells.

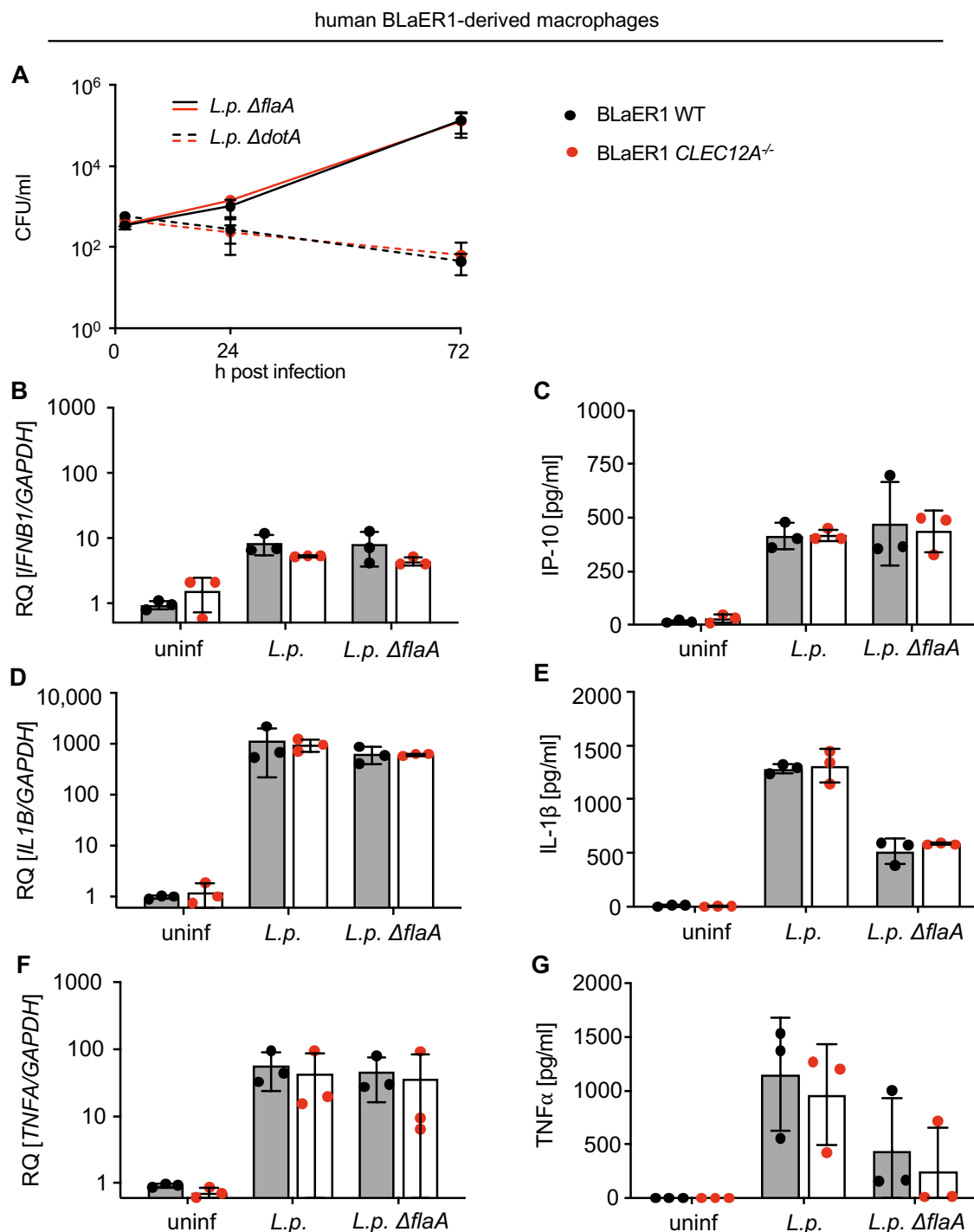


Figure 10) CLEC12A does not impact replication of *L. pneumophila* nor immune response in human BLaER1-derived macrophages. (A) Replication of *L. pneumophila* (*L.p.*) $\Delta flaA$ and $\Delta dotA$ in BLaER1 WT and *CLEC12A*^{-/-} cells was assessed after infecting cells at MOI 0.1 and evaluating CFUs at 2, 24 and 72 h post infection. Next, BLaER1 WT and *CLEC12A*^{-/-} cells were infected with *L. p.* WT and $\Delta flaA$ at MOI 10 and expression of *IFNB1* (B), *IL1B* (D) and *TNFA* (F) was measured after 8 h by qPCR and compared to uninfected controls. Data are shown as relative quantification (RQ) of the target mRNAs relative to *GAPDH*. Production of IP-10 (CXCL10) (C), IL-1β (E) and TNFα (G) was measured in supernatants of infected BLaER1 WT and *CLEC12A*^{-/-} cells after 18 h. All data represent the mean ± SD of 3 independent experiments carried out in triplicates. Differences were assessed using a multiple paired t-test. Comparisons with a $p < 0.05$ were considered significant.

This figure and figure description were similarly published and taken from Klatt et al (2023), IJMS ²⁶¹ with permission of MDPI.

CFUs from cells infected with *AflaA* and *ΔdotA* at an MOI of 0.1 were evaluated after 2 h, 24 h, and 72 h. The *ΔdotA* strain used in this study is a non-replicative and avirulent strain of *L. pneumophila*, as it carries a mutation disrupting the expression of the *dot/icm* genes required to express a functional T4SS ^{24,35}. Evaluating bacterial burdens from cells and supernatants revealed no difference between WT and *CLEC12A*^{-/-} cells (see Figure 10A). For evaluation of cytokine production, WT and *CLEC12A*^{-/-} cells were infected with an MOI of 10 and expression of *IFNB1*, *IL1B*, and *TNFA* mRNA (see Figure 10B, D, F) and production of IFN-inducible cytokine IP-10, IL-1β and TNFα (see Figure 10C, E, G) were evaluated by qPCR after 8 h and ELISA after 18 h, respectively. *CLEC12A* deficiency did not affect gene expression or cytokine production. Thus, the results do not support the hypothesis that human *CLEC12A* significantly impacts the immune response to *L. pneumophila* infection.

3.2. Investigating the innate immune response of AMs to *L. pneumophila* infection

The second part of this thesis focused on investigating the response of AMs to an infection with *L. pneumophila in vivo*. B6 WT mice were intranasally infected with 10⁸ CFU GFP-expressing *L. pneumophila* JR32 *AflaA* (virulent) or *ΔdotA* (avirulent). A control group of mice was intranasally mock-treated with PBS. After 12 to 14 h, BALF samples of infected mice were collected, pooled within the respective groups, and FACS-sorted to discriminate between infected, bystander (non-infected), and mock-infected (uninfected) AMs (Siglec-F⁺ and CD11c⁺) based on the internalized bacterial GFP signal. This experimental approach was used to (i) collect RNA samples, as well as (ii) total proteins from FACS-sorted cell populations to perform a bulk RNA-seq and a mass spectrometry analysis, respectively. The selected approach allowed me to investigate the response of AMs to *L. pneumophila* infection on transcriptome and proteome levels (see Figure 11).

FACS-sorted AMs from murine BALF samples 12 -14 h p.i.

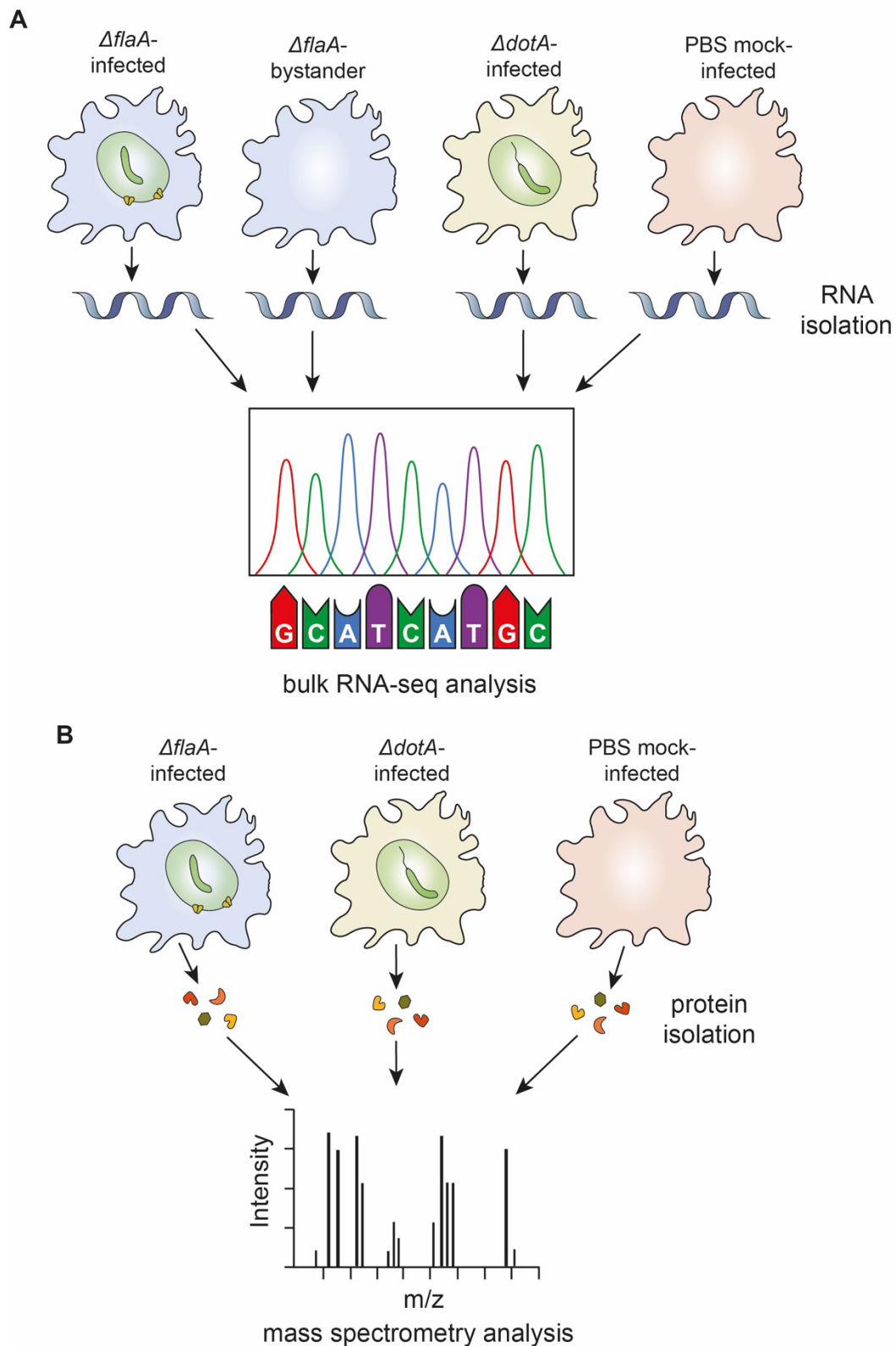


Figure 11) The immune response of AMs to infection with *L. pneumophila* was investigated on the transcriptional and proteome level. FACS-sorted AMs collected from BALF samples of $\Delta flaA$ - and $\Delta dotA$ -infected, as well as PBS mock-treated mice, were further processed to investigate the (A) transcriptomic and (B) proteomic response to the infection by performing bulk RNA-seq and mass spectrometry analysis, respectively.

3.2.1. GFP-expressing *L. pneumophila* allow discrimination of infected and non-infected bystander AMs from BALF samples

To set up the experiment, first, the applicability of the *in vivo* model was tested to confirm that the FACS sort of BALF samples allowed for clean discrimination of *L. pneumophila* JR32 $\Delta flaA$ - or $\Delta dotA$ -infected AMs and corresponding bystander cells. To this end, FACS-sorted AM populations were evaluated by fluorescence microscopy (see Figure 12A - C).

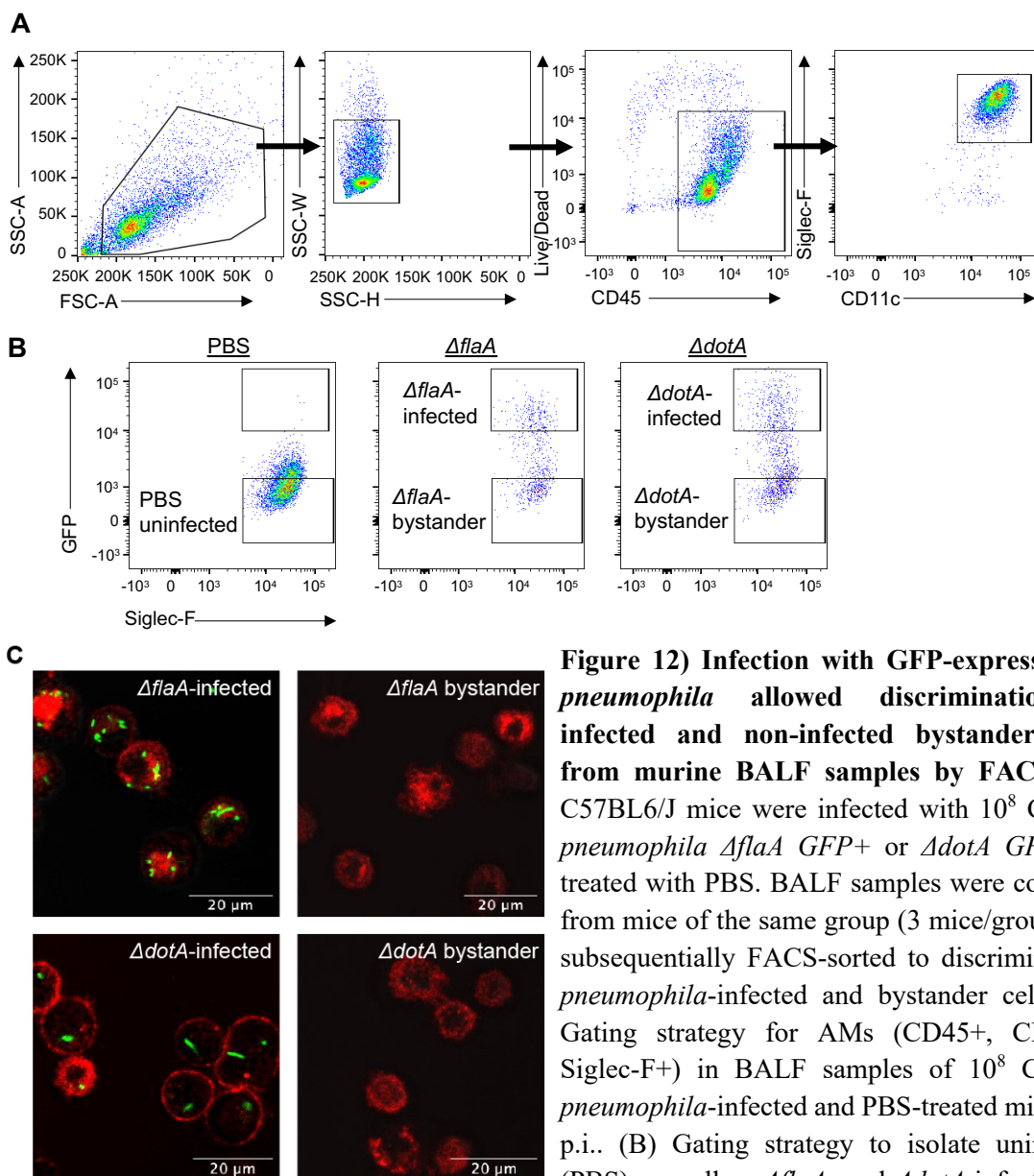


Figure 12) Infection with GFP-expressing *L. pneumophila* allowed discrimination of infected and non-infected bystander AMs from murine BALF samples by FACS-sort. C57BL6/J mice were infected with 10^8 CFU *L. pneumophila* $\Delta flaA$ GFP+ or $\Delta dotA$ GFP+ or treated with PBS. BALF samples were collected from mice of the same group (3 mice/group) and subsequently FACS-sorted to discriminate *L. pneumophila*-infected and bystander cells. (A) Gating strategy for AMs (CD45+, CD11c+, Siglec-F+) in BALF samples of 10^8 CFU *L. pneumophila*-infected and PBS-treated mice 12 h p.i.. (B) Gating strategy to isolate uninfected (PBS) as well as $\Delta flaA$ - and $\Delta dotA$ -infected and corresponding bystander AMs in a FACS-sort based on the bacterial GFP signal. (C) Fluorescence microscopy analysis of FACS-sorted AMs confirmed clean discrimination of infected and bystander cells.

The examination of the FACS-sorted AMs by fluorescence microscopy showed the presence of the bacterial GFP signal in infected cell populations. On the contrary, no GFP signal was detected in the bystander fraction (see Figure 12C), confirming clean discrimination by FACS-sort and allowing the repeat of the *in vivo* infection at a larger scale for further downstream analysis of the transcriptome and proteome of AMs during *L. pneumophila* infection.

3.2.2. *L. pneumophila* Δ *flaA*-infected, and to a slightly lesser extent Δ *dotA*-infected AMs, show a robust upregulation of proinflammatory genes

Upon performing the above-described *in vivo* infection and isolating RNA from FACS-sorted populations of AMs, a bulk RNA-seq analysis of AMs from *L. pneumophila* Δ *flaA*- or Δ *dotA*-infected and PBS-treated mice was conducted. Figures 13A and 13B depict the differentially regulated genes (DEGs) identified in AMs from Δ *flaA*- and Δ *dotA*-infected mice compared to AMs from PBS-treated animals. It was found that Δ *flaA*-infected AMs and Δ *dotA*-infected cells share a similar set of upregulated genes. Thus, proinflammatory cytokines such as *Ccl3*, *Ccl9*, *Il1a*, and *Tnfa* were upregulated in both groups. Additionally, genes encoding for proteins involved in the recruitment of other leucocyte cell populations (e.g., *Cxcl1*, *Cxcl2*, or *Cxcl3*), as well as genes encoding for proteins with an immune regulatory function (e.g., the NF- κ B inhibitor *Tnfaip3* and the transcription factor *Nfkbiz*) were found in both data sets. The observation that virulent and avirulent infected AMs upregulate similar genes was further examined by evaluating the correlation between the fold changes of DEGs in Δ *flaA*- as well as Δ *dotA*-infected AMs in comparison to AMs from PBS-treated animals (see Figure 13C). A trend towards slightly higher mRNA fold changes in AMs of Δ *flaA*-infected vs. AMs from Δ *dotA*-infected animals was observed, indicating that the proinflammatory response is more robust in virulent infected cells. In line with this, induction for genes encoding for the transcription factor IRF1, as well as the cytokines GDF15 and IL23A, was stronger in AMs from Δ *flaA*-infected mice compared to AMs from PBS-treated or Δ *dotA*-infected animals. Another gene that was found to be more strongly upregulated in AMs from Δ *flaA*-infected mice compared to AMs from PBS-treated or Δ *dotA*-infected animals was *Cdkn1b*, which encodes for a cell cycle inhibitor (see Figure 13A, C).

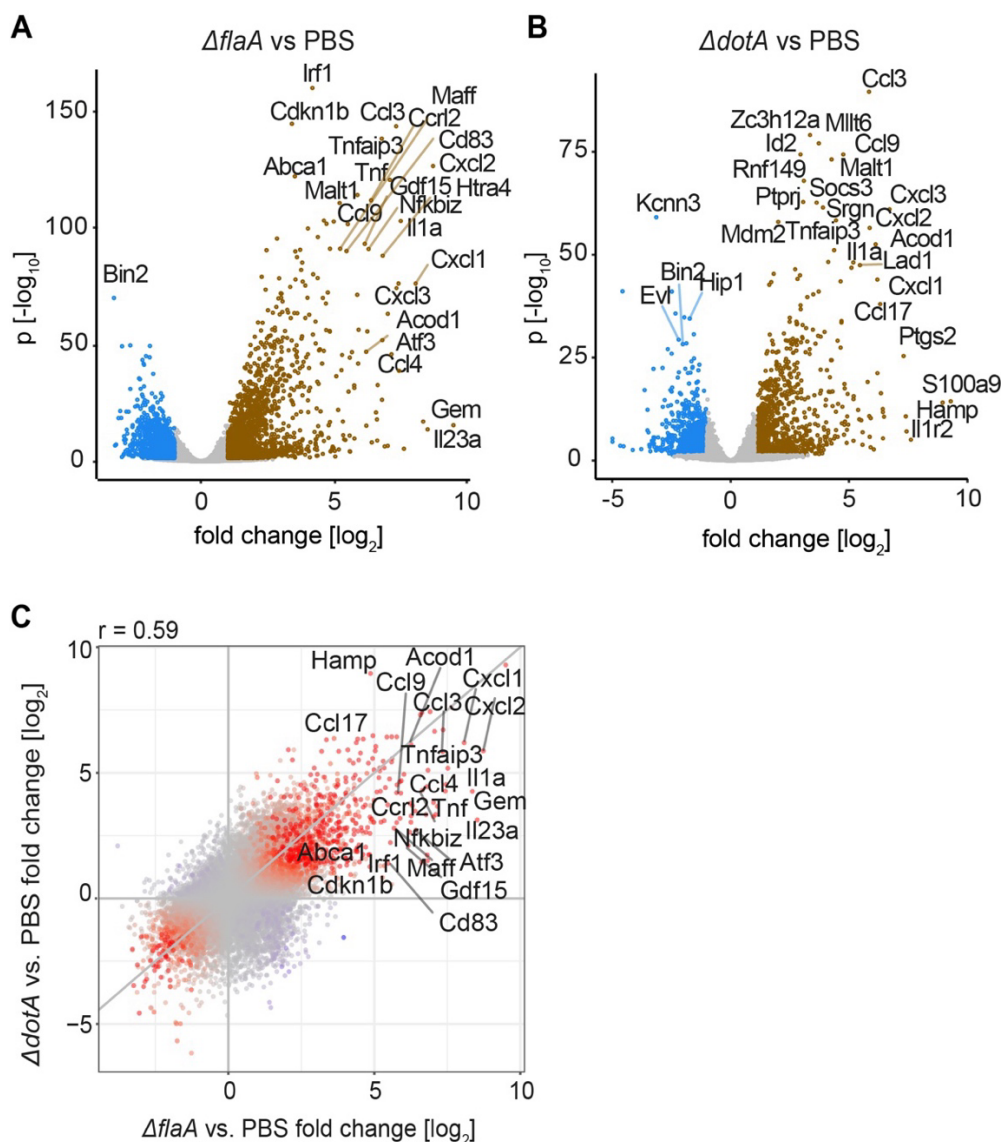


Figure 13 DEGs in AMs of mice infected with *L. pneumophila* $\Delta flaA$ or $\Delta dotA$ and of animals treated with PBS. BALF samples from $\Delta flaA$ - (10 mice/group) and $\Delta dotA$ -infected (10 mice/group) as well as PBS-treated (5 mice/group) mice at 12-14 h p.i. were collected and pooled for each group, FACS-sorted and RNA was isolated. Subsequently, a bulk RNA-seq analysis was conducted. (A, B) Volcano plots show differentially regulated genes (DEGs) in AMs from $\Delta flaA$ -infected ($\Delta flaA$) vs. PBS-treated mice and $\Delta dotA$ -infected ($\Delta dotA$) vs. PBS-treated animals. Significant DEGs with a log₂FC threshold of ≥ 1 were considered upregulated, and significant DEGs with a log₂FC threshold of ≤ -1 were downregulated, with $p \leq 0.05$. (C) The scatter plot shows log₂FCs of DEGs detected in $\Delta flaA$ - and $\Delta dotA$ -infected AMs compared to AMs from PBS-treated animals. Additionally, a correlation analysis of the respective log₂FC of DEGs was conducted. The bulk RNA-seq analysis was performed in quadruplicates, with each replicate derived from an independent infection experiment.

In addition, a gene set enrichment analysis (GSEA) was conducted to identify regulated pathways in $\Delta flaA$ - and $\Delta dotA$ -infected AMs. To this end, genes obtained from the individual comparisons were ranked based on their fold change and significance and compared to published Hallmark and Reactome data sets from the Molecular Signatures

Database (MSigDB) and Reactome Knowledgebase^{276–278}. Filters were set to diminish redundancy among resulting terms. Figure 14 shows the most enriched gene sets and regulation of the DEGs specifically associated with them for each comparison. Based on these findings, enriched DEGs in *L. pneumophila*-infected AMs seem to drive the “inflammatory response” (M5932 Hallmark), the “IL6 JAK STAT3 Signaling” (M5897 Hallmark), the “TNFA signaling via NF- κ B” (M5890 Hallmark), the “Interleukin 10 signaling” (M27605 Reactome) and the “Toll-like receptor TLR1 and TLR2 Cascade” (M27013 Reactome). Genes involved in these gene sets were found to be mostly upregulated or unchanged in Δ *flaA*- and Δ *dotA*-infected AMs compared to PBS-treated AMs.

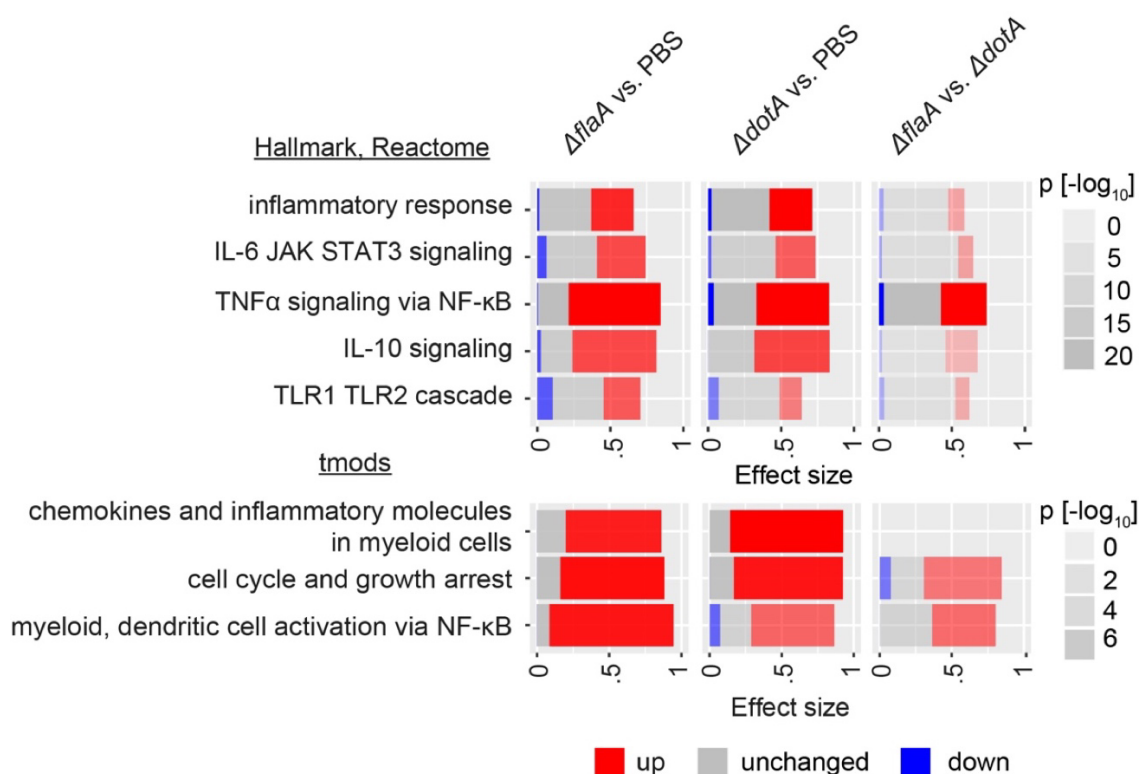


Figure 14) *L. pneumophila*-infected AMs show enrichment and upregulation of proinflammatory and cell cycle pathways in AMs 12-14 h p.i. *in vivo*. Data from bulk RNA-seq analysis of Δ *flaA*-, Δ *dotA*-infected AMs, and AMs from PBS-treated mice were further analyzed by performing a gene set enrichment analysis (GSEA). The panel plot shows enriched *Hallmark* and *Reactome* and *tmod* terms for each comparison, with indicated effect size and adjusted p values, with $p \leq 0.05$ considered significant. The direction of DEG regulation within the individual gene sets is highlighted (up: red, unchanged: grey, down: blue).

The direct comparison of Δ *flaA*- and Δ *dotA*-infected AMs revealed that enrichment of individual gene sets was slightly more substantial in virulent infected AMs. This effect is seen most prominently for the “TNFA signaling via NF- κ B pathway”, suggesting that the induction of genes related to this pathway is partly dependent on a functional T4SS. In

addition to the Hallmark and Reactome database, enrichment of transcriptional modules from the *tmod* package was evaluated^{279–281}. Transcriptional modules that came up in the analysis were “chemokines and inflammatory molecules in myeloid cells” (LI.M86.0, *tmod*), “cell cycle and growth arrest” (LI.M31, *tmod*), and “myeloid, dendritic cell activation via NF- κ B (I)” (LI.M43.0, *tmod*). The first module was enriched to a similar extent in both Δ *flaA*- and Δ *dotA*-infected AMs. In contrast, the module comprised of genes regulating the myeloid cell activation via NF- κ B was found to be more strongly upregulated in Δ *flaA*-infected cells. Similarly, genes associated with the module “cell cycle and growth arrest” were more enriched in Δ *flaA*-infected AMs compared to Δ *dotA*-infected AMs, with more genes being up- than downregulated in the direct comparison.

Overall, the data collected from this bulk RNA-seq study suggest that the transcriptomic response in *L. pneumophila*-infected AMs is mainly driven by a significant upregulation of proinflammatory genes that drive various proinflammatory pathways in the early phase of infection *in vivo*. This response seems slightly stronger in Δ *flaA*-infected AMs compared to Δ *dotA*-infected cells, which is potentially in line with the fact that innate immune sensing of *L. pneumophila* by some PRRs depends on an intact T4SS.

3.2.3. The DEGs in Δ *flaA*-infected vs. bystander AMs are similar to the DEGs in AMs from Δ *flaA*-infected mice vs. PBS-treated animals

The complete replication cycle of *L. pneumophila* in macrophages before host cell lysis and release of the bacterial progeny takes about 24 h^{27,32}. Consequentially, the FACS-sort of BALF samples from infected mice at 12 to 14 h upon infection allowed isolation of bystander AMs that had not internalized bacteria yet but might be activated due to extracellular signaling. Therefore, I next examined if bystander AMs showed a transcriptomic response at 12 to 14 h p.i. *in vivo*. Figure 15A depicts the top DEGs for Δ *flaA*-infected and corresponding bystander AMs. Upregulated DEGs that were found to have a higher expression level in infected AMs were also detected to be upregulated in Δ *flaA* vs PBS, e.g., *Irf1*, *Cdkn1b*, *Ccl3*, *Gdf15*, *Ccrl2*, *Tnf*, and *Htra4* (compare to Figure 13A). Further analysis revealed a high correlation ($r = 0.72$) between mRNA fold changes of genes detected in Δ *flaA* vs bystander and Δ *flaA* vs PBS (see Figure 15B). These findings indirectly show that bystander AMs have a similar transcriptomic profile as AMs from PBS-treated animals at the early time of infection. Therefore, bystander AMs were excluded from the subsequent mass spectrometry analysis.

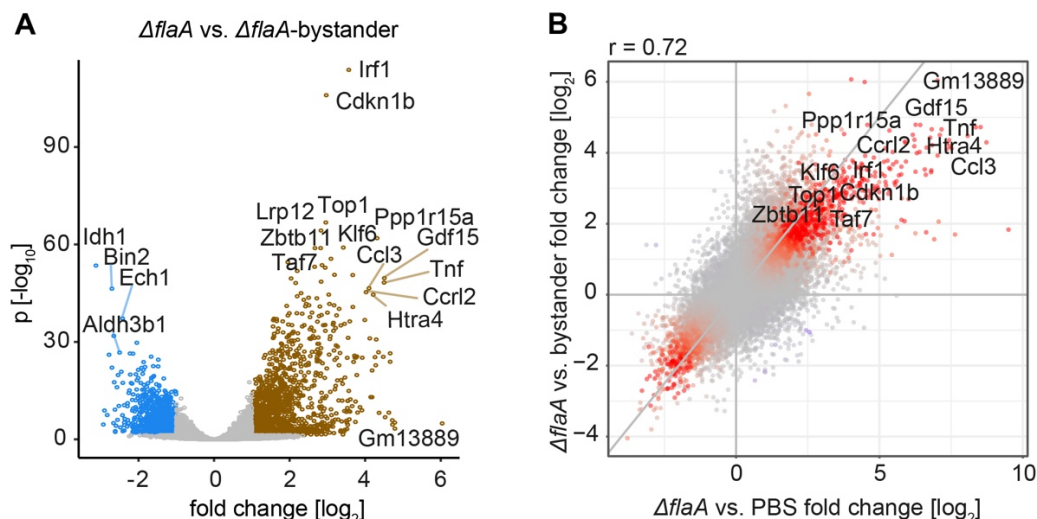


Figure 15) DEGs in *ΔflaA*-infected vs. bystander AMs are similar to DEGs in AMs from *ΔflaA*-infected mice vs. PBS-treated mice. (A) The volcano plot shows DEGs for comparing infected and bystander AMs from the lungs of *ΔflaA*-infected mice. Significant DEGs with a \log_2FC threshold of ≥ 1 were considered as upregulated, and significant DEGs with a \log_2FC threshold of ≤ -1 as downregulated, with $p \leq 0.05$. B) Correlation for fold changes of DEGs detected in both *ΔflaA* vs. bystander and *ΔflaA* vs. PBS was assessed.

3.2.4. *L. pneumophila*-infected AMs show a significant upregulation of proteins that are not consistently regulated on mRNA level

Next, a new round of *in vivo* infection experiments was performed to isolate total proteins from FACS-sorted AMs at 12-14 h p.i.. A mass spectrometry analysis investigated the proteomic response in AMs from *ΔflaA*- and *ΔdotA*-infected and PBS-treated animals. The analysis identified 7,835 proteins, specifically 213 *L. pneumophila*- and 7,622 mouse-derived proteins (see Figure 16A). A strain-specific comparison was performed for the host proteins to identify differentially regulated proteins (DEPs) in *ΔflaA*- and *ΔdotA*-infected AMs compared to AMs from PBS-treated mice (see Figure 16B, C). Comparing the top regulated DEPs to the DEGs revealed that some of the upregulated DEPs in *ΔflaA*- and *ΔdotA*-infected AMs were not consistently regulated at the transcriptional level, as defined by RNA fold changes categorized as “unchanged” (between 1 and -1) or a p-value > 0.05 (e.g., *Mmp8*, *Gpx3*, *C3*, *Abca3*). Moreover, several upregulated proteins exhibited a low base mean in the corresponding bulk RNA-seq data (e.g., *C4b*, *Mtus1*, *Mgam*, *Stx2*), suggesting a generally low average mRNA expression level.

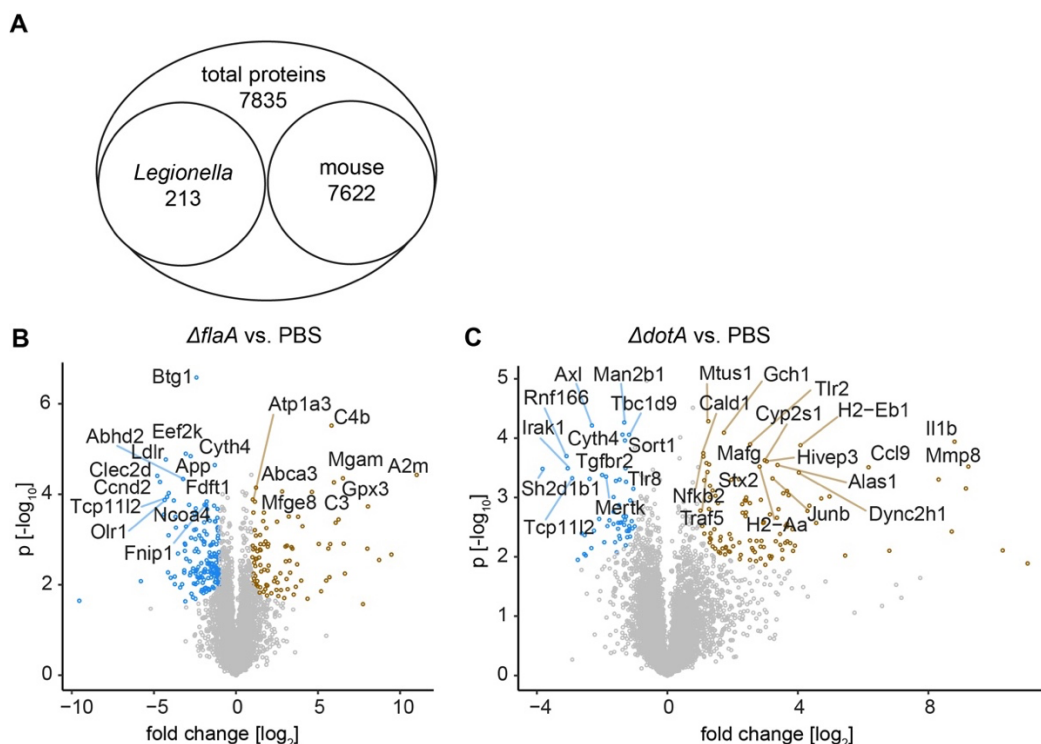


Figure 16) The proteome analysis revealed that some top-upregulated proteins in *L. pneumophila*-infected AMs are not consistently regulated on mRNA level. AMs from $\Delta flaA$ - (20 mice/group) and $\Delta dotA$ -infected (20 mice/group) and PBS-treated (5 mice/group) mice were isolated by FACS sorting at 12 to 14 h p.i., and proteins were isolated. (A) A mass spectrometry analysis of AM proteins isolated from $\Delta flaA$ - and $\Delta dotA$ -infected as well as PBS-treated animals led to the identification of 7,622 host proteins. The volcano plots illustrate differentially regulated proteins (DEPs) for (B) $\Delta flaA$ - and (C) $\Delta dotA$ -infected AMs in comparison to cells from PBS-treated mice. The mass spectrometry analysis was conducted in quadruplicates, with each replicate derived from an independent *in vivo* infection experiment. The significance of DEPs was evaluated by ANOVA test with a threshold of FDR 5%. DEPs with a log₂FC of ≥ 1 and ≤ -1 and with $p < 0.05$ were highlighted.

It could not be fully excluded that the observed discrepancy of proteome and transcriptome data was due to contamination with, e.g., murine serum. However, extensive washing steps during the experimental procedure and preparation of total protein samples make this explanation highly unlikely, and we consider it more likely that the engulfment of dead cells or cellular debris by the highly phagocytotic AMs is responsible. To minimize the effect of phagocytosis-driven “contamination”, the proteome data were further evaluated for concordance with bulk RNA-seq data. As a first step, data were aligned to identify molecules found in both the bulk RNA-seq and proteome datasets of FACS-sorted AMs from $\Delta flaA$ -infected or $\Delta dotA$ -infected mice and PBS-treated animals (see Figure 17).

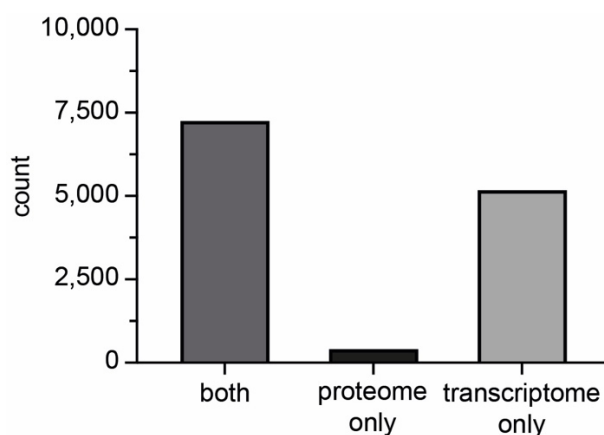


Figure 17) Numbers of molecules identified in AMs from $\Delta flaA$ -infected or $\Delta dotA$ -infected mice and PBS-treated animals on protein and mRNA levels by bulk RNA-seq and proteome analysis, respectively. Data from the bulk RNA-seq and mass spectrometry analysis was analyzed for concordance by identifying the number of molecules identified in both or only one of the two data sets. The bar diagram shows the numbers of molecules found in both or only the proteome or transcriptome data sets of $\Delta flaA$ -infected or $\Delta dotA$ -infected mice and PBS-treated animals.

A total of 7,231 protein-encoding genes were found both on mRNA and protein levels. In contrast, 5,158 genes from the bulk RNA-seq data set were not detected in the mass spectrometry analysis, and no corresponding transcripts were detected for 391 proteins. The absence of corresponding proteins for 5,158 transcripts could be a result of technical limitation of the mass spectrometry analysis, as they were neither detected in any of the three AM total protein samples from $\Delta flaA$ - or $\Delta dotA$ -infected mice and PBS-treated animals. The absence of corresponding transcripts for the 391 proteins, on the other hand, indicates that these proteins might be phagocytosis-driven “contamination”, as explained above. Therefore, I performed subsequent analyses with only the molecules that were detected on both transcript and protein levels.

3.2.5. Concordantly regulated molecules in $\Delta flaA$ -infected AMs are related proinflammatory pathways and cholesterol biosynthesis

As a next step, I first investigated the regulation of detected molecules on both transcript and protein levels in AMs from $\Delta flaA$ -infected, $\Delta dotA$ -infected, and PBS-treated mice on a global level. To this end, a differential concordance (DISCO) analysis was conducted. This analysis aimed to identify which of the proteins were regulated in the same direction on the mRNA level (referred to as “concordant”) and which displayed regulation in opposite directions (referred to as “discordant”). Figure 18A-C depicts the concordantly (brown) and discordantly (blue) regulated genes and proteins for each comparison.

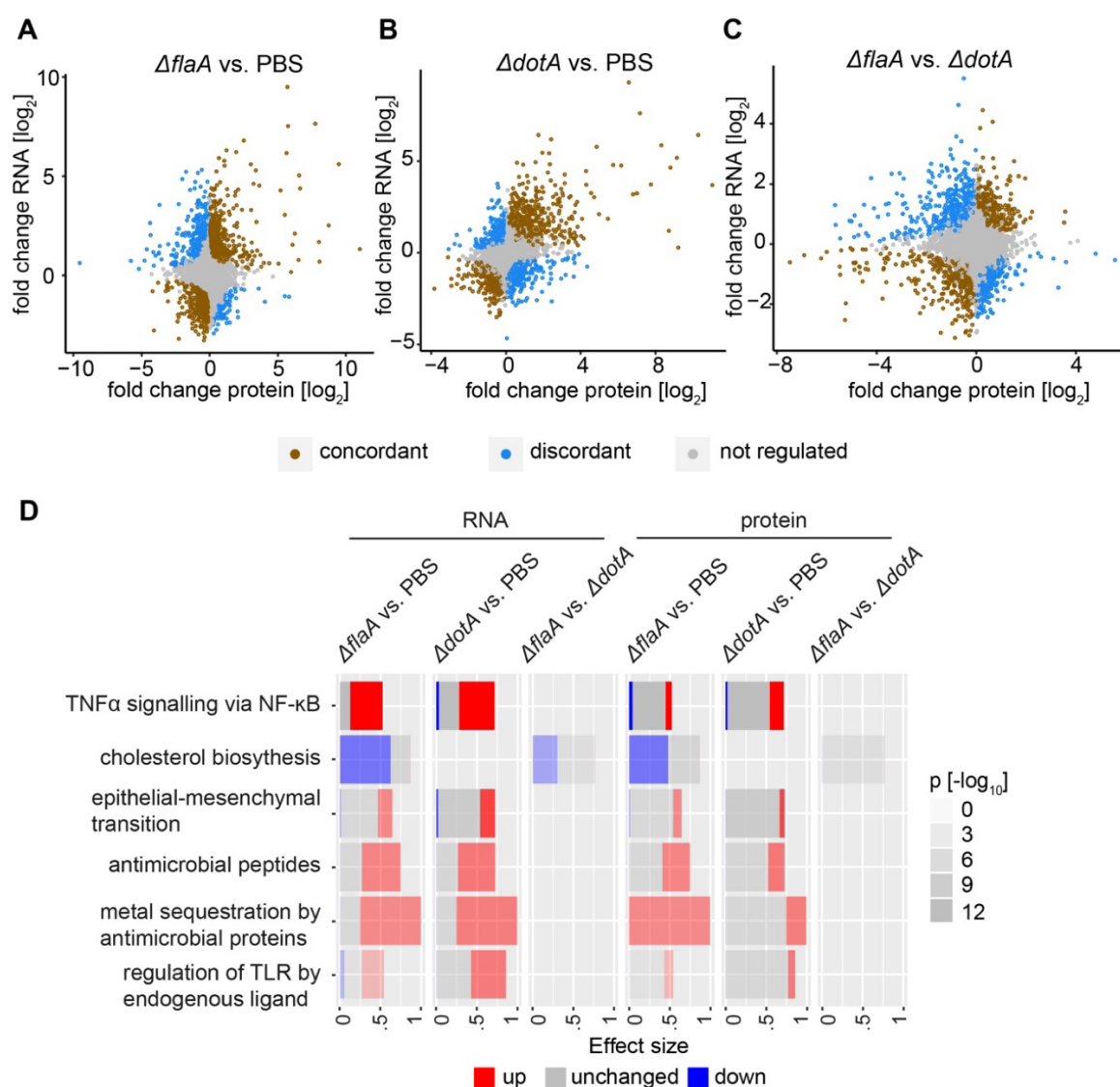


Figure 18) *L. pneumophila* $\Delta flaA$ -infected AMs upregulate transcripts involved in TNF α signaling and to a lesser extent the corresponding proteins, whereas transcripts and proteins related to cholesterol biosynthesis are simultaneously downregulated. A differential concordance (DISCO) analysis was performed for molecules detected in the bulk RNA-seq and proteome data set. Disco scores were calculated and ranked, and the top 10% of concordant (brown) and discordant (blue) molecules were highlighted in scatter plots, showing \log_2 FCs of DEGs and DEPs for (A) $\Delta flaA$ vs PBS, (B) $\Delta dotA$ vs PBS and (C) $\Delta flaA$ vs $\Delta dotA$. (D) Enrichment analysis was performed for concordantly regulated proteins. The panel plot shows enriched Hallmark and Reactome terms of concordantly regulated proteins. For each identified term, enriched DEGs and DEPs were plotted independently of their concordance score in a panel plot, indicating the direction of their regulation, effect size and corrected p value for each pathway, with $p < 0.05$ considered significant.

To identify enriched pathways among concordantly and discordantly regulated molecules, an enrichment analysis was performed for both categories of molecules. To this end, concordantly and discordantly regulated molecule sets were compared to published MSigDB Hallmark and Reactome datasets. The analysis gave no result for specifically enriched

pathways by discordantly enriched molecules. On the contrary, six pathways were identified as specifically enriched by concordantly regulated genes and proteins in AMs from *AflaA*-infected and *ΔdotA*-infected mice, as shown in Figure 18D. These pathways were “TNF α signaling via NF- κ B” (M5890, Hallmark), “cholesterol biosynthesis” (M16227, Reactome), “epithelial-mesenchymal transition” (M5930, Hallmark), “antimicrobial peptides” (M27627, Reactome), “metal sequestration by antimicrobial proteins” (M27622, Reactome), “regulation of TLR by endogenous ligands” (M27571, Reactome). For each identified concordantly regulated pathway in this analysis, enriched genes and proteins from the bulk RNA-seq and proteomic dataset were plotted independently of their DISCO score (meaning that discordant regulated proteins were plotted as well if they were associated with the respective pathway). This allowed us to better visualize the detailed regulation of the respective pathways on both mRNA and protein levels (see Figure 18D). Most identified gene sets were upregulated on mRNA and protein levels similarly in AMs from *AflaA*-infected and *ΔdotA*-infected mice.

In *AflaA*-infected AMs, I observed a significant downregulation of mRNAs and proteins involved in cholesterol biosynthesis. This downregulation was exclusively observed in AMs from *AflaA*-infected animals, which suggests that the cholesterol synthesis is affected in a T4SS-dependent manner during the early stages of infection in AMs. Interestingly, further investigation of the proteomic data found that the low-density lipoprotein receptor (LDLR), which is a transmembrane receptor involved in sensing intracellular cholesterol levels, was found to be downregulated on protein level in AMs of *AflaA*-infected mice (Data not shown). Another interesting observation was the regulation of the “TNF α signaling via NF- κ B” pathway, which describes a set of genes, whose expression is regulated by NF- κ B in response to TNF α -signaling. This data set was found to be the most significantly enriched pathway for AMs from *AflaA*-infected and *ΔdotA*-infected mice compared to AMs from PBS-treated animals, respectively (see Figure 18D). While both *AflaA*-infected and *ΔdotA*-infected AMs showed a strong upregulation of this pathway on the mRNA level, only some of the corresponding proteins were found to be upregulated in AMs of both animal groups. This discordant regulation of proteins appeared to be stronger in *AflaA*-infected AMs compared to *ΔdotA*-infected AMs, potentially suggesting that the translation of some of the proinflammatory genes involved in TNF α signaling is specifically suppressed by *L. pneumophila ΔflaA*. Indeed, a closer look at the regulation of this pathway on mRNA and protein levels revealed that 76 molecules were upregulated on the mRNA level, but only 13 of them also on the protein level in *AflaA*-infected AMs. For the comparison of *ΔdotA*-

infected AMs vs. AMs from PBS-treated mice, on the contrary, 56 mRNAs and 25 corresponding proteins were identified as upregulated.

Given that *L. pneumophila* infection leads to an impairment of inflammation-associated proteins in a T4SS-dependent manner in BMMs *in vitro*^{36,41,67}, it is possible that some proteins of the “TNF α signaling via NF- κ B” may also be translationally blocked during infection of AMs with *L. pneumophila* Δ *flaA*. The regulation of individual molecules in AMs from Δ *flaA*- and Δ *dotA*-infected mice was further investigated in the next step.

3.2.6. Comparison of mRNA and protein expression allows identification of molecules that appear to be exclusively up- and downregulated in AMs from Δ *flaA*-infected mice, as well as of genes whose translation seems to be T4SS-dependently impaired

Several *in vitro* studies in hematopoietic macrophages have demonstrated that *L. pneumophila* effectors impair the translation of various host proteins in a T4SS-dependent manner. In contrast, some proteins seem to be able to bypass the translational block^{36,41,67}. To investigate how single genes and proteins are regulated in *in vivo* infection in AMs that differ ontogenetically and concerning the life cycle, life span, function, and phenotype, molecules detected in both the bulk RNA-seq as well as the proteome analyses of AMs from Δ *flaA*- or Δ *dotA*-infected mice were categorized into different categories. These categories were based on fold changes and p values from the individual comparisons of the transcripts and proteins. Nine classes of mRNA and protein expression were identified for AMs from both Δ *flaA*- or Δ *dotA*-infected mice, such as, e.g., “mRNA \uparrow protein \uparrow ” (indicating upregulation on both mRNA and protein level) and “mRNA= protein \downarrow ” (indicating no changes in mRNA expression and downregulation on protein level). Figure 19 illustrates the regulation for genes and proteins detected in Δ *flaA*- and Δ *dotA*-infected AMs compared to AMs from PBS-treated mice.

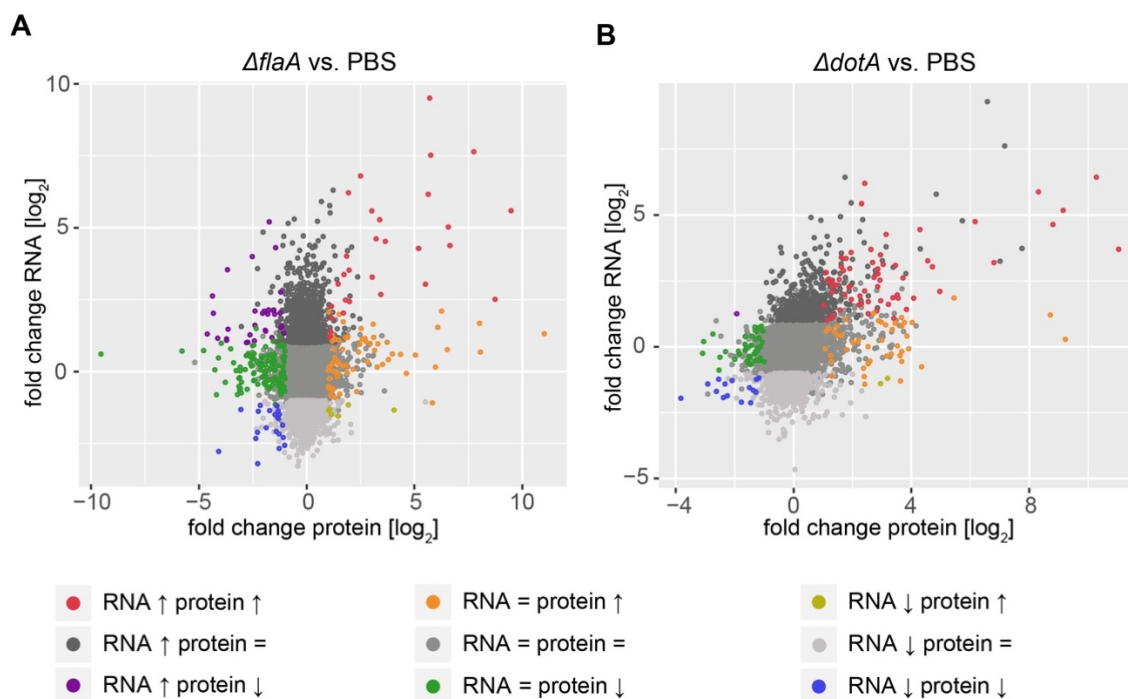


Figure 19) Assignment of proteins detected in AMs of *L. pneumophila*-infected mice to classes based on their transcriptional and translational regulation. Corresponding genes and proteins detected in $\Delta flaA$ vs. PBS and $\Delta dotA$ vs. PBS were assigned to classes based on their mRNA and protein \log_2 FC and significance. Thresholds for upregulated (“↑”) mRNAs and proteins were set as FC [\log_2] > 1, $p < 0.05$, while thresholds for downregulated (“↓”) mRNAs and proteins were set as FC [\log_2] < -1, $p < 0.05$. Genes and proteins with \log_2 FCs between 1 and -1, as well as >1 and <-1 with $p > 0.05$, were classified as unchanged (“=”). Classes of genes and proteins were highlighted in scatter plots for (A) $\Delta flaA$ vs. PBS and (B) $\Delta dotA$ vs. PBS.

The next step was to identify the single proteins within these classes to get a better view of which molecules were i) upregulated and which molecules were ii) downregulated in AMs responding to *L. pneumophila* $\Delta flaA$, respectively. By comparing these two subsets of molecules in $\Delta flaA$ -infected AMs to molecules that were up- and down-regulated in AMs infected with $\Delta dotA$, it was possible to identify molecules that were specifically regulated in $\Delta flaA$ -infected AMs. In addition, it was investigated which molecules were upregulated on mRNA but unchanged or downregulated on protein level, thus, assigned to the categories “mRNA ↑ protein =” and “mRNA ↑ protein ↓” in $\Delta flaA$ -infected AMs. By subtracting molecules assigned to the same categories in $\Delta dotA$ -infected AMs, I aimed to identify molecules potentially impaired in their translation in a T4SS-dependent manner during *L. pneumophila* infection in AMs *in vivo*.

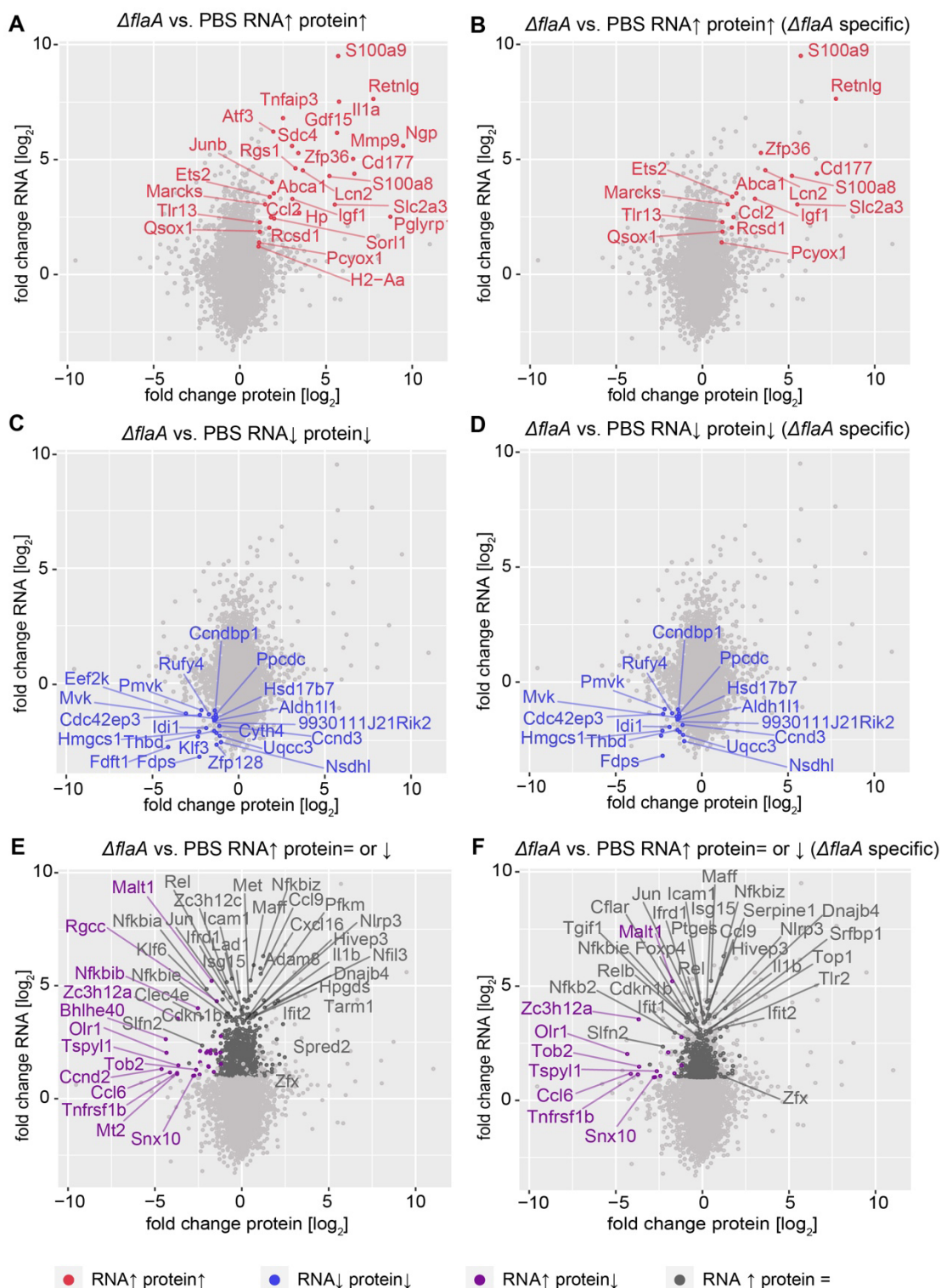


Figure 20) Molecules that were exclusively up- and downregulated in *L. pneumophila* $\Delta flaA$ -infected AMs, as well as proteins that were identified to be potentially impaired in their translation in a T4SS-dependent manner. Molecules identified on both bulk RNA-seq and proteomic analyses were categorized based on their regulation on mRNA and protein level in $\Delta flaA$ - and $\Delta dotA$ -infected AMs. This allowed to identify molecules specifically up- and downregulated in $\Delta flaA$ -infected AMs, as well as to screen for proteins that were potentially impaired in translation in a T4SS-dependent manner. The scatter plots show proteins that were found to be up- (A) (“mRNA \uparrow

protein \uparrow ”) and downregulated (C) (“mRNA \downarrow protein \downarrow ”) in *AflaA*-infected AMs. Scatter plots (B) and (D) highlight the respective subsets of these proteins that were only identified to be regulated in that manner in *AflaA*- but not in *AdotA*-infected AMs (referred to as “*AflaA* vs. PBS specific”). The scatter plot (E) shows 905 proteins identified in *AflaA*-infected AMs that were upregulated on mRNA-level but either unchanged (“mRNA \uparrow protein=”) or downregulated (“mRNA \uparrow protein \downarrow ”) on protein level. Scatter plot (F) highlights some of the 576 the proteins that fell into these categories in *AflaA*- but not in *AdotA*-infected AMs.

29 molecules were upregulated on mRNA and protein levels in *AflaA*-infected AMs (see Figure 20A). These molecules included cytokines and chemokines (IL-1 α , CCL2, GDF15), transcriptional regulators (ATF3, JUNB), growth factors (IGF1), metabolic enzymes (ABCA1, SLC2A3), negative regulators of TNF α response (ZFP36, TNFAIP3) and antimicrobial and inflammatory proteins (S100A8, S100A9). To identify molecules that were specifically upregulated on both mRNA and protein level in *AflaA*-infected AMs but not in *AdotA*-infected AMs, molecules found to be induced on transcript and protein level in *AdotA*-infected AMs were subtracted from the 29 molecules induced in *AflaA*-infected cells (referred to as “*AflaA* vs. PBS specific”). This subset of proteins specifically upregulated in *AflaA*-infected AMs contained 16 proteins (see Figure 20B). Notably, some of these 16 molecules were found to have a very low base mean (< 100), namely RETNLG, CD177, SLC2A3, S100A8, LCN2, HP, SDC4, SORL1, CCL2, RCSD1 and MARCKS, indicating a very low average expression on mRNA level. Therefore, the data related to these molecules should be interpreted with care, and further investigation will be necessary to assess if some of the proteins found in this analysis have a significant role in modulating the immune response in *L. pneumophila AflaA*-infected AMs.

Similarly, 21 molecules were downregulated in *AflaA*-infected AMs on both transcript and protein levels (see Figure 20C), with 16 specifically regulated upon infection with *AflaA* but not *AdotA* (see Figure 20D). Many of these exclusively downregulated molecules in *AflaA*-infected AMs are proteins associated with cholesterol biosynthesis, such as HMGCS1, MVD, PMVK, IDI1, NSDHL, FDPS, and HSD17B7, which is in line with the observations from the pathway analysis of concordant regulated molecules in *L. pneumophila*-infected AMs (see Figure 18D). Other proteins found to be downregulated specifically in *AflaA*-infected AMs were involved in the cell cycle (CCND3, CCNDBP1), autophagy (RUFY4), and ATP synthesis (UQCC3) (see Figure 20D).

Based on the categories defined for transcriptional and translational regulation, proteins that were potentially impaired in their translation in AMs of *AflaA*-infected mice were expected to be upregulated on the mRNA level while either unchanged or downregulated on the

protein level. A total of 905 proteins fell into these two categories defined for *AflaA*-infected AMs, as shown in Figure 20D. Among those, the majority were classified as “unchanged” on the protein level (n = 874), and fewer molecules were “downregulated” in their translation (n = 31) in comparison to AMs from PBS-treated mice. Of these 905 molecules, 576 proteins could be “exclusively” assigned to the categories mentioned above in *AflaA*-infected AMs (see Figure 20F), whereas 329 proteins were regulated similarly in *ΔdotA*-infected AMs. Based on the results from the analysis, the translation for some proinflammatory proteins (IL-1 β , CCL9, CCL6) seems to be exclusively impaired in *AflaA*-infected AMs. Furthermore, two PRRs fell into the category “RNA \uparrow protein=” in *AflaA*-infected AMs but not *ΔdotA*-infected AMs, namely TLR2 and NLRP3. Moreover, proteins involved in NF- κ B-signaling as the transcriptional regulator NFKBIZ²⁸² or the enzyme MALT1²⁸³ seem to be specifically blocked in AMs of mice infected with *AflaA* (see Figure 20F). In line with the results from the DISCO analysis (see Figure 18) that indicated a potential the translation impairment of proteins associated with the “TNF α signaling via NF- κ B” pathway, also TNFRSF1B (TNFR2), one of the two membrane receptors binding TNF α , was downregulated on protein level in *AflaA*- but not in *ΔdotA*-infected AMs (see Figure 20F). Collectively, the results suggest that translation of various proinflammatory and regulatory proteins is inhibited in a T4SS-dependent manner during infection of AMs *in vivo* with *L. pneumophila*. Further investigation is required to test if and which T4SS-dependently secreted bacterial effector proteins might be involved in translational inhibition.

3.2.7. A single cell RNA sequencing analysis demonstrated upregulation of potential targets for further investigation of their role in the immune response to *L. pneumophila* in AMs *in vivo*.

Finally, a sc RNA-seq analysis was conducted. Groups of mice were again infected with *AflaA* for 6 h and 20 h and with *ΔdotA* for 6 h only. A control group of mice treated with PBS was included for each time point. After the indicated time points, BALF samples of mice from each group were collected and pooled in the individual groups, and GFP+ and GFP- leucocytes (CD45+) were FACS-sorted. The purity of the FACS-sorted cells was validated by fluorescence microscopy (see Figure 21) before sc RNA-seq analysis was performed.

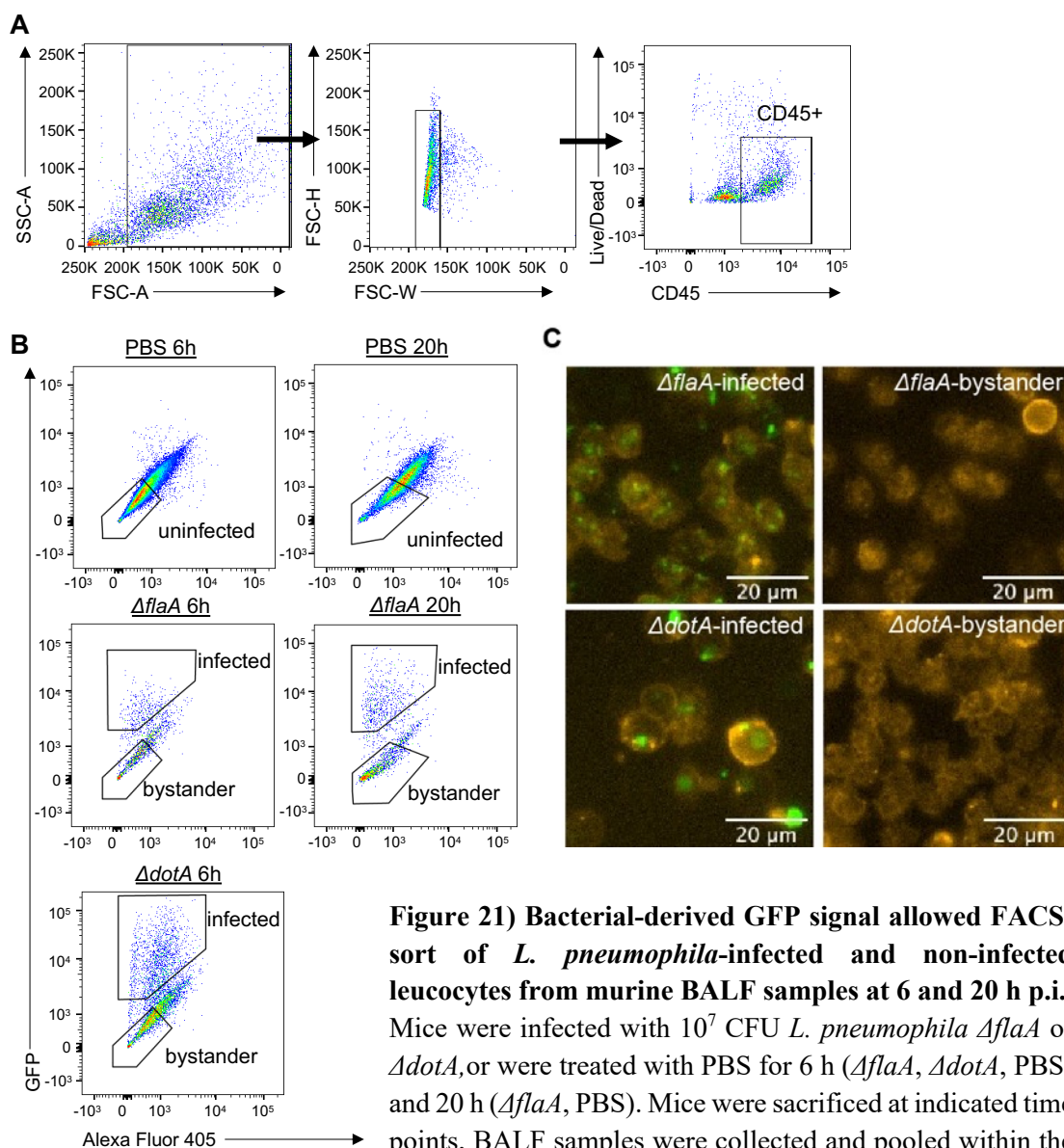


Figure 21) Bacterial-derived GFP signal allowed FACS-sort of *L. pneumophila*-infected and non-infected leucocytes from murine BALF samples at 6 and 20 h p.i. Mice were infected with 10^7 CFU *L. pneumophila* $\Delta flaA$ or $\Delta dotA$, or were treated with PBS for 6 h ($\Delta flaA$, $\Delta dotA$, PBS) and 20 h ($\Delta flaA$, PBS). Mice were sacrificed at indicated time points, BALF samples were collected and pooled within the same group (6 mice/group), and cells were FACS-sorted. (A) Gating strategy for leucocytes (CD45+) in BALF samples of mice. (B) Gating strategy for sorting cells from PBS-treated, $\Delta flaA$ -infected, and $\Delta dotA$ -infected animals as well as corresponding bystander leucocytes (C) Fluorescence microscopy of $\Delta flaA$ - and $\Delta dotA$ -infected and bystander leucocytes confirmed the purity of FACS-sorted cells.

Leucocyte populations found in the BALF samples were annotated based on the expression of selected cell population markers (see Figure 22A). Two main cell populations were identified in BALF samples of *L. pneumophila*-infected mice, namely PMNs and AMs. While AMs were the most abundant cell population at 6 h p.i., a substantial PMN influx was observed at 20 h p.i. (see Figure 22B). For the 6 h timepoint, 2879 AMs from $\Delta flaA$ -infected mice, 256 corresponding $\Delta flaA$ -bystander AMs were analyzed and compared to 479 $\Delta dotA$ -

infected AMs and 1834 AMs from BALF samples of mice treated with PBS. At 20 h p.i. 113 $\Delta flaA$ -infected AMs and 308 $\Delta flaA$ -bystander AMs were analyzed, and gene expression was compared to 2330 AMs from PBS-treated mice.

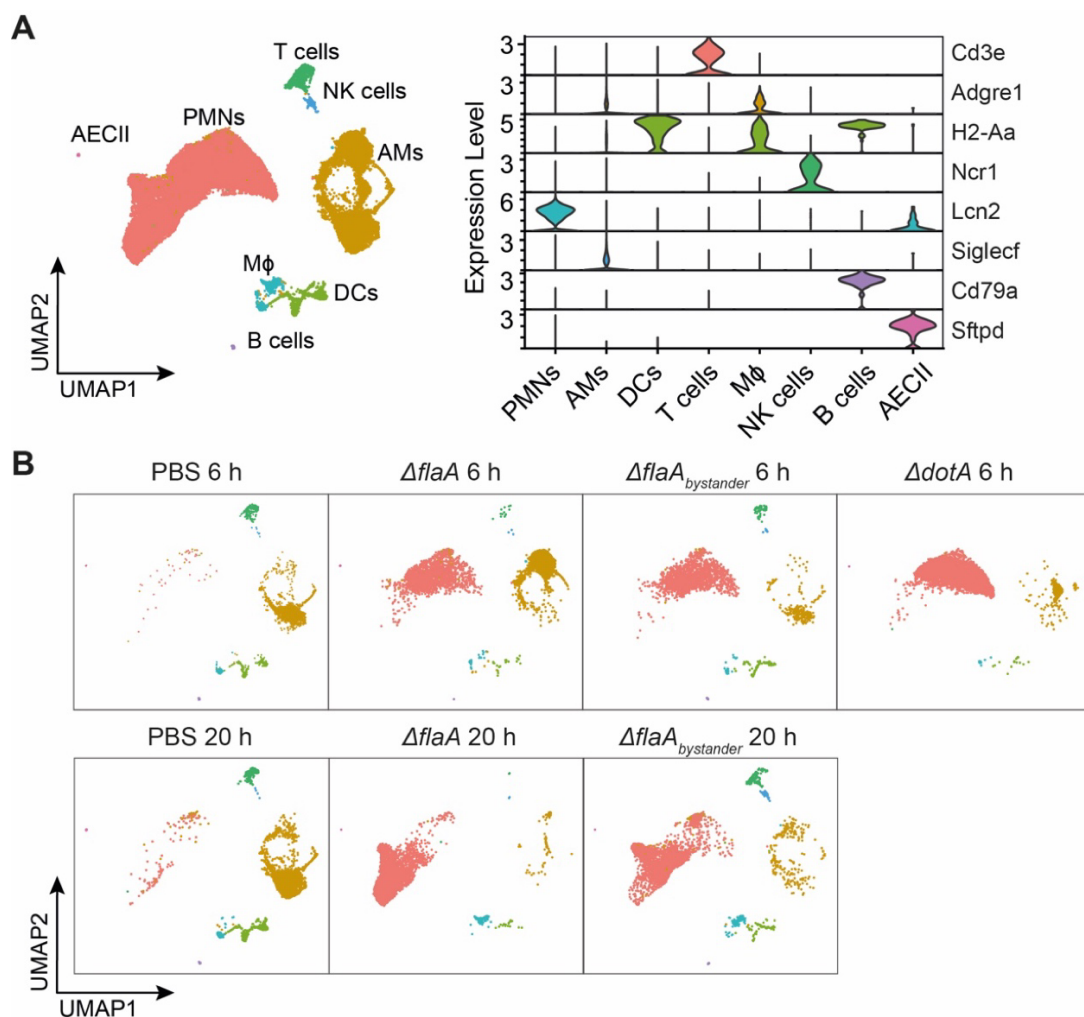


Figure 22) AMs and PMNs were the two main leukocyte populations in BALF samples of *L. pneumophila*-infected mice at 6 and 20 h p.i.. A sc RNA-seq analysis of FACS-sorted *L. pneumophila*-infected, bystander, and uninfected CD45⁺ cells of the 6 and 20 h timepoint was conducted. (A) Cell populations in BALF samples were annotated based on expression of selected cell population markers as the following: Polymorphonuclear monocyte (PMN), alveolar macrophage (AM), dendritic cells (DCs), monocytic macrophages (Mφ), natural killer (NK) cells, T lymphocyte (T cells), B lymphocyte (B cells), type 2 alveolar epithelial cells (AECII). (B) UMAP embedding shows the distribution of cell population found in BALF samples of PBS-treated (6 h, 20 h), $\Delta flaA$ -infected (6 h, 20 h), $\Delta flaA$ -bystander ($\Delta flaA_{bystander}$, 6 h, 20 h), and $\Delta dotA$ -infected (6 h) mice at each time point.

Next, a sub-clustering approach for the AM population revealed that $\Delta flaA$ - and $\Delta dotA$ -infected cells cluster distinct from each other, as well as from bystander AMs and AMs from PBS-treated cells (see Figure 23A).

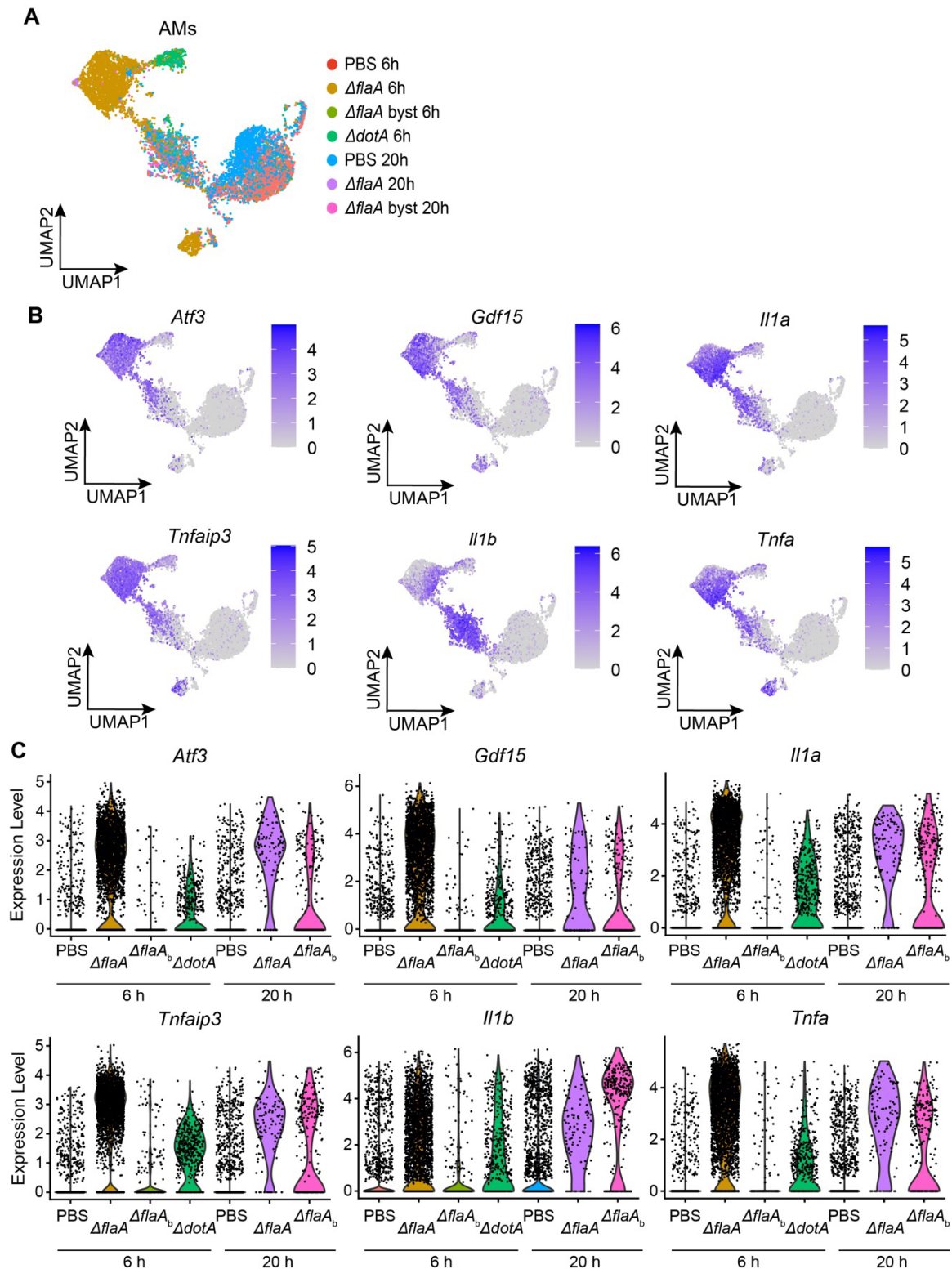


Figure 23) AMs isolated from mice infected with *L. pneumophila* $\Delta flaA$ upregulate gene expression of inflammatory genes at 6 and 20 h p.i.. (A) AMs of individual experimental groups were sub-clustered based on their gene expression and plotted in a UMAP embedding. The normalized expression of *Atf3*, *Gdf15*, *Il1a*, *Tnfaip3*, *Il1b*, and *Tnf* in AM subclusters and individual experimental groups was shown in (B) UMAP embeddings and (C) violin plots.

Interestingly, two groups of *AflaA*-infected AMs were observed at the 6 h time point (see Figure 23A). A direct comparison of the top DEGs between the two *AflaA*-infected AM clusters at the 6 h time point revealed strong upregulation of mitochondrial RNA in the smaller cluster (Data not shown), indicating that the differential clustering of *AflaA*-infected AMs at 6 h p.i. is likely an artifact as the high content of mitochondrial genes potentially overlaps similar gene signatures in both clusters.

Expression analysis of individual molecules in the different experimental groups was in line with the findings from the bulk RNA-seq analysis, as *Atf3*, *Gdf15*, *Tnfaip3*, *Il1a*, *Il1b*, and *Tnfa* were found to be upregulated in *AflaA*-infected cells at the 6 and 20 h time point, as well as - to less extent - in *ΔdotA*-infected AMs (see Figure 23B, C). Furthermore, upregulation of these genes was also found in bystander AMs at the 20 h time point but not at the 6 h time point. Overall, the data collected from the sc RNA-seq analysis support the hypothesis that these genes and their corresponding proteins might be involved in the immune response against *L. pneumophila* in AMs *in vivo* and, therefore, could be of interest for functional investigations in the future.

4. Discussion

4.1. Summary – Investigating the potential role of the CLR CLEC12A during *L. pneumophila* infection

Several studies have aimed to investigate the mechanisms of the immune response of macrophages to an infection with the intracellular pathogen *L. pneumophila*, which can cause a pulmonary infection, referred to as LD, with a potentially fatal outcome^{284,285}. To clear the infection and prevent the spreading of pulmonary disease, fast detection of the pathogen in the pulmonary environment and inside infected cells is necessary. Various PRRs, such as TLRs and NLRs, recognize *L. pneumophila* and *L. pneumophila*-derived PAMPs at the surface and in the cytosol of infected macrophages²⁵⁴. Another family of PRRs that have been found to modulate the immune response in the context of infections caused by intracellular pathogens, such as *Mycobacteria* or *Salmonella*, are CLRs^{147,148}. However, the role of CLRs in the context of *L. pneumophila* is poorly investigated, and no CLRs were reported to be involved in the immune response against the bacterium. A preliminary screening analysis had shown that among a library of CLR fusion proteins, the receptor CLEC12A (also referred to as MICL), primarily expressed on myeloid cells, including macrophages, binds to *L. pneumophila*. Therefore, CLEC12A was assumed to contribute to the immune response to the intracellular pathogen²⁶¹. Using an *in vivo* model in which WT and CLEC12A-deficient mice were intranasally infected with *L. pneumophila*, I found that CLEC12A neither had a significant role in clearing the bacterial burden from the lungs of mice nor that it impacted leucocyte recruitment or cytokine production during infection.

Additionally, functional *in vitro* analysis performed on murine BMDMs from WT and *Clec12a*^{-/-} animals did not provide clear evidence for a non-redundant functional role of the CLR in the innate immune response to *L. pneumophila*. Similarly, studies conducted in human BLaER1-cells, in which I introduced a KO for CLEC12A using CRISPR/Cas9, did not reveal an effect of CLEC12A deficiency in the infection. Taken together, CLEC12A seems to bind *L. pneumophila* but does not play a significant role in the innate immune response against the pathogen. This chapter will discuss the results of this study in more detail.

4.1.1. The hemITIM-containing receptor CLEC12A has no critical function in the response to *L. pneumophila* infection *in vitro* and *in vivo*

CLRs are hardly investigated in the context of *L. pneumophila* infection. Some studies have addressed the potential epidemiological relevance of CLRs^{286–288}, but there is no evidence for a functional relevance of this receptor family during *L. pneumophila* infection. Using a murine infection model, the impact of CLEC12A on bacterial clearance and cytokine production during intranasal *L. pneumophila* infection was evaluated *in vivo*. Assessment of CFU levels at 24 h p.i. showed no differences in the lungs of WT and CLEC12A-deficient mice (see Figure 6A). However, a non-significant trend at 48 and 96 h towards lower bacterial burdens in the lungs of CLEC12A-deficient mice suggested that the receptor might have a small negative modulatory effect on the immune response *in vivo*. CLEC12A is a CLR harboring an ITIM domain in its cytoplasmic tail. Upon binding of its ligands MSU, plasmodial hemozoin, or *mycobacterial* mycolic acids, CLEC12A was found to counteract the cell-activating kinase Syk, thereby inducing either an anti-inflammatory or stimulating an adaptive immunity-promoting signaling cascade^{140,146,148}. The by-trend lower bacterial burdens in the lungs of *Clec12a*^{-/-} mice potentially suggest that the receptor might be involved in anti-inflammatory signaling and the subsequent suppression of various proinflammatory cytokines during *L. pneumophila* infection. However, no differences in expression levels of *Ifnb1* in the lungs of WT and *Clec12a*^{-/-} mice were observed at the 24 h time point after infection (see Figure 6D).

The analysis of some cytokines known to play a crucial role in the immune response against *L. pneumophila*, such as IFN γ , TNF α , and IL-6^{28,51,255,289}, did not show differences between WT and *Clec12a*^{-/-} animals, and the results therefore do not support any non-redundant role of CLEC12A in the early immune response against the bacterium (see Figure 6E, F, G). However, it should be noted that even though no significant difference in cytokine levels in the lungs of WT and *Clec12a*^{-/-} mice was observed, data points derived from samples of *Clec12a*^{-/-} mice showed some variance. This variability could be due to technical issues during sample processing. However, no variance was observed for the WT samples obtained during the same experiment and processed at the same. Still, it cannot be fully excluded that a potential effect of the receptor on cytokine levels during pulmonary infection is present but masked by the variance observed here.

The action of many PRRs during *L. pneumophila* infection leads to the secretion of proteins from AMs with functions in the subsequent immune response, such as the recruitment of

other immune cell populations to the site of infection. For example, PMNs and iMonos are rapidly recruited into the lung during *L. pneumophila* infection, and critically contribute to the host defense²¹³. Considering the recently described anti-inflammatory role of CLEC12A and the small trend towards lower CFU levels in *Clec12a*^{-/-} compared to WT mice at later time points during infection, potential differences in the recruitment of specific cell populations were considered possible. However, a flow cytometry analysis of PMNs and iMonos and of the tissue-resident AMs revealed no differences between WT and *Clec12a*^{-/-} mice at the 24 h time point post infection (see Figure 7). Conclusively, the results of the *in vivo* analysis indicate no impact of the receptor during an *L. pneumophila*-induced pneumonia in mice. It should be noted that only the 24 h time point was investigated for cytokine production during *L. pneumophila* infection. I cannot exclude the possibility that CLEC12A has a function in suppressing cytokine response at earlier stages of infection, which later becomes masked by other PRR-mediated signaling cascades. Investigation of the pulmonary immune response at, e.g., 12 h after infection, could aid to further exclude an impact of the receptor on the immune response against *L. pneumophila*. Furthermore, it is essential to consider that the impact of specific CLRs on bacterial infections might vary based on factors such as the mouse model and the bacterial strain used, like in the case of Mincle in pneumococcal infections, as demonstrated in recent studies^{123,290}. Consequently, it remains possible that an effect of CLEC12A on the immune response would have been observed with a different *L. pneumophila* strain.

The *in vivo* model used in this study allowed for the assessment of the role of the receptor during pulmonary infection. Studies on various CLRs, such as Dectin-1, mannose receptor, and Mincle in the context of *Mycobacterium tuberculosis* infection had shown that the receptors were implicated in the control of the infection *in vitro* but seemed to have a redundant role during *in vivo* infection²⁹¹⁻²⁹³. To investigate if a similar effect could become observed for CLEC12A and if the receptor has a specific function in macrophages during *L. pneumophila* infection, an *in vitro* study was conducted using BMMs isolated from WT and *Clec12a*^{-/-} mice. The infection studies revealed that the receptor does not seem to have a role in bacterial replication, type I IFN expression, or TNF α production (see Figure 8). In addition to the *L. pneumophila* wt strain, the flagellin-deficient mutant Δ *flaA* was used in this study. As for the infection with wt bacteria, no differences were observed between WT and CLEC12A^{-/-} cells infected with Δ *flaA*, suggesting no major agonistic activity of *L. pneumophila*-derived flagellin. Studies from the group of Prof. Bernd Lepenies

(Tierärztliche Hochschule Hanover), with whom we have collaborated, aimed to investigate which part of *L. pneumophila* is recognized by CLEC12A. As mentioned before, CLEC12A was identified to bind crystalline ligands, such as MSU and hemozoin^{140,146}. In addition, pathogen-derived molecules were reported as ligands for the receptor^{140,148}, and the results from the binding study suggest that CLEC12A binds to PAMPs of *L. pneumophila*²⁶¹. No specific binding to a flagellin mutant (*AflaA*) was observed in a flow cytometry assay. Furthermore, by using the *L. pneumophila* LPS mutant TF 3/1, as well as purified *L. pneumophila* LPS, an interaction of CLEC12A and LPS was excluded, as no specific binding was observed in flow cytometry and ELISA assay, respectively²⁶¹. Finally, a dot-blot-based lectin assay that investigated the binding of CLEC12A to proteinase K-treated *L. pneumophila* lysates led to the exclusion of (glyco-)proteins as putative bacterial ligands²⁶¹. Given the recent findings that have shown the binding of CLEC12A to mycolic acids, a major and specific lipid component of the mycobacterial cell envelope, from different mycobacterial species¹⁴⁸, it would be interesting to investigate the binding of isolated *L. pneumophila*-derived lipid fractions to CLEC12A and to evaluate their agonistic activity. However, based on the results from the group of Prof. Lepenies, it cannot be fully excluded that the observed binding of CLEC12A to *L. pneumophila* might be unspecific, particularly with regard to the results from the *in vivo* and *in vitro* assays conducted in this study.

Finally, a functional infection study was conducted in human BLaER1-derived macrophages to assess the receptors' role during *L. pneumophila* infection in human cells. The use of the BLaER1 cell line was considered a well-suited model for studying the immune response to *L. pneumophila*, as these cells have been reported to share more resemblance with primary human monocytes and macrophages than many of the commonly used cell culture models such as the U937 and THP1 cell lines^{274,275}. I demonstrated that BLaER1-derived macrophages express CLEC12A and allow replication of *L. pneumophila* to a similar extent as human primary AMs (see Figure 9), indicating that these cells represent a suitable model for the study of *L. pneumophila* interaction with human macrophages. However, the investigation of bacterial replication as well as of cytokine production in WT cells and CLEC12A-deficient BLaER1-derived macrophages revealed no differences: Specifically, no differences in CFU levels as well as in expression levels of *IFNB1*, *IL1B*, and *TNFA* nor in levels of IP-10, IL-1 β , and TNF α were detected upon infection (see Figure 10). Taken together, the data indicate that CLEC12A has no major impact on the immune response in

human macrophages. However, it cannot be excluded that the receptor might be involved in the production of cytokines that were not assayed in this study.

To conclude, my studies do not support a functionally relevant role of CLEC12A during the early phase of *L. pneumophila* infection. Since neither bacterial control nor cytokine production seemed to be influenced by the receptor, additional potential effects of the receptor upon binding of *L. pneumophila*, e.g., its intracellular signaling or autophagy, were not investigated. A previous study indicated a role of CLEC12A in regulating autophagy in *Salmonella*-infected cells¹⁴⁷. It cannot be excluded that CLEC12A affects autophagy during *L. pneumophila* infection and this effect is masked by the action of bacterial effectors of *L. pneumophila* that were found to interfere with autophagic degradation of bacteria in the LCV^{294,295}. Further studies using a different *L. pneumophila* strain that lacks such effectors might help to further exclude a role of CLEC12A in *Legionella* infection. Furthermore, PRRs are often somewhat functionally redundant and exhibit cross-talk between receptors from their own and different PRR families²⁹⁶. It is, therefore, possible that the single loss-of-function approach used in this study to investigate the role of CLEC12A might not pinpoint a visible phenotype during *L. pneumophila* infection. This phenomenon was often seen with other PRRs, e.g., for TLRs during bacterial infections^{93,297}, and may cause difficulties in assessing the impact of the receptors to, e.g., susceptibility of host cells and the activated immune cascades. It can, therefore, not be fully excluded that a phenotype would have been observed when evaluating CLEC12A-deficiency in combination with other PRR knock-outs during *L. pneumophila* infection.

4.2. Summary - A global view on the transcriptomic and proteomic response in *L. pneumophila* infected AMs

Most studies investigating the host-pathogen interaction between *L. pneumophila* and its eucaryotic host cell have been done in hematopoietic macrophages as cell culture models, such as immortalized cell lines, human PBMCs or murine BMDMs^{262–264}. In general, these macrophage models have provided very important insights into the interaction of the bacterium with host cells but likely do not fully recapitulate the biological processes induced by the intracellular infection in tissue-resident AMs for several reasons: First, most tissue-resident macrophages have a greater life-span compared to hematopoietic macrophages. Second, they have a self-replicating capacity, which has not been observed for hematopoietic macrophages. Third, tissue-resident AMs are mostly of embryotic origin, while

hematopoietic macrophages originate from the bone marrow^{158,298,159,299}. Finally, *in vitro* culture systems lack most of the specific factors characterizing the microenvironment in the lung that might shape the transcriptomic, proteomic, and metabolomic phenotype of tissue-resident AMs^{187,262,266}. As a consequence, responses of cells to infections *in vitro* might differ from the *in vivo* scenario, as it has been recently observed for *M. tuberculosis* infection: While *in vitro* infected BMDMs showed a fast proinflammatory response upon infection with *M. tuberculosis*, *in vivo* infected AMs showed a delayed proinflammatory phenotype due to transcription factor NRF2-dependent activation of cell protective gene expression programs²⁹⁹.

To address this issue, the second part of this study focused on the transcriptomic and proteomic response in AMs in the early phase of infection (12-14 h after infection) of *L. pneumophila* infection *in vivo*. By using GFP-expressing virulent, intracellularly replicating *L. pneumophila* (Δ *flaA* lacking flagellin and therefore evading restriction by the NAIP5/NLRC4 inflammasome) as well as avirulent, not intracellularly replicating *L. pneumophila* strains (Δ *dotA* lacking the T4SS), a subsequent FACS-sort allowed to discriminate infected- and non-infected bystander AMs from murine BALF samples. Sorted AMs were subsequently investigated regarding their transcriptomic and proteomic response to the infection by bulk RNA-seq and mass spectrometry. Additionally, a sc RNA-seq analysis of leucocytes isolated from *L. pneumophila*-infected mice was performed at 6 and 20 h after infection.

I found that AMs isolated from Δ *flaA*-infected mice upregulate proinflammatory and immunoregulatory genes. The Δ *flaA*-induced upregulation appeared to be slightly more robust compared to the induction of these genes in AMs from Δ *dotA*-infected mice, perhaps related to the enhanced T4SS-dependent activation of the transcription factor NF- κ B in Δ *flaA*-infected AMs^{49,67,300}. DEGs between Δ *flaA*-infected vs. Δ *flaA*-bystander were similar to the DEGs in AMs from Δ *flaA*-infected mice vs. PBS-treated animals, indicating that bystander AMs show a similar expression profile as AMs from PBS-treated mice and are thus not activated at this early stage of infection.

By correlating the transcriptome to the proteome data obtained from AMs of Δ *flaA*- or Δ *dotA*-infected mice as well as from AMs of PBS-treated animals, it was found that concordantly upregulated genes and proteins in Δ *flaA*-infected AMs are associated with inflammatory pathways and that the cholesterol biosynthesis is downregulated in Δ *flaA*-infected cells on both mRNA and protein levels. An investigation of the differential

regulation of the mRNAs and corresponding proteins found that the translation of some proinflammatory transcripts, such as IL-1 β , CCL6, and CCL9, seemed to be impaired in a T4SS-dependent manner in AMs during *L. pneumophila* infection *in vivo*. On the contrary, some proteins appear to bypass the potential translational impairment in *AflaA*-infected AMs, including the proinflammatory cytokine IL-1 α , the transcription factor ATF3, the cytokine GDF15, and the NF- κ B regulator A20. The results from the sc RNA-seq analysis also demonstrated upregulation of these genes at 6 and 20 h p.i. in *AflaA*-infected AMs.

In conclusion, the presented study provided a unique insight into the global transcriptomic and proteomic response in tissue-resident AMs during early *L. pneumophila* infection *in vivo*. The results will be discussed in more depth in the following chapters.

4.2.1. A slightly stronger proinflammatory gene transcription was observed in AMs infected with *L. pneumophila AflaA* as compared to cells infected with *AdotA*

The activation of the antibacterial defense during *L. pneumophila* infection in macrophages is mediated by PAMP recognition by various PRRs at the cell surface, e.g., by TLR5 and TLR2, or in the host-cytosol, e.g., by NOD1^{220,221,228}. PRR activation induces different downstream signaling cascades that result in the transcription of different proinflammatory cytokines and antibacterial molecules via the transcriptional regulator NF- κ B as well as MAPK signaling^{263,301–303}. In the presented study, AMs isolated from mice that were infected for 12 to 14 h with virulent *L. pneumophila AflaA* strain showed a strong upregulation of several proinflammatory and immunoregulatory genes, such as *Ccl3*, *Ccl9*, *Illa*, *Tnfa*, and *Tnfaip3* (see Figure 13). Additionally, the enrichment of pathways that were associated with different immune responses and immunoregulatory activity, such as, e.g., the Hallmark term M5932 “inflammatory response”, were observed in *AflaA*-infected AMs, suggesting an overall proinflammatory transcriptomic state of *AflaA*-infected AMs (see Figure 14). Most of these upregulated genes and pathways in *AflaA*-infected AMs were also upregulated in *AdotA*-infected AMs. This suggests that their expression is, at least partly, independent of the T4SS, cellular uptake, and cytosolic PRRs but driven by detection at the cell surface by, e.g., TLRs. In support of this assumption, the results from the GSEA analysis revealed the upregulation of genes driving the “TLR1 TLR2 cascade” (see Figure 14) in both *AflaA*- and *AdotA*-infected AMs. In theory, this gene set describes the co-activation of TLR2 and TLR1 by various bacterial ligands, e.g., *mycobacterial* triacylated lipoproteins, which trigger the subsequent activation of the transcriptional regulator NF- κ B as well as apoptotic

cascades³⁰⁴. However, whereas similar genes were found to be upregulated in *ΔflaA*- and *ΔdotA*-infected AMs, fold changes for most of the proinflammatory transcripts were observed to be lower in *ΔdotA*-infected compared to *ΔflaA*-infected AMs (see Figure 13C). This observation is potentially due to the enhanced activity of NF-κB caused by cytosolic PRR-activation, such as NOD1, NOD2, and cGAS in *ΔflaA*-infected AMs^{68,228,241}. This observation is also reflected by the results of the enrichment analysis (see Figure 14): Most of the genes driving the upregulated Hallmark and Reactome pathways in AMs were more strongly induced upon *ΔflaA*- as compared to *ΔdotA* infection (see Figure 14). This effect was most prominent for the gene set “TNFα signaling via NF-κB”, which describes a set of genes regulated in their expression by NF-κB in response to TNFα signaling. TNFα, thought to be mainly produced by uninfected bystander cells such as AMs, PMNs, iMonos, and DCs, plays a critical role in the host defense against *L. pneumophila* infection⁷¹. Several *in vitro* studies demonstrated that TNFα restricts the replication of the bacterium in murine BMDMs, rat AMs, and human airway epithelial cells *in vitro* and that NF-κB signaling downstream of TNFR1 activation is critical during this process^{255,259,260,305}. The findings from the presented bulk RNA-seq study suggest that NF-κB activation by TNFα also plays a significant role during *L. pneumophila* infection in murine tissue-resident AMs *in vivo*. The overall stronger enrichment of this pathway in *ΔflaA*-infected cells could either indicate that the pathway is reinforced in a T4SS-dependent manner in AMs or that production of TNFα by activated bystander cell populations is overall stronger during the *ΔflaA*-infection, as the *ΔdotA* strain is faster cleared due to phagocytic degradation within AMs itself^{24,35,36}. Finally, the prominent role of NF-κB regulation during *ΔflaA* infection in AMs *in vivo* is also emphasized by the additional investigation of gene set enrichment using the *tmod* package, which showed a stronger enrichment of the module “myeloid, dendritic cell activation via NF-κB” in *ΔflaA*-infected compared to *ΔdotA*-infected AMs.

The overall stronger proinflammatory response in virulent infected AMs could also be explained by the *effector-triggered response*, a hallmark of the *L. pneumophila* infection, observed *in vitro* (see Chapter 1.1.2.)⁴⁹. The effector-driven blockage of host protein synthesis leads to a prolonged NF-κB activation as well as prolonged MAPK-signaling, which results in a hyper-induction of specific proinflammatory transcripts that bypass the translational impairment and drive the immune response in infected cells^{67,69,300}. Among the top upregulated transcripts in *ΔflaA*-infected AMs were genes that have already been

described as being expressed in the course of the T4SS-dependent effector-triggered response in BMDMs as well as in human monocyte-derived macrophages upon virulent *L. pneumophila* infection, such as e.g. *Il23a*, *Gem* or *Cd83*^{67,306} (see Figure 13). Consequentially, these genes' expression was lower in $\Delta dotA$ -infected AMs (see Figure 13C). Whereas it seems that tissue-resident AMs exhibit an effector-triggered transcriptomic profile upon virulent *L. pneumophila* infection, the full range of genes regulated in this manner remains unclear and would need further investigation. A possible approach to identify the full set of genes would be to perform a similar *in vivo* infection experiment using different *L. pneumophila* strains that lack one or more of the effector proteins, such as Lgt1-3, SidI, and SidL⁶⁷, which were so far identified to impair the host-protein synthesis and trigger the hyper-induction of specific genes in macrophages⁴⁵. A subsequent global comparison of the gene expression between mutant and *L. pneumophila* WT or $\Delta flaA$ infection could highlight which host genes are affected in their expression by bacterial effector proteins and part of the effector-triggered response in *L. pneumophila*-infected AMs *in vivo*.

4.2.2. Many proinflammatory transcripts induced upon $\Delta flaA$ infection in AMs seem not to be translated into proteins

Given that *L. pneumophila* has been described to manipulate hematopoietic macrophages *in vitro* by blocking host protein synthesis^{36,41,67}, this study aimed to compare transcription and protein expression in $\Delta flaA$ -infected AMs *in vivo*. The enrichment analysis of concordantly regulated genes and proteins provided insight into which pathways are affected in their regulation in virulent and avirulent infected AMs on an mRNA and protein level (see Figure 18). It was found that molecules in *L. pneumophila*-infected AMs were strongly associated with the Hallmark term “TNF α signaling via NF- κ B”. Whereas most of the transcripts driving this pathway were found to be upregulated in both $\Delta flaA$ - and $\Delta dotA$ -infected AMs, several proteins were classified to be not regulated (“unchanged”) or even downregulated for this pathway. This effect was seen as more prominent in $\Delta flaA$ - compared to $\Delta dotA$ -infected AMs. Given that no bacterial effector translocation into the host cytosol occurs during $\Delta dotA$ infection, this finding indicates that transcripts of this pathway might be impaired in their translation by $\Delta flaA$ due to T4SS-dependent effector activity.

As an approach to characterize differential regulation of molecules on transcript and protein levels in $\Delta flaA$ - and $\Delta dotA$ -infected AMs, nine categories were defined, based on whether

they were up- or downregulation or unchanged in their expression on mRNA and protein levels (see Figure 19). This allowed to identify 29 proteins that were upregulated on both mRNA and protein levels in *AflaA*-infected AMs (see Figure 20A). Of these proteins, 16 were specifically upregulated in *AflaA*-infected AMs, whereas 13 molecules were also detected as upregulated on mRNA and protein levels in *ΔdotA*-infected AMs (see Figure 20B). Given the numerous upregulated transcripts in *AflaA*-infected AMs that were observed in the bulk RNA-seq analysis (see Figure 13), the small number of transcripts that translate into proteins in *AflaA*-infected AMs further supports a potential global block of translation due to T4SS-dependent effector activity that only a few proteins may bypass. Based on the categories defined for mRNA and protein expression (see Figure 19), potentially translation-impaired targets were assumed to be upregulated on the mRNA level and either downregulated (RNA↑ protein↓) or not regulated (RNA↑ protein=) on the protein level. By investigating which proteins were assigned to these two categories in *AflaA*- but not in *ΔdotA*-infected AMs, 576 proteins could be identified that are potentially impaired in their translation in a T4SS-dependent manner in AMs *in vivo* (see Figure 20E). In line with the observations published from *in vitro* studies, it was found that AMs seem to upregulate transcripts of inflammatory molecules that are not translated on protein level^{36,41,67}. Among those transcripts were, e.g., *Ccl9*, *Cxcl16*, *Ccl6*, *Il1b*, and *Nfkbiz*, supporting the hypothesis that numerous proinflammatory proteins are globally impaired during virulent *L. pneumophila* infection. Unfortunately, some of the proteins previously shown to be blocked during *L. pneumophila* infection in macrophages *in vitro* studies, such as TNFα, IL-6, and IL-12⁴⁹⁻⁵¹, were not detected in our mass spectrometry analysis of AMs from both *AflaA*- and *ΔdotA*-infected mice. Therefore, a conclusion about whether these molecules are also translationally blocked in AMs during *in vivo* infection with *L. pneumophila ΔflaA* is not possible. The absence of these proinflammatory molecules in the proteome of AMs from *AflaA*- and *ΔdotA*-infected mice, as well as PBS-treated animals, is potentially due to a technical limitation of the mass spectrometry approach used in this study rather than a biological phenomenon. Due to the low number of infected AMs in this study, an unstimulated murine BMDM sample of 1*10⁶ cells was used as a reference for protein annotation and quantification. Hence, only proteins detected in the reference BMDM sample were quantified in the protein samples from AMs of *L. pneumophila* or PBS-treated mice. It cannot be excluded that more proinflammatory proteins would have been detected if, e.g.,

an LPS-stimulated BMDM sample had been used to cover the detection of more proinflammatory molecules.

However, an interesting finding of this study was that the proinflammatory cytokine IL-1 β was also categorized as “RNA \uparrow protein=” in *AflaA*-infected AMs. In contrast, *AdotA*-infected AMs show upregulation of IL-1 β on both mRNA and protein levels. Published data from *in vitro* infection studies in BMDMs indicate that IL-1 β is one of the proteins that bypasses the effector-mediated impairment of protein synthesis during *L. pneumophila* infection and play a role in bystander activation⁷¹. An *in vivo* study demonstrated that while IL-1 α seems to indeed play a critical role in the clearance of the infection, IL-1 β seems to be dispensable for PMN recruitment during *L. pneumophila* WT infection⁷⁰. The data from the bulk RNA-seq and proteome analysis shown here support the assumption that the role of IL-1 β might be limited *in vivo*, as its translation appears to be blocked in a T4SS-dependent manner, whereas IL-1 α seems to bypass the translational block and is upregulated on both mRNA and protein levels in *AflaA*-infected AMs (see Figure 20A). However, further studies would need to explore the potential impairment of IL-1 β , e.g., by performing western blot analysis or intracellular FACS-staining of infected AMs from *AflaA*-infected mice.

Finally, the data presented in this study indicate that several proteins involved in the NF- κ B-signaling might be potentially impaired in translation in a T4SS-dependent manner. The results from the DISCO analysis and subsequent enrichment analysis showed that several upregulated transcripts, which are part of the Hallmark pathway “TNF α signaling via NF- κ B” and are, by definition, assumed to be regulated in their expression by NF- κ B in response to TNF α -signaling, were not concordantly regulated on protein level (see Figure 18D). This supports the hypothesis that a major percentage of proinflammatory transcripts regulated by NF- κ B are blocked in their translation. Another transcript that was found among the molecules defined as “RNA \uparrow , protein=” in *AflaA*-infected, but not *AdotA*-infected AMs (see Figure 18D) was NFKBIZ. *Nfkbiz* is considered a primary response gene induced rapidly in macrophages as a response to LPS³⁰⁷. The transcript encodes for the protein I κ B ζ , a transcription factor that binds to NF- κ B in the nucleus and co-regulates several secondary response genes such as *Il6*, *Il12*, and *Ifng*^{308,309}. Studies have indicated that the transcription factor might have a dual role in regulating gene transcription. Depending on the respective target genes, I κ B ζ seemingly acts as a coactivator or repressor of proinflammatory genes, e.g., by inducing expression of *Il6* or repressing expression of *Tnfa*, during inflammation^{309,310}. Given the dual role of the protein, its potential impairment during *L. pneumophila*

infection could be in favor of the bacterium or the host cell. Loss-of-function and overexpression studies could thereby aid in addressing the question of how a potential effector-driven translation impairment affects the outcome of the infection with *AflaA*. Interestingly, the gene *Tnfrsf1b*, which encodes for one of the two TNF α -receptors (namely TNFR2), was among the candidates that were identified as potentially blocked in their translation (see Figure 18D). TNF α -signaling has been described as an essential component of the host-response during *L. pneumophila* infection. TNF α -signaling via TNFR1 is considered to contribute to bacterial clearance as well as regulation of proinflammatory cytokine production in AMs²⁵⁸. Deficiency of TNFR2 in mice seems to induce excessive inflammation during the infection *in vivo* and is accompanied by PMN accumulation in the lung and high mortality rates. However, the precise mechanism of how TNFR2 controls inflammation remains unclear²⁵⁸. It is possible that the putative impairment of TNFR2 observed in our study could contribute to establishing a high inflammatory state in the lung *in vivo* and might contribute to an increased PMN influx. Despite the protective role of PMNs during *L. pneumophila* infection, the increased influx of these cells is also assumed to contribute to the pathology associated with LD^{70,311,312}. Furthermore, studies indicate that an exaggerated local inflammation might favor intracellular bacterial replication of, e.g., *Pseudomonas aeruginosa* or *Staphylococcus aureus* in human monocytes *in vitro*³¹³. Thus, further investigation is requested to unravel if and how a potential effector-driven impairment of TNFR2 in AMs could favor bacterial infection.

Conclusively, the data obtained from this study suggest that a broad number of proinflammatory transcripts is translationally impaired in *AflaA*-infected AMs in a T4SS-dependent manner and that only a small number of proteins bypasses this transcriptional block, which will be discussed in the next chapter (see 4.2.3.). However, as mentioned above, further studies need to be conducted to evaluate the translation-impairment of selected transcripts and to assess their absolute quantity in *AflaA*-infected cells compared to *AdotA*-infected or uninfected AMs.

4.2.3. Molecules that were upregulated on mRNA and protein levels in *AflaA*-infected AMs might have relevance for the immune response to *L. pneumophila* infection

One main objective of this thesis was to identify molecules that bypass the translational block in *L. pneumophila* infected AMs and, therefore, might have an essential role in regulating the immune response. Those molecules were expected to be upregulated on both

the mRNA and the protein level, and 29 proteins fell into this category in *ΔflaA*-infected AMs (see Figure 20A), with 16 of them being exclusively upregulated in *ΔflaA*- but not *ΔdotA*-infected AMs (see Figure 20B). Many of these 29 proteins were found to have a low base mean in the bulk RNA-seq data, indicating a generally low average mRNA expression, and this effect was especially seen for the 16 proteins that were upregulated specifically in *ΔflaA*- but not *ΔdotA*-infected AMs. A similar effect was observed for the initial investigation of upregulated proteins in *ΔflaA*- and *ΔdotA*-infected AMs (see Chapter 3.2.4.) and highlights one of the limitations of this study: The location of AMs in the airways makes them the first cells to encounter and phagocytize inhaled particles, pollutants, and pathogens. At the same time, AMs are constantly active in cleaning the airways from the pulmonary surfactant and mediate efferocytosis, the ingestion of dying or dead cells, to prevent an unwanted overshooting of inflammation in the unperturbed lung^{19,149,150,179}. During infection, activated AMs remain highly phagocytic³¹⁴. It cannot be excluded that some of the proteins identified by the proteomic analysis of AMs represent molecules from engulfed cells rather than infection-induced upregulation of endogenous proteins. I, therefore, only included proteins in the downstream analyses for which the corresponding mRNA was also found in AMs. However, in the case of the 16 proteins mentioned above, the expression of the corresponding mRNA was very low. Therefore, it cannot be excluded that some of these molecules are the result of phagocytic “contamination”. Additional studies are requested to clarify if the concordantly upregulated molecules identified in this study (see Figure 20A, B) are all endogenously expressed in *L. pneumophila*-infected AMs on both the mRNA and the protein level. Recently, the cultivation of murine AMs *ex vivo* has been described and proposed as a model to investigate AMs during, e.g., inflammation and infection, as these cells show a phenotype largely similar to tissue-resident AMs^{267,268}. Preliminary unpublished results of our lab have indicated that these cells serve as replication niches for *L. pneumophila* and show similar upregulation of gene expression and cytokine production upon infection as primary murine AMs (master thesis of Léa Boillot, master thesis of Lisbeth Hasler, unpublished). Evaluating the expression of both the mRNA and the protein level of the upregulated molecules found in this study in *ex vivo* cultivated AMs upon *L. pneumophila* infection might further elucidate if upregulation occurs in a cell-intrinsic manner.

However, some molecules classified as upregulated on mRNA and protein levels in *ΔflaA*-infected AMs have robust mRNA expression levels and might play a pivotal role during *L. pneumophila* infection in AMs *in vivo*. Among those proteins were e.g., IL-1 α , ATF3,

GDF15, and A20 (*Tnfaip3*) (see Figure 20A). The results from the sc RNA-seq study also demonstrated the upregulation of these candidate genes at 6 h and 20 h in AMs infected with *AflaA* (see Figure 23B, C) and support their potential role during the immune response *in vivo*.

The role of the cytokine IL-1 α was already intensively studied during *L. pneumophila* infection. It was found to be one of the proteins that bypass translation impairment in macrophages, thereby having an essential role during infection by activating bystander cells^{49,70}. The data collected in this study support these findings and suggest that the protein has an important role in the immune response against *L. pneumophila* in AMs *in vivo*.

An interesting molecule discovered to be upregulated in *AflaA*-infected AMs is the activating transcription factor 3 (ATF3). ATF3 was reported to have essential roles in the modulation of metabolic and immunity pathways. In macrophages, its expression is upregulated in response to TLR stimulation by, e.g., LPS and various other stimuli, such as type I and II IFNs. ATF3 subsequently acts in a negative feedback loop, as it binds to the promoter region of target genes, including *Il6*, *Tnfa*, and *Ifnb* and the pro-apoptotic genes *Bak* and *Bax*, where it acts as a repressor and promotes an anti-inflammatory state^{315–317}.

Besides its anti-inflammatory role, the transcription factor was also found to have a proinflammatory function: During *Streptococcus pneumoniae* infection in murine macrophages, pneumolysin was reported to induce the expression of ATF3. Upon complex formation with the transcription factor activator-protein-1 (AP-1) family protein JUN (*c-Jun*), ATF3 was shown to stimulate the production of TNF- α , IL-1 β , and IFN- γ ^{318,319}. The protein c-Jun, encoded by *Jun*, was found to be among the proteins regulated as “RNA \uparrow protein=” in *AflaA*-infected AMs *in vivo* and, therefore, might also be impaired in translation (see Figure 20F). However, among the concordantly upregulated proteins in *AflaA*-infected AMs was JUNB (*Junb*), another transcription factor of the AP-1 family, and it might be possible that ATF3 and JUNB complex formation could have a similar proinflammatory effect on the gene regulation in *L. pneumophila*-infected AMs. Investigating expression levels of *Il1b* and *Tnfa* upon *L. pneumophila* infection in AMs with a single and double *knock-out* for ATF3 and JUNB could provide insight into if and how ATF3 regulates gene expression. A recently published study by Subramanian *et al.* (2023) reported that ATF3 bypasses the translational block mediated by the *L. pneumophila* effector protein SidI in human macrophages³²⁰. The results from the study suggest that the transcription factor has a major role in the ribosomal stress response and orchestrates the transcription of stress-

inducible genes to promote cell death of infected cells ³²⁰. Further studies need to be conducted to unravel whether the transcription factor has a similar role during the immune response to *L. pneumophila* in tissue-resident AMs *in vivo*.

Another potentially interesting candidate for further investigation is the cytokine growth differentiation factor 15 (GDF15), which was among the upregulated proteins in *AflaA*-infected AMs and has a binding site for ATF3 and for several other transcription factors on its promoter region ³²¹. The receptor belongs to the transforming growth factor beta (TGF- β) superfamily of proteins. It is assumed to have a role in many biological processes, including energy homeostasis, body weight regulation, inflammation regulation, apoptosis, growth, and differentiation, as well as several diseases, including diabetes, cancer, cardiovascular disease, and obesity ^{321,321,322}. Over the past years the proteins' role has mainly been studied in the context of metabolic health and body weight control. In this context, the GDNF Family Receptor Alpha Like (GFRAL) protein was revealed to be the receptor for GDF15 and critical for the appetite-suppressing effects of GDF15 ³²²⁻³²⁴. Interestingly, GFRAL has so far only been found to be expressed in a small cell population in the brain stem, indicating that the signaling effects of GDF15 could be translated via the sympathetic nervous system ³²⁴. The expression of *Gdf15* in various cell types and subsequent increasing circulating GDF15 levels has been found under conditions often linked to mitochondrial stress, which could be a mechanism involved in its regulation during *L. pneumophila* infection. Therefore, similar to ATF3, upregulation of GDF15 might result from the bacterial modulation of mitochondrial dynamics and subsequent dysfunction ^{29,325}. Finally, the protein A20, encoded by *Tnfrsf3*, could be of interest for further functional studies in the context of *L. pneumophila* infection in AMs *in vivo*. A20 is a deubiquitinase and an essential negative regulator of NF- κ B and inflammation ³²⁶. It was found that mice deficient for A20 died prematurely due to the development of spontaneous and uncontrolled multi-organ inflammation ³²⁷. The upregulation of A20 in *L. pneumophila*-infected AMs may balance the hyper-induction of non-translated transcripts that accumulate in infected AMs during the *effector-triggered response* (see Chapter 4.2.1.) ⁶⁷. While TNF α -signaling was found to induce A20 expression globally, A20 suppresses TNF α -induced apoptosis and stress response ³²⁸. It remains open to explore if A20 has a similar role in the context of an *L. pneumophila* infection, as a shift of infected AMs towards an anti-inflammatory state would rather have an adverse outcome for the host cell.

Further investigation will be necessary to unravel the possible effects of the identified molecules during infection with *L. pneumophila* and to assess further if their upregulation in

AMs has an essential function in the immune response *in vivo*. A possible first step could be to study *L. pneumophila* infection in selected murine knock-out models, e.g., with *Atf3*^{-/-} or *Gdf15*^{-/-} mice. Comparing the outcome of the infection by various readouts such as, e.g., bacterial loads, body weight, and expression and production of proinflammatory cytokines to WT control mice, more insight could be gained to answer the question of how these molecules may affect antibacterial immunity and inflammation. Another approach to study the impact of these individual molecules in AMs during infection with *L. pneumophila in vivo* would be using *Csf2ra*^{-/-} or *Csf2rb*^{-/-} mice. Mice of both these lines show impaired GM-CSF signaling due to a mutation in the α or β -chain of the GM-CSF receptor. Consequentially, the maturation and function of AMs are impaired in the lungs of *Csf2ra*^{-/-} and *Csf2rb*^{-/-} animals, leading to insufficient surfactant clearance and development of PAP^{159,164,165}. Recently, the intranasal transfer of *ex vivo* cultivated and primary AMs into *Csf2ra*^{-/-} and *Csf2rb*^{-/-} animals at a neonatal age was shown to restore the alveolar niche and to prevent PAP development^{267,268}. Isolation of primary AMs from mice carrying a single knock-out for proteins of interest, e.g., *Atf3*^{-/-}, and transferring these AMs into lungs of neonatal *Csf2ra*^{-/-} or *Csf2rb*^{-/-} mice, would allow the generation of a murine model in which the investigation of specific proteins and their role in AMs during *L. pneumophila* infection is possible.

4.2.4. Bystander AMs in lungs of *L. pneumophila* infected mice might only be activated at the end of the bacterial replication cycle *in vivo*

As the manipulation of the host cell by *L. pneumophila* dampens the proinflammatory response of the infected cells, the antibacterial immune response might at least partly depend on the early activation of uninfected bystander cells. This effect was, e.g., recently observed for *M. tuberculosis* infection, where *in vivo* infected AMs showed an anti-inflammatory state due to an NRF2-driven antioxidant program for the first days of infection, while bystander AMs upregulate several proinflammatory pathways²⁹⁹. In the presented study, both *ΔflaA*- and *ΔdotA*-infected AMs were found to express chemokines such as *Cxcl1*, *Cxcl2*, or *Cxcl3* that have a known function in recruiting other leucocyte cell populations^{202,329}. Additionally, a strong expression of *Il1a* was observed in both *ΔflaA*- and *ΔdotA*-infected AMs (see Figure 13), and upregulation of IL-1 α was also observed on the protein level in *L. pneumophila*-infected AMs (see Figure 20A). Expression and secretion of IL-1 α have been described as critical in activating uninfected bystander AMs to produce proinflammatory cytokines, e.g.,

TNF α during *L. pneumophila* infection^{70,71}. Therefore, I initially assumed that bystander cells might already be activated at this early point of infection and might show a distinct proinflammatory profile. However, the results from the bulk RNA-seq study indicate that no distinct transcriptional activation of bystander AMs had taken place at the investigated time point (see Figure 15). On the contrary, bystander AMs exhibited a transcriptomic profile similar to AMs collected from BALF samples of PBS-treated mice. A possible explanation for this observation might be the early time point after infection chosen for this analysis, and activation of bystander AMs would perhaps have been observed at a later time point. As the bulk RNA-seq and the mass spectrometry analysis only allowed a relative but no absolute quantification of gene and protein expression, respectively, no explicit conclusion about the absolute IL-1 α levels in infected AMs at this time point can be drawn. It might, therefore, be possible that IL-1 α -signaling is not yet sufficient at the investigated time point to induce a bystander response. In favor of this were the results of the sc RNA-seq study, where an increased expression of proinflammatory cytokines such as *Tnfa*, *Il1a*, and *Il1b* in bystander AMs from *AflaA*-infected mice was observed at 20 h but not at 6 h p.i. with *AflaA* (see Figure 23). In line with this, a strong PMN influx was observed at 20 h of infection, arguing for sufficient IL-1 α signaling at this time point (see Figure 22B). However, the data derived from the sc RNA-seq study should be handled with care due to the lower bacterial dose of infection that was used for this experiment, compared to the bulk RNA-seq and proteome analysis. Therefore, the cellular response might differ from the observation of the bulk RNA-seq analysis. Additionally, only a few infected and non-infected bystander AMs were evaluated for the 20 h time point, as the strong influx of PMNs into the alveolar space at this stage of infection led to a relative decrease in the number of AMs being analyzed from the BALF samples. To further investigate the response of bystander AMs during *in vivo* infection of *L. pneumophila*, it would be advisable to repeat the infection experiment under the same condition as for the bulk RNA-seq analysis and investigate the transcriptome at later stages during infection to identify at which stage a bystander response can be observed *in vivo*.

4.2.5. The downregulation of the cholesterol biosynthesis in *AflaA*-infected AMs – an interplay between bacterial effectors and the antibacterial defense?

Finally, I found that AMs infected with *L. pneumophila AflaA* downregulate many molecules associated with the cholesterol biosynthesis on a mRNA and protein level (see Figure 18D

& 20C, D). During inflammation, macrophages can quickly reprogram their metabolism to promote or reduce inflammation and modulate their effector functions³³⁰. These changes in metabolism may be caused by environmental cues, such as the surrounding cytokine milieu, and might be associated with the polarization status of macrophages^{330,331}. Modulation of the cellular metabolism has been observed during infections with intracellular pathogens, e.g., due to the detection of PAMPs and the subsequent induction of antibacterial defense cascades⁶⁶. Another potential cause for changes in metabolism is the bacterial manipulation of the host cell, e.g., by effector molecules for nutrient supply to facilitate the pathogen's survival^{66,332}. *In vitro* studies in human macrophages have found that *L. pneumophila* infection induces a shift towards a Warburg-like metabolism characterized by increased glycolysis levels quickly upon infection and a decrease in OXPHOS. These alterations of metabolism occur partly in a T4SS-dependent manner, as the bacterial effector MitF has been found to mediate the OXPHOS downregulation due to mitochondrial fragmentation in the infected host cell. In contrast, the increase of glycolysis seems to occur independently of bacterial effector translocation from the LCV²⁹. It is assumed that the metabolic changes during *L. pneumophila* infection favor the bacterium and are essential for its replication, as amino acids, the primary energy source for growing *L. pneumophila*, can be synthesized from redirected glycolytic and TCA intermediate^{29,66}. The transcriptome and proteome data collected in this study provide no evidence for alterations in the metabolism of infected tissue-resident AMs regarding glycolysis or OXPHOS. This observation could be due to the kinetics of changes in metabolism that might not be present at the inspected time point or may result from metabolic differences between hematopoietic and tissue-resident macrophages, as tissue-resident macrophages are less dependent on glycolysis due to low glucose availability in their surrounding milieu³³³. Notably, no experimental quantification of metabolites was performed, and it cannot be excluded that changes are present but not directly visible on mRNA and protein expression levels. A quantification of glycolysis and OXPHOS rate by, e.g., Seahorse-Assay or in a FACS-based approach³³⁴, would be advisable to investigate if changes of metabolism are present in AMs during *L. pneumophila* infection. However, as mentioned before, the data from this study suggest changes in cholesterol metabolism during *L. pneumophila* infection in AMs *in vivo*. Cholesterol is an essential lipid in mammalian cells. As a crucial component of the eukaryotic membrane, it ensures its integrity, fluidity, and permeability by regulating the packing and phase separation of phospholipids³³⁵. Regulation of the cholesterol homeostasis occurs at the ER membrane, where intracellular cholesterol levels are sensed, to locally induce cholesterol biosynthesis

and packing of excessive cholesterol in its esterified form within lipid droplets for storage or export via ABC transporters³³⁶. Several enzymes involved in the cholesterol *de novo* biosynthesis, which is one possible way cells regulate their intracellular cholesterol homeostasis, were downregulated specifically in *AflaA*-infected AMs, such as HMGCS1, MVD, PMVK, or NSDHL (see Figure 20D). The expression of the enzymes driving cholesterol synthesis is regulated by the transcription factor sterol regulatory element-binding protein 2 (SREBP2) in response to cholesterol levels in the ER³³⁷. A critical enzyme for this regulatory mechanism is 3-hydroxy-3-methyl glutaryl coenzyme A (HMGCR), a rate-limiting enzyme in the cholesterol biosynthesis, as increased levels of cholesterol induce its proteolytic cleavage, which downstream signals to block SREBP2 activation³³⁸. In this study, HMGCR was classified as “mRNA =, protein level↓” (data not shown) in *AflaA*-infected AMs, which would explain the downregulation of cholesterol biosynthesis. Interestingly, the low-density lipoprotein receptor (LDLR) was significantly downregulated on protein level (see Chapter 3.2.5.). LDLR is expressed in the plasma membrane of most cells and regulates the import of low-density lipoproteins (LDL) from the extracellular space, which is another mechanism of how cells maintain their cholesterol homeostasis³³⁷. Finally, the upregulation of the cholesterol exporter ABCA1 on both mRNA and protein levels, specifically for *AflaA*-infected AMs (see Figure 20B), was observed. These findings suggest that while *de novo*-synthesis and cholesterol uptake in *AflaA*-infected AMs are specifically downregulated, *AflaA*-infected cells might also actively remove intracellular cholesterol via the cholesterol exporter. At this stage, it would be interesting to quantify the absolute levels of intracellular cholesterol at this time point of infection with *AflaA*, e.g., by flow cytometry using fluorescence-labeled perfringolysin O (PFO), a *Clostridium*-derived toxin, capable of binding to cholesterol, as described by Li et al. (2017)³³⁹.

A recent study by Ondari et al. (2023) aimed to investigate the link between intracellular cholesterol and *L. pneumophila* infection in BMDMs and found that successful infection is promoted by cholesterol³⁴⁰. The authors could show that disruption of cholesterol biosynthesis or cholesterol trafficking into the cell negatively affects bacterial survival, as it was associated with membrane rupture of the LCV at the early stages of infection. In line with this, early bacterial replication was enhanced in macrophages with a high cholesterol capacity and saturation. Microscopy analysis of different replication stages during *L. pneumophila* infection indicated that cholesterol presumably has a role in the replication onset in the established LCV³⁴⁰. Given that the downregulation of enzymes associated with the cholesterol biosynthesis was observed for *AflaA*-infected AMs, it seems that the cellular

response observed in AMs *in vivo* counteracts the replication-promoting effect of cholesterol at this time point. Therefore, the downregulation of cholesterol biosynthesis might be a cellular defense mechanism to restrict bacterial growth.

However, it is also possible that the observed downregulation of enzymes associated with cholesterol biosynthesis is due to the activity of bacterial effector proteins. It was found that the expression of cholesterol synthesis enzymes by SREBP2 is positively regulated by activation of mTOR³⁴¹. In murine BMDMs, mTOR activity has been found to be dampened in a Myd88-dependent manner during *L. pneumophila* infection, most likely as an antibacterial defense strategy, as reduced mTOR-dependent lipogenesis has been found to lead to LCV membrane instability^{341,342}. At the same time, bacterial effector proteins secreted from the T4SS have been found to regulate mTOR activity (see Chapter 1.1.2.). Whereas the impairment of mTOR by the effector protein SidE occurs most likely to facilitate the acquisition of free amino acids, the Lgt effector family was found to activate mTOR to suppress autophagy⁵⁷. It is possible that during temporal activation of mTOR by the *L. pneumophila* Lgt effector family, AMs might synthesize cholesterol, which promotes bacterial replication and LCV membrane integrity. On the contrary, impairment of mTOR for amino acid acquisition by the SidE effector family might be accompanied by a downregulation of cholesterol biosynthesis. It would, therefore, be interesting to investigate the temporal activity of SidE and Lgts effector translocation from the LCV *in vivo*. Furthermore, infection studies with *L. pneumophila* strains lacking these effectors could provide further evidence if the intracellular cholesterol homeostasis in AMs *in vivo* is affected by bacterial effectors or if its regulation is part of the cell-intrinsic defense.

5. Conclusion & Outlook

The intracellular pathogen *L. pneumophila* is one of the most common causes of community-acquired pneumonia in many parts of the world, and the severe form of the infection, Legionnaire's disease, is associated with high mortality rates. A global understanding of the pathogen-host interaction is inevitable to develop effective therapies. Moreover, acquiring a deeper understanding of how AMs, the main replication niche of *L. pneumophila*, respond to the infection could provide transferrable insights into the host-pathogen interaction of other medically relevant pathogens that target AMs, such as, e.g., *Mycobacterium tuberculosis*.

To this end, the cellular host's immune response to the bacterium and the pathways modulated due to the intracellular infection must be fully explored. Up to date, several *in vitro* studies using murine and human hematopoietic cell culture systems have aimed to unravel the mechanisms of how the infection is detected and which cell-intrinsic antibacterial defense strategies become activated in response to *L. pneumophila* in macrophages. However, the full range of the detection and defense strategies remains incompletely understood, and conventionally used infection models often only provide a limited reflection of how tissue-resident AMs respond to an infection *in vivo*.

Previous studies have found that the C-type lectin receptor CLEC12A binds to *L. pneumophila*. However, the data derived from the first part of this study demonstrated that CLEC12A does not seem to have a critical role in the innate immune response against *L. pneumophila* infection *in vivo* and in murine and human macrophages *in vitro*. Even though it cannot be entirely excluded that some effects of CLEC12A were missed due to the bacterial strain used, the choice of the mouse model, or the read-outs and time points chosen, the receptors' role seems to be rather redundant or not existing.

To address how tissue-resident AMs respond to the infection, the transcriptome and proteome of AMs during *in vivo* infections with virulent and avirulent *L. pneumophila* were investigated. Upregulation of proinflammatory genes and pathways was found to be, to some extent, enforced in a T4SS-dependent manner. The comparison of the transcriptome and proteome data further indicates that numerous transcripts associated with a proinflammatory and immunoregulatory function are impaired in translation in a seemingly T4SS-dependent manner, e.g., the proinflammatory cytokines IL-1 β and CCL9 or the transcription factor NFKBIZ. However, a few molecules seem to bypass the translational impairment in *AflaA*-infected AMs, including IL-1 α , ATF3, GDF15, and TNFAIP3. Although upregulation of IL-

1 α on mRNA and protein level was observed at 12 to 14 h p.i., uninfected bystander AMs seem to be only activated towards the end of the replication cycle, as indicated by the scRNA-seq study. Furthermore, the virulent infection seems to induce a downregulation of cholesterol biosynthesis.

The data collected from this study provides insight into the global response of AM to *L. pneumophila* on a transcriptome and proteome level. However, further studies are needed to confirm and expand some findings. Functional investigations into the role of identified candidate molecules, which are upregulated on mRNA and protein levels in response to the infection with virulent bacteria, are necessary to assess their impact on the immune response. Furthermore, it would be interesting to evaluate additional time points during the infection cycle of *L. pneumophila* in AMs to get better insight into the cellular response and, e.g., metabolic changes. At this point, it would be advisable to quantify different metabolites to detect changes that are not directly visible on the mRNA or protein level of the enzymes regulating the respective metabolic pathways.

Moreover, additional infection studies with different *L. pneumophila* strains lacking specific effector proteins would be interesting to obtain further information regarding which of the observed changes in infected AMs are due to bacterial manipulation. Finally, it would be interesting to compare the findings from this study to the transcriptional and proteome response in human AMs to investigate whether the observed regulatory mechanisms and pathways also have a role in human *L. pneumophila* infection.

6. References

1. Cordes, L. G. & Fraser, D. W. Legionellosis: Legionnaires' disease; Pontiac fever. *Med. Clin. North Am.* **64**, 395–416 (1980).
2. Fraser, D. W. *et al.* Legionnaires' Disease. *N. Engl. J. Med.* **297**, 1189–1197 (1977).
3. McDade, J. E. *et al.* Legionnaires' Disease: Isolation of a Bacterium and Demonstration of Its Role in Other Respiratory Disease. *N. Engl. J. Med.* **297**, 1197–1203 (1977).
4. Cunha, B. A., Thekkel, V. & Schoch, P. E. Community-acquired versus nosocomial Legionella pneumonia: Lessons learned from an epidemiologic investigation. *Am. J. Infect. Control* **39**, 901–903 (2011).
5. Graham, F. F., Finn, N., White, P., Hales, S. & Baker, M. G. Global Perspective of Legionella Infection in Community-Acquired Pneumonia: A Systematic Review and Meta-Analysis of Observational Studies. *Int. J. Environ. Res. Public Health* **19**, 1907 (2022).
6. Qin, T. *et al.* Distribution of Sequence-Based Types of Legionella pneumophila Serogroup 1 Strains Isolated from Cooling Towers, Hot Springs, and Potable Water Systems in China. *Appl. Environ. Microbiol.* **80**, 2150–2157 (2014).
7. Doebbeling, B. N. & Wenzel, R. P. The epidemiology of Legionella pneumophila infections. *Semin. Respir. Infect.* **2**, 206–221 (1987).
8. Leoni, E., Catalani, F., Marini, S. & Dallolio, L. Legionellosis Associated with Recreational Waters: A Systematic Review of Cases and Outbreaks in Swimming Pools, Spa Pools, and Similar Environments. *Int. J. Environ. Res. Public Health* **15**, 1612 (2018).
9. Hoffman, P. S. A common strategy for all hosts? *Can J Infect Dis* **8**, 139–146 (1997).
10. Rowbotham, T. J. Preliminary report on the pathogenicity of Legionella pneumophila for freshwater and soil amoebae. *J. Clin. Pathol.* **33**, 1179–1183 (1980).
11. Hoffmann, C., Harrison, C. F. & Hilbi, H. The natural alternative: protozoa as cellular models for Legionella infection: Protozoa models for Legionella infection. *Cell. Microbiol.* **16**, 15–26 (2014).
12. O'Connor, T. J., Adepoju, Y., Boyd, D. & Isberg, R. R. Minimization of the Legionella pneumophila genome reveals chromosomal regions involved in host range expansion. *Proc. Natl. Acad. Sci.* **108**, 14733–14740 (2011).
13. Boamah, D. K., Zhou, G., Ensminger, A. W. & O'Connor, T. J. From Many Hosts,

-
- One Accidental Pathogen: The Diverse Protozoan Hosts of Legionella. *Front. Cell. Infect. Microbiol.* **7**, 477 (2017).
14. Mercante, J. W. & Winchell, J. M. Current and Emerging Legionella Diagnostics for Laboratory and Outbreak Investigations. *Clin. Microbiol. Rev.* **28**, 95–133 (2015).
 15. Correia, A. M. *et al.* Probable Person-to-Person Transmission of Legionnaires' Disease. *N. Engl. J. Med.* **374**, 497–498 (2016).
 16. Ginevra, C. *et al.* Host-Related Risk Factors and Clinical Features of Community-Acquired Legionnaires Disease Due to the Paris and Lorraine Endemic Strains, 1998–2007, France. *Clin. Infect. Dis.* **49**, 184–191 (2009).
 17. Stout, J. E. & Yu, V. L. Legionellosis. *N. Engl. J. Med.* **337**, 682–687 (1997).
 18. Bollin, G. E., Plouffe, J. F., Para, M. F. & Hackman, B. Aerosols containing Legionella pneumophila generated by shower heads and hot-water faucets. *Appl. Environ. Microbiol.* **50**, 1128–1131 (1985).
 19. Neupane, A. S. *et al.* Patrolling Alveolar Macrophages Conceal Bacteria from the Immune System to Maintain Homeostasis. *Cell* **183**, 110–125 (2020).
 20. Horwitz, M. A. Formation of a novel phagosome by the Legionnaires' disease bacterium (*Legionella pneumophila*) in human monocytes. *J. Exp. Med.* **158**, 1319–1331 (1983).
 21. Isberg, R. R., O'Connor, T. & Heidtman, M. The Legionella pneumophila replication vacuole: making a cozy niche inside host cells. *Nat Rev Microbiol.* **7**, 13–24 (2009).
 22. Gruenberg, J. The endocytic pathway: a mosaic of domains. *Nat. Rev. Mol. Cell Biol.* **2**, 721–730 (2001).
 23. Clemens, D. L., Lee, B.-Y. & Horwitz, M. A. Deviant Expression of Rab5 on Phagosomes Containing the Intracellular Pathogens *Mycobacterium tuberculosis* and *Legionella pneumophila* Is Associated with Altered Phagosomal Fate. *Infect. Immun.* **68**, 2671–2684 (2000).
 24. Roy, C. R., Berger, K. H. & Isberg, R. R. Legionella pneumophila DotA protein is required for early phagosome trafficking decisions that occur within minutes of bacterial uptake. *Mol. Microbiol.* **28**, 663–674 (1998).
 25. Horwitz, M. A. & Maxfield, F. R. Legionella pneumophila inhibits acidification of its phagosome in human monocytes. *J. Cell Biol.* **99**, 1936–1943 (1984).
 26. Ninio, S. & Roy, C. R. Effector proteins translocated by Legionella pneumophila: strength in numbers. *Trends Microbiol.* **15**, 372–380 (2007).
 27. Tilney, L. G., Harb, O. S., Connelly, P. S., Robinson, C. G. & Roy, C. R. How the
-

-
- parasitic bacterium *Legionella pneumophila* modifies its phagosome and transforms it into rough ER: implications for conversion of plasma membrane to the ER membrane. *J. Cell Sci.* **114**, 4637–4650 (2001).
28. Naujoks, J. *et al.* IFNs Modify the Proteome of Legionella-Containing Vacuoles and Restrict Infection Via IRG1-Derived Itaconic Acid. *PLOS Pathog.* **12**, e1005408 (2016).
29. Escoll, P. *et al.* Legionella pneumophila Modulates Mitochondrial Dynamics to Trigger Metabolic Repurposing of Infected Macrophages. *Cell Host Microbe* **22**, 302–316.e7 (2017).
30. Finsel, I. & Hilbi, H. Formation of a pathogen vacuole according to *Legionella pneumophila*: how to kill one bird with many stones: Legionella pathogen vacuole formation. *Cell. Microbiol.* **17**, 935–950 (2015).
31. Sturgill-Koszycki, S. & Swanson, M. S. Legionella pneumophila replication vacuoles mature into acidic, endocytic organelles. *J. Exp. Med.* **192**, 1261–1272 (2000).
32. Horwitz, M. A. The Legionnaires' disease bacterium (*Legionella pneumophila*) inhibits phagosome-lysosome fusion in human monocytes. *J. Exp. Med.* **158**, 2108–2126 (1983).
33. Zhu, W. *et al.* Comprehensive Identification of Protein Substrates of the Dot/Icm Type IV Transporter of Legionella pneumophila. *PLoS ONE* **6**, e17638 (2011).
34. Voth, D. E., Broederdorf, L. J. & Graham, J. G. Bacterial Type IV secretion systems: versatile virulence machines. *Future Microbiol.* **7**, 241–257 (2012).
35. Roy, C. R. & Isberg, R. R. Topology of Legionella pneumophila DotA: an inner membrane protein required for replication in macrophages. *Infect. Immun.* **65**, 571–578 (1997).
36. Ge, J. & Shao, F. Manipulation of host vesicular trafficking and innate immune defence by Legionella Dot/Icm effectors. *Cell. Microbiol.* **13**, 1870–1880 (2011).
37. Newton, H. J., Ang, D. K. Y., Van Driel, I. R. & Hartland, E. L. Molecular Pathogenesis of Infections Caused by *Legionella pneumophila*. *Clin. Microbiol. Rev.* **23**, 274–298 (2010).
38. Bandyopadhyay, P., Liu, S., Gabbai, C. B., Venitelli, Z. & Steinman, H. M. Environmental Mimics and the Lvh Type IVA Secretion System Contribute to Virulence-Related Phenotypes of *Legionella pneumophila*. *Infect. Immun.* **75**, 723–735 (2007).
39. Söderberg, M. A., Dao, J., Starkenburg, S. R. & Cianciotto, N. P. Importance of Type
-

-
- II Secretion for Survival of *Legionella pneumophila* in Tap Water and in Amoebae at Low Temperatures. *Appl. Environ. Microbiol.* **74**, 5583–5588 (2008).
40. Chauhan, D. & Shames, S. R. Pathogenicity and Virulence of *Legionella* : Intracellular replication and host response. *Virulence* **12**, 1122–1144 (2021).
41. Kellermann, M., Scharte, F. & Hensel, M. Manipulation of Host Cell Organelles by Intracellular Pathogens. *Int. J. Mol. Sci.* **22**, 6484 (2021).
42. Galán, J. E. Common Themes in the Design and Function of Bacterial Effectors. *Cell Host Microbe* **5**, 571–579 (2009).
43. Belyi, Y., Levanova, N. & Schroeder, G. N. Glycosylating Effectors of *Legionella pneumophila*: Finding the Sweet Spots for Host Cell Subversion. *Biomolecules* **12**, 255 (2022).
44. Mondino, S. *et al.* Legionnaires' Disease: State of the Art Knowledge of Pathogenesis Mechanisms of *Legionella*. *Annu. Rev. Pathol. Mech. Dis.* **15**, 439–466 (2020).
45. Belyi, Y. Targeting Eukaryotic mRNA Translation by *Legionella pneumophila*. *Front. Mol. Biosci.* **7**, 80 (2020).
46. Belyi, Y. *et al.* *Legionella pneumophila* glucosyltransferase inhibits host elongation factor 1A. *Proc. Natl. Acad. Sci.* **103**, 16953–16958 (2006).
47. Moss, S. M. *et al.* A *Legionella pneumophila* Kinase Phosphorylates the Hsp70 Chaperone Family to Inhibit Eukaryotic Protein Synthesis. *Cell Host Microbe* **25**, 454–462.e6 (2019).
48. Ivanov, S. S. & Roy, C. R. Pathogen signatures activate a ubiquitination pathway that modulates the function of the metabolic checkpoint kinase mTOR. *Nat. Immunol.* **14**, 1219–1228 (2013).
49. Asrat, S., Dugan, A. S. & Isberg, R. R. The Frustrated Host Response to *Legionella pneumophila* Is Bypassed by MyD88-Dependent Translation of Pro-inflammatory Cytokines. *PLoS Pathog.* **10**, e1004229 (2014).
50. Copenhaver, A. M. *et al.* Alveolar Macrophages and Neutrophils Are the Primary Reservoirs for *Legionella pneumophila* and Mediate Cytosolic Surveillance of Type IV Secretion. *Infect. Immun.* **82**, 4325–4336 (2014).
51. Liu, X. & Shin, S. Viewing *Legionella pneumophila* Pathogenesis through an Immunological Lens. *J. Mol. Biol.* **431**, 4321–4344 (2019).
52. Hempstead, A. D. & Isberg, R. R. Inhibition of host cell translation elongation by *Legionella pneumophila* blocks the host cell unfolded protein response. *Proc. Natl. Acad. Sci. U. S. A.* **112**, E6790–6797 (2015).
-

-
53. Treacy-Abarca, S. & Mukherjee, S. Legionella suppresses the host unfolded protein response via multiple mechanisms. *Nat. Commun.* **6**, 7887 (2015).
 54. Walter, P. & Ron, D. The unfolded protein response: from stress pathway to homeostatic regulation. *Science* **334**, 1081–1086 (2011).
 55. Qiu, J. & Luo, Z.-Q. Hijacking of the Host Ubiquitin Network by Legionella pneumophila. *Front. Cell. Infect. Microbiol.* **7**, 487 (2017).
 56. Kitao, T., Nagai, H. & Kubori, T. Divergence of Legionella Effectors Reversing Conventional and Unconventional Ubiquitination. *Front. Cell. Infect. Microbiol.* **10**, 448 (2020).
 57. De Leon, J. A. *et al.* Positive and Negative Regulation of the Master Metabolic Regulator mTORC1 by Two Families of Legionella pneumophila Effectors. *Cell Rep.* **21**, 2031–2038 (2017).
 58. Qiu, J. *et al.* Ubiquitination independent of E1 and E2 enzymes by bacterial effectors. *Nature* **533**, 120–124 (2016).
 59. Kotewicz, K. M. *et al.* A Single Legionella Effector Catalyzes a Multistep Ubiquitination Pathway to Rearrange Tubular Endoplasmic Reticulum for Replication. *Cell Host Microbe* **21**, 169–181 (2017).
 60. Gan, N., Nakayasu, E. S., Hollenbeck, P. J. & Luo, Z.-Q. Legionella pneumophila inhibits immune signalling via MavC-mediated transglutaminase-induced ubiquitination of UBE2N. *Nat. Microbiol.* **4**, 134–143 (2018).
 61. Gan, N. *et al.* Legionella pneumophila regulates the activity of UBE 2N by deamidase-mediated deubiquitination. *EMBO J.* **39**, e102806 (2020).
 62. Tesh, M. J. & Miller, R. D. Amino acid requirements for Legionella pneumophila growth. *J. Clin. Microbiol.* **13**, 865–869 (1981).
 63. Price, C. T. D., Al-Khodor, S., Al-Quadani, T. & Abu Kwaik, Y. Indispensable Role for the Eukaryotic-Like Ankyrin Domains of the Ankyrin B Effector of Legionella pneumophila within Macrophages and Amoebae. *Infect. Immun.* **78**, 2079–2088 (2010).
 64. Lomma, M. *et al.* The Legionella pneumophila F-box protein Lpp2082 (AnkB) modulates ubiquitination of the host protein parvin B and promotes intracellular replication: L. pneumophila modulates ParvB. *Cell. Microbiol.* **12**, 1272–1291 (2010).
 65. Efeyan, A., Zoncu, R. & Sabatini, D. M. Amino acids and mTORC1: from lysosomes to disease. *Trends Mol. Med.* **18**, 524–533 (2012).
 66. Escoll, P. & Buchrieser, C. Metabolic reprogramming: an innate cellular defence
-

-
- mechanism against intracellular bacteria? *Curr. Opin. Immunol.* **60**, 117–123 (2019).
67. Fontana, M. F. *et al.* Secreted Bacterial Effectors That Inhibit Host Protein Synthesis Are Critical for Induction of the Innate Immune Response to Virulent *Legionella pneumophila*. *PLoS Pathog.* **7**, e1001289 (2011).
68. Shin, S. *et al.* Type IV Secretion-Dependent Activation of Host MAP Kinases Induces an Increased Proinflammatory Cytokine Response to *Legionella pneumophila*. *PLoS Pathog.* **4**, e1000220 (2008).
69. Fontana, M. F., Shin, S. & Vance, R. E. Activation of host mitogen-activated protein kinases by secreted *Legionella pneumophila* effectors that inhibit host protein translation. *Infect. Immun.* **80**, 3570–3575 (2012).
70. Barry, K. C., Fontana, M. F., Portman, J. L., Dugan, A. S. & Vance, R. E. IL-1 α signaling initiates the inflammatory response to virulent *Legionella pneumophila* in vivo. *J. Immunol. Baltim. Md 1950* **190**, 6329–6339 (2013).
71. Copenhaver, A. M., Casson, C. N., Nguyen, H. T., Duda, M. M. & Shin, S. IL-1R signaling enables bystander cells to overcome bacterial blockade of host protein synthesis. *Proc. Natl. Acad. Sci.* **112**, 7557–7562 (2015).
72. Lipo, E. *et al.* 5' Untranslated mRNA Regions Allow Bypass of Host Cell Translation Inhibition by *Legionella pneumophila*. *Infect. Immun.* e00179-22 (2022).
73. Delves, P. J. & Roitt, I. M. The Immune System. *N. Engl. J. Med.* **343**, 37–49 (2000).
74. Janeway, C. A. Approaching the Asymptote? Evolution and Revolution in Immunology. *Cold Spring Harb. Symp. Quant. Biol.* **54**, 1–13 (1989).
75. Avendaño Carvajal, L. & Perret Pérez, C. Epidemiology of Respiratory Infections. in *Pediatric Respiratory Diseases* (eds. Bertrand, P. & Sánchez, I.) 263–272 (Springer International Publishing, 2020).
76. Schlingmann, B., Molina, S. A. & Koval, M. Claudins: Gatekeepers of lung epithelial function. *Semin. Cell Dev. Biol.* **42**, 47–57 (2015).
77. Wittekindt, O. H. Tight junctions in pulmonary epithelia during lung inflammation. *Pflüg. Arch. - Eur. J. Physiol.* **469**, 135–147 (2017).
78. Higgins, G. *et al.* Lipoxin A₄ prevents tight junction disruption and delays the colonization of cystic fibrosis bronchial epithelial cells by *Pseudomonas aeruginosa*. *Am. J. Physiol.-Lung Cell. Mol. Physiol.* **310**, L1053–L1061 (2016).
79. Short, K. R. *et al.* Influenza virus damages the alveolar barrier by disrupting epithelial cell tight junctions. *Eur. Respir. J.* **47**, 954–966 (2016).
80. Galeas-Pena, M., McLaughlin, N. & Pociask, D. The role of the innate immune system
-

-
- on pulmonary infections. *Biol. Chem.* **400**, 443–456 (2019).
81. Opitz, B., Van Laak, V., Eitel, J. & Suttorp, N. Innate Immune Recognition in Infectious and Noninfectious Diseases of the Lung. *Am. J. Respir. Crit. Care Med.* **181**, 1294–1309 (2010).
 82. Desaki, Y. *et al.* Bacterial Lipopolysaccharides Induce Defense Responses Associated with Programmed Cell Death in Rice Cells. *Plant Cell Physiol.* **47**, 1530–1540 (2006).
 83. Wolf, A. J. & Underhill, D. M. Peptidoglycan recognition by the innate immune system. *Nat. Rev. Immunol.* **18**, 243–254 (2018).
 84. Korf, J., Stoltz, A., Verschoor, J., De Baetselier, P. & Grooten, J. The Mycobacterium tuberculosis cell wall component mycolic acid elicits pathogen-associated host innate immune responses. *Eur. J. Immunol.* **35**, 890–900 (2005).
 85. Zhong, M., Yan, H. & Li, Y. Flagellin: a unique microbe-associated molecular pattern and a multi-faceted immunomodulator. *Cell. Mol. Immunol.* **14**, 862–864 (2017).
 86. Hemmi, H. *et al.* A Toll-like receptor recognizes bacterial DNA. *Nature* **408**, 740–745 (2000).
 87. Alexopoulou, L., Holt, A. C., Medzhitov, R. & Flavell, R. A. Recognition of double-stranded RNA and activation of NF- κ B by Toll-like receptor 3. *Nature* **413**, 732–738 (2001).
 88. Pichlmair, A. *et al.* RIG-I-Mediated Antiviral Responses to Single-Stranded RNA Bearing 5'-Phosphates. *Science* **314**, 997–1001 (2006).
 89. Kumar, H., Kawai, T. & Akira, S. Pathogen Recognition by the Innate Immune System. *Int. Rev. Immunol.* **30**, 16–34 (2011).
 90. Zasloff, M. Antimicrobial peptides of multicellular organisms. *Nature* **415**, 389–395 (2002).
 91. O'Neill, L. A. J., Golenbock, D. & Bowie, A. G. The history of Toll-like receptors — redefining innate immunity. *Nat. Rev. Immunol.* **13**, 453–460 (2013).
 92. Medzhitov, R., Preston-Hurlburt, P. & Janeway, C. A. A human homologue of the Drosophila Toll protein signals activation of adaptive immunity. *Nature* **388**, 394–397 (1997).
 93. Kawai, T. & Akira, S. The role of pattern-recognition receptors in innate immunity: update on Toll-like receptors. *Nat. Immunol.* **11**, 373–384 (2010).
 94. Takeuchi, O. & Akira, S. Pattern Recognition Receptors and Inflammation. *Cell* **140**, 805–820 (2010).
 95. Kumar, H., Kawai, T. & Akira, S. Pathogen recognition in the innate immune
-

-
- response. *Biochem. J.* **420**, 1–16 (2009).
96. Kawasaki, T. & Kawai, T. Toll-Like Receptor Signaling Pathways. *Front. Immunol.* **5**, (2014).
 97. Franchi, L., Warner, N., Viani, K. & Nuñez, G. Function of Nod-like receptors in microbial recognition and host defense. *Immunol. Rev.* **227**, 106–128 (2009).
 98. Elinav, E., Strowig, T., Henao-Mejia, J. & Flavell, R. A. Regulation of the Antimicrobial Response by NLR Proteins. *Immunity* **34**, 665–679 (2011).
 99. Keestra-Gounder, A. M. & Tsolis, R. M. NOD1 and NOD2: Beyond Peptidoglycan Sensing. *Trends Immunol.* **38**, 758–767 (2017).
 100. Broz, P. & Dixit, V. M. Inflammasomes: mechanism of assembly, regulation and signalling. *Nat. Rev. Immunol.* **16**, 407–420 (2016).
 101. Schroder, K. & Tschopp, J. The Inflammasomes. *Cell* **140**, 821–832 (2010).
 102. Zhang, P. *et al.* NLRC4 inflammasome-dependent cell death occurs by a complementary series of three death pathways and determines lethality in mice. *Sci. Adv.* **7**, eabi9471 (2021).
 103. Luo, D. Toward a crystal-clear view of the viral RNA sensing and response by RIG-I-like receptors. *RNA Biol.* **11**, 25–32 (2014).
 104. Loo, Y.-M. & Gale, M. Immune Signaling by RIG-I-like Receptors. *Immunity* **34**, 680–692 (2011).
 105. Hornung, V. *et al.* 5'-Triphosphate RNA is the ligand for RIG-I. *Science* **314**, 994–997 (2006).
 106. Chiu, Y.-H., MacMillan, J. B. & Chen, Z. J. RNA Polymerase III Detects Cytosolic DNA and Induces Type I Interferons through the RIG-I Pathway. *Cell* **138**, 576–591 (2009).
 107. Rodriguez, K. R., Bruns, A. M. & Horvath, C. M. MDA5 and LGP2: accomplices and antagonists of antiviral signal transduction. *J. Virol.* **88**, 8194–8200 (2014).
 108. Bhat, N. & Fitzgerald, K. A. Recognition of cytosolic DNA by cGAS and other STING-dependent sensors. *Eur. J. Immunol.* **44**, 634–640 (2014).
 109. Holm, C. K., Paludan, S. R. & Fitzgerald, K. A. DNA recognition in immunity and disease. *Curr. Opin. Immunol.* **25**, 13–18 (2013).
 110. Abe, T. & Barber, G. N. Cytosolic-DNA-mediated, STING-dependent proinflammatory gene induction necessitates canonical NF- κ B activation through TBK1. *J. Virol.* **88**, 5328–5341 (2014).
 111. Sun, L., Wu, J., Du, F., Chen, X. & Chen, Z. J. Cyclic GMP-AMP synthase is a
-

-
- cytosolic DNA sensor that activates the type I interferon pathway. *Science* **339**, 786–791 (2013).
112. Decout, A., Katz, J. D., Venkatraman, S. & Ablasser, A. The cGAS–STING pathway as a therapeutic target in inflammatory diseases. *Nat. Rev. Immunol.* **21**, 548–569 (2021).
113. Wu, J. *et al.* Cyclic GMP-AMP is an endogenous second messenger in innate immune signaling by cytosolic DNA. *Science* **339**, 826–830 (2013).
114. Wang, B., Tian, Y. & Yin, Q. AIM2 Inflammasome Assembly and Signaling. *Adv. Exp. Med. Biol.* **1172**, 143–155 (2019).
115. Hornung, V. & Latz, E. Intracellular DNA recognition. *Nat. Rev. Immunol.* **10**, 123–130 (2010).
116. Sharma, S. & Fitzgerald, K. A. Innate Immune Sensing of DNA. *PLoS Pathog.* **7**, e1001310 (2011).
117. Brown, G. D., Willment, J. A. & Whitehead, L. C-type lectins in immunity and homeostasis. *Nat. Rev. Immunol.* **18**, 374–389 (2018).
118. Fischer, S., Stegmann, F., Gnanapragassam, V. S. & Lepenies, B. From structure to function – Ligand recognition by myeloid C-type lectin receptors. *Comput. Struct. Biotechnol. J.* **20**, 5790–5812 (2022).
119. Brown, G. D. & Gordon, S. A new receptor for β -glucans. *Nature* **413**, 36–37 (2001).
120. Brown, G. D. *et al.* Dectin-1 Is A Major β -Glucan Receptor On Macrophages. *J. Exp. Med.* **196**, 407–412 (2002).
121. Saijo, S. *et al.* Dectin-2 Recognition of α -Mannans and Induction of Th17 Cell Differentiation Is Essential for Host Defense against *Candida albicans*. *Immunity* **32**, 681–691 (2010).
122. Yamasaki, S. *et al.* C-type lectin Mincle is an activating receptor for pathogenic fungus, *Malassezia*. *Proc. Natl. Acad. Sci.* **106**, 1897–1902 (2009).
123. Behler-Janbeck, F. *et al.* C-type Lectin Mincle Recognizes Glucosyl-diacylglycerol of *Streptococcus pneumoniae* and Plays a Protective Role in Pneumococcal Pneumonia. *PLOS Pathog.* **12**, e1006038 (2016).
124. Ishikawa, E. *et al.* Direct recognition of the mycobacterial glycolipid, trehalose dimycolate, by C-type lectin Mincle. *J. Exp. Med.* **206**, 2879–2888 (2009).
125. Schoenen, H. *et al.* Cutting Edge: Mincle Is Essential for Recognition and Adjuvanticity of the Mycobacterial Cord Factor and its Synthetic Analog Trehalose-Dibehenate. *J. Immunol.* **184**, 2756–2760 (2010).
-

-
126. Ahrens, S. *et al.* F-Actin Is an Evolutionarily Conserved Damage-Associated Molecular Pattern Recognized by DNGR-1, a Receptor for Dead Cells. *Immunity* **36**, 635–645 (2012).
 127. Yamasaki, S. *et al.* Mincle is an ITAM-coupled activating receptor that senses damaged cells. *Nat. Immunol.* **9**, 1179–1188 (2008).
 128. Nagata, M. *et al.* Intracellular metabolite β -glucosylceramide is an endogenous Mincle ligand possessing immunostimulatory activity. *Proc. Natl. Acad. Sci.* **114**, (2017).
 129. Mayer, S., Raulf, M.-K. & Lepenies, B. C-type lectins: their network and roles in pathogen recognition and immunity. *Histochem. Cell Biol.* **147**, 223–237 (2017).
 130. Sancho, D. & Reis e Sousa, C. Signaling by Myeloid C-Type Lectin Receptors in Immunity and Homeostasis. *Annu. Rev. Immunol.* **30**, 491–529 (2012).
 131. Sato, K. *et al.* Dectin-2 is a pattern recognition receptor for fungi that couples with the Fc receptor gamma chain to induce innate immune responses. *J. Biol. Chem.* **281**, 38854–38866 (2006).
 132. Bakker, A. B. H., Baker, E., Sutherland, G. R., Phillips, J. H. & Lanier, L. L. Myeloid DAP12-associating lectin (MDL)-1 is a cell surface receptor involved in the activation of myeloid cells. *Proc. Natl. Acad. Sci.* **96**, 9792–9796 (1999).
 133. Mata-Martínez, P., Bergón-Gutiérrez, M. & Del Fresno, C. Dectin-1 Signaling Update: New Perspectives for Trained Immunity. *Front. Immunol.* **13**, 812148 (2022).
 134. Del Fresno, C., Iborra, S., Saz-Leal, P., Martínez-López, M. & Sancho, D. Flexible Signaling of Myeloid C-Type Lectin Receptors in Immunity and Inflammation. *Front. Immunol.* **9**, 804 (2018).
 135. Rogers, N. C. *et al.* Syk-Dependent Cytokine Induction by Dectin-1 Reveals a Novel Pattern Recognition Pathway for C Type Lectins. *Immunity* **22**, 507–517 (2005).
 136. Fuller, G. L. J. *et al.* The C-type Lectin Receptors CLEC-2 and Dectin-1, but Not DC-SIGN, Signal via a Novel YXXL-dependent Signaling Cascade. *J. Biol. Chem.* **282**, 12397–12409 (2007).
 137. Geijtenbeek, T. B. H. & Gringhuis, S. I. C-type lectin receptors in the control of T helper cell differentiation. *Nat. Rev. Immunol.* **16**, 433–448 (2016).
 138. Bates, E. E. M. *et al.* APCs Express DCIR, a Novel C-Type Lectin Surface Receptor Containing an Immunoreceptor Tyrosine-Based Inhibitory Motif. *J. Immunol.* **163**, 1973–1983 (1999).
 139. Ishiguro, T. *et al.* Absence of DCIR1 reduces the mortality rate of endotoxemic hepatitis in mice. *Eur. J. Immunol.* **47**, 704–712 (2017).
-

-
140. Raulf, M.-K. *et al.* The C-type Lectin Receptor CLEC12A Recognizes Plasmodial Hemozoin and Contributes to Cerebral Malaria Development. *Cell Rep.* **28**, 30–38.e5 (2019).
 141. Redelinghuys, P. & Brown, G. D. Inhibitory C-type lectin receptors in myeloid cells. *Immunol. Lett.* **136**, 1–12 (2011).
 142. Marshall, A. S. J. *et al.* Human MICL (CLEC12A) is differentially glycosylated and is down-regulated following cellular activation. *Eur. J. Immunol.* **36**, 2159–2169 (2006).
 143. Pyż, E. *et al.* Characterisation of murine MICL (CLEC12A) and evidence for an endogenous ligand. *Eur. J. Immunol.* **38**, 1157–1163 (2008).
 144. Redelinghuys, P. *et al.* MICL controls inflammation in rheumatoid arthritis. *Ann. Rheum. Dis.* **75**, 1386–1391 (2016).
 145. Sagar, D. *et al.* Antibody blockade of CLEC12A delays EAE onset and attenuates disease severity by impairing myeloid cell CNS infiltration and restoring positive immunity. *Sci. Rep.* **7**, 2707 (2017).
 146. Neumann, K. *et al.* Clec12a Is an Inhibitory Receptor for Uric Acid Crystals that Regulates Inflammation in Response to Cell Death. *Immunity* **40**, 389–399 (2014).
 147. Begun, J. *et al.* Integrated Genomics of Crohn’s Disease Risk Variant Identifies a Role for CLEC12A in Antibacterial Autophagy. *Cell Rep.* **11**, 1905–1918 (2015).
 148. Nishimura, N. *et al.* Mycobacterial mycolic acids trigger inhibitory receptor Clec12A to suppress host immune responses. *Tuberculosis* **138**, 102294 (2023).
 149. Joshi, N., Walter, J. M. & Misharin, A. V. Alveolar Macrophages. *Cell. Immunol.* **330**, 86–90 (2018).
 150. Hussell, T. & Bell, T. J. Alveolar macrophages: plasticity in a tissue-specific context. *Nat. Rev. Immunol.* **14**, 81–93 (2014).
 151. the Immunological Genome Consortium *et al.* Gene-expression profiles and transcriptional regulatory pathways that underlie the identity and diversity of mouse tissue macrophages. *Nat. Immunol.* **13**, 1118–1128 (2012).
 152. Misharin, A. V., Morales-Nebreda, L., Mutlu, G. M., Budinger, G. R. S. & Perlman, H. Flow Cytometric Analysis of Macrophages and Dendritic Cell Subsets in the Mouse Lung. *Am. J. Respir. Cell Mol. Biol.* **49**, 503–510 (2013).
 153. Rodriguez-Rodriguez, L., Gillet, L. & Machiels, B. Shaping of the alveolar landscape by respiratory infections and long-term consequences for lung immunity. *Front. Immunol.* **14**, 1149015 (2023).
-

-
154. Mitchell, A. J. *et al.* Technical Advance: Autofluorescence as a tool for myeloid cell analysis. *J. Leukoc. Biol.* **88**, 597–603 (2010).
 155. Maus, U., Rosseau, S., Seeger, W. & Lohmeyer, J. Separation of human alveolar macrophages by flow cytometry. *Am. J. Physiol.-Lung Cell. Mol. Physiol.* **272**, L566–L571 (1997).
 156. van Furth, R. & Cohn, Z. A. The origin and kinetics of mononuclear phagocytes. *J. Exp. Med.* **128**, 415–435 (1968).
 157. van Furth, R. Macrophage activity and clinical immunology. Origin and kinetics of mononuclear phagocytes. *Ann. N. Y. Acad. Sci.* **278**, 161–175 (1976).
 158. Guilliams, M. *et al.* Alveolar macrophages develop from fetal monocytes that differentiate into long-lived cells in the first week of life via GM-CSF. *J. Exp. Med.* **210**, 1977–1992 (2013).
 159. Schneider, C. *et al.* Induction of the nuclear receptor PPAR- γ by the cytokine GM-CSF is critical for the differentiation of fetal monocytes into alveolar macrophages. *Nat. Immunol.* **15**, 1026–1037 (2014).
 160. Tarling, J. D., Lin, H. S. & Hsu, S. Self-renewal of pulmonary alveolar macrophages: evidence from radiation chimera studies. *J. Leukoc. Biol.* **42**, 443–446 (1987).
 161. Hashimoto, D. *et al.* Tissue-resident macrophages self-maintain locally throughout adult life with minimal contribution from circulating monocytes. *Immunity* **38**, 792–804 (2013).
 162. Janssen, W. J. *et al.* Fas determines differential fates of resident and recruited macrophages during resolution of acute lung injury. *Am. J. Respir. Crit. Care Med.* **184**, 547–560 (2011).
 163. Guilliams, M. *et al.* Alveolar macrophages develop from fetal monocytes that differentiate into long-lived cells in the first week of life via GM-CSF. *J. Exp. Med.* **210**, 1977–1992 (2013).
 164. Nishinakamura, R. *et al.* Mice deficient for the IL-3/GM-CSF/IL-5 β c receptor exhibit lung pathology and impaired immune response, while β IL3 receptor-deficient mice are normal. *Immunity* **2**, 211–222 (1995).
 165. Robb, L. *et al.* Hematopoietic and lung abnormalities in mice with a null mutation of the common beta subunit of the receptors for granulocyte-macrophage colony-stimulating factor and interleukins 3 and 5. *Proc. Natl. Acad. Sci.* **92**, 9565–9569 (1995).
 166. Yu, X. *et al.* The Cytokine TGF- β Promotes the Development and Homeostasis of
-

-
- Alveolar Macrophages. *Immunity* **47**, 903-912.e4 (2017).
167. Nakamura, A. *et al.* Transcription repressor Bach2 is required for pulmonary surfactant homeostasis and alveolar macrophage function. *J. Exp. Med.* **210**, 2191–2204 (2013).
168. Cain, D. W. *et al.* Identification of a Tissue-Specific, C/EBP β -Dependent Pathway of Differentiation for Murine Peritoneal Macrophages. *J. Immunol.* **191**, 4665–4675 (2013).
169. Todd, E. M. *et al.* Alveolar macrophage development in mice requires L-plastin for cellular localization in alveoli. *Blood* **128**, 2785–2796 (2016).
170. Keating, E. *et al.* Effect of Cholesterol on the Biophysical and Physiological Properties of a Clinical Pulmonary Surfactant. *Biophys. J.* **93**, 1391–1401 (2007).
171. Griese, M. Pulmonary surfactant in health and human lung diseases: state of the art. *Eur Respir J* 1455–1476 (1999).
172. Postle, A. D., Heeley, E. L. & Wilton, D. C. A comparison of the molecular species compositions of mammalian lung surfactant phospholipids. *Comp. Biochem. Physiol. A. Mol. Integr. Physiol.* **129**, 65–73 (2001).
173. Schiller, J., Hammerschmidt, S., Wirtz, H., Arnhold, J. & Arnold, K. Lipid analysis of bronchoalveolar lavage fluid (BAL) by MALDI-TOF mass spectrometry and ³¹P NMR spectroscopy. *Chem. Phys. Lipids* **112**, 67–79 (2001).
174. Cockshutt, A. M., Weitz, J. & Possmayer, F. Pulmonary surfactant-associated protein A enhances the surface activity of lipid extract surfactant and reverses inhibition by blood proteins in vitro. *Biochemistry* **29**, 8424–8429 (1990).
175. Rodriguez-Capote, K., Nag, K., Schürch, S. & Possmayer, F. Surfactant protein interactions with neutral and acidic phospholipid films. *Am. J. Physiol. Lung Cell. Mol. Physiol.* **281**, L231-242 (2001).
176. Venkitaraman, A. R., Hall, S. B., Whitsett, J. A. & Notter, R. H. Enhancement of biophysical activity of lung surfactant extracts and phospholipid-apoprotein mixtures by surfactant protein A. *Chem. Phys. Lipids* **56**, 185–194 (1990).
177. Borie, R. *et al.* Pulmonary alveolar proteinosis. *Eur. Respir. Rev.* **20**, 98–107 (2011).
178. Ortega-Gómez, A., Perretti, M. & Soehnlein, O. Resolution of inflammation: an integrated view. *EMBO Mol. Med.* **5**, 661–674 (2013).
179. Grabiec, A. M. & Hussell, T. The role of airway macrophages in apoptotic cell clearance following acute and chronic lung inflammation. *Semin. Immunopathol.* **38**, 409–423 (2016).
180. Fadok, V. A. *et al.* Macrophages that have ingested apoptotic cells in vitro inhibit
-

-
- proinflammatory cytokine production through autocrine/paracrine mechanisms involving TGF-beta, PGE2, and PAF. *J. Clin. Invest.* **101**, 890–898 (1998).
181. Huynh, M.-L. N., Fadok, V. A. & Henson, P. M. Phosphatidylserine-dependent ingestion of apoptotic cells promotes TGF-beta1 secretion and the resolution of inflammation. *J. Clin. Invest.* **109**, 41–50 (2002).
182. Coleman, M. M. *et al.* Alveolar Macrophages Contribute to Respiratory Tolerance by Inducing FoxP3 Expression in Naive T Cells. *Am. J. Respir. Cell Mol. Biol.* **48**, 773–780 (2013).
183. Soroosh, P. *et al.* Lung-resident tissue macrophages generate Foxp3⁺ regulatory T cells and promote airway tolerance. *J. Exp. Med.* **210**, 775–788 (2013).
184. Iwasaki, A., Foxman, E. F. & Molony, R. D. Early local immune defences in the respiratory tract. *Nat. Rev. Immunol.* **17**, 7–20 (2017).
185. Westphalen, K. *et al.* Sessile alveolar macrophages communicate with alveolar epithelium to modulate immunity. *Nature* **506**, 503–506 (2014).
186. Mayer, A. K., Bartz, H., Fey, F., Schmidt, L. M. & Dalpke, A. H. Airway epithelial cells modify immune responses by inducing an anti-inflammatory microenvironment. *Eur. J. Immunol.* **38**, 1689–1699 (2008).
187. Martin, F. P., Jacqueline, C., Poschmann, J. & Roquilly, A. Alveolar Macrophages: Adaptation to Their Anatomic Niche during and after Inflammation. *Cells* **10**, 2720 (2021).
188. Murray, P. J. *et al.* Macrophage Activation and Polarization: Nomenclature and Experimental Guidelines. *Immunity* **41**, 14–20 (2014).
189. Orecchioni, M., Ghosheh, Y., Pramod, A. B. & Ley, K. Macrophage Polarization: Different Gene Signatures in M1(LPS⁺) vs. Classically and M2(LPS⁻) vs. Alternatively Activated Macrophages. *Front. Immunol.* **10**, 1084 (2019).
190. Dumigan, A. *et al.* *In vivo* single-cell transcriptomics reveal *Klebsiella pneumoniae* skews lung macrophages to promote infection. *EMBO Mol. Med.* **14**, e16888 (2022).
191. Okabe, Y. & Medzhitov, R. Tissue-Specific Signals Control Reversible Program of Localization and Functional Polarization of Macrophages. *Cell* **157**, 832–844 (2014).
192. Fernandez, S., Jose, P., Avdiushko, M. G., Kaplan, A. M. & Cohen, D. A. Inhibition of IL-10 receptor function in alveolar macrophages by Toll-like receptor agonists. *J. Immunol. Baltim. Md 1950* **172**, 2613–2620 (2004).
193. Bhatia, M., Zemans, R. L. & Jeyaseelan, S. Role of Chemokines in the Pathogenesis of Acute Lung Injury. *Am. J. Respir. Cell Mol. Biol.* **46**, 566–572 (2012).
-

-
194. Tino, M. J. & Wright, J. R. Surfactant protein A stimulates phagocytosis of specific pulmonary pathogens by alveolar macrophages. *Am. J. Physiol.* **270**, L677-688 (1996).
 195. Iles, K. E. & Forman, H. J. Macrophage Signaling and Respiratory Burst. *Immunol. Res.* **26**, 095–106 (2002).
 196. Nagre, N., Cong, X., Pearson, A. C. & Zhao, X. Alveolar Macrophage Phagocytosis and Bacteria Clearance in Mice. *J. Vis. Exp. JoVE* (2019).
 197. Marriott, H. M. *et al.* Interleukin-1 β regulates CXCL8 release and influences disease outcome in response to *Streptococcus pneumoniae*, defining intercellular cooperation between pulmonary epithelial cells and macrophages. *Infect. Immun.* **80**, 1140–1149 (2012).
 198. Nathan, C. F., Murray, H. W., Wiebe, M. E. & Rubin, B. Y. Identification of interferon-gamma as the lymphokine that activates human macrophage oxidative metabolism and antimicrobial activity. *J. Exp. Med.* **158**, 670–689 (1983).
 199. Su, X. *et al.* Interferon- γ regulates cellular metabolism and mRNA translation to potentiate macrophage activation. *Nat. Immunol.* **16**, 838–849 (2015).
 200. Furze, R. C. & Rankin, S. M. Neutrophil mobilization and clearance in the bone marrow. *Immunology* **125**, 281–288 (2008).
 201. Kolaczowska, E. & Kubes, P. Neutrophil recruitment and function in health and inflammation. *Nat. Rev. Immunol.* **13**, 159–175 (2013).
 202. Craig, A., Mai, J., Cai, S. & Jeyaseelan, S. Neutrophil Recruitment to the Lungs during Bacterial Pneumonia. *Infect. Immun.* **77**, 568–575 (2009).
 203. Tateda, K. *et al.* Early Recruitment of Neutrophils Determines Subsequent T1/T2 Host Responses in a Murine Model of *Legionella pneumophila* Pneumonia. *J. Immunol.* **166**, 3355–3361 (2001).
 204. Kaufmann, S. H. E. & Dorhoi, A. Molecular Determinants in Phagocyte-Bacteria Interactions. *Immunity* **44**, 476–491 (2016).
 205. Fuchs, T. A. *et al.* Novel cell death program leads to neutrophil extracellular traps. *J. Cell Biol.* **176**, 231–241 (2007).
 206. Pechous, R. D. With Friends Like These: The Complex Role of Neutrophils in the Progression of Severe Pneumonia. *Front. Cell. Infect. Microbiol.* **7**, 160 (2017).
 207. Scapini, P. *et al.* The neutrophil as a cellular source of chemokines. *Immunol. Rev.* **177**, 195–203 (2000).
 208. Wang, S. *et al.* S100A8/A9 in Inflammation. *Front. Immunol.* **9**, 1298 (2018).
 209. McCubbrey, A. L. & Curtis, J. L. Efferocytosis and Lung Disease. *Chest* **143**, 1750–
-

-
- 1757 (2013).
210. Worbs, T., Hammerschmidt, S. I. & Förster, R. Dendritic cell migration in health and disease. *Nat. Rev. Immunol.* **17**, 30–48 (2017).
211. Cook, P. C. & MacDonald, A. S. Dendritic cells in lung immunopathology. *Semin. Immunopathol.* **38**, 449–460 (2016).
212. Lambrecht, B. N., Prins, J. B. & Hoogsteden, H. C. Lung dendritic cells and host immunity to infection. *Eur. Respir. J.* **18**, 692–704 (2001).
213. Casson, C. N. *et al.* Neutrophils and Ly6Chi monocytes collaborate in generating an optimal cytokine response that protects against pulmonary *Legionella pneumophila* infection. *PLoS Pathog.* **13**, e1006309 (2017).
214. Brown, A. S. *et al.* Cooperation between Monocyte-Derived Cells and Lymphoid Cells in the Acute Response to a Bacterial Lung Pathogen. *PLOS Pathog.* **12**, e1005691 (2016).
215. Si, Y., Tsou, C.-L., Croft, K. & Charo, I. F. CCR2 mediates hematopoietic stem and progenitor cell trafficking to sites of inflammation in mice. *J. Clin. Invest.* **120**, 1192–1203 (2010).
216. Jia, T. *et al.* Additive roles for MCP-1 and MCP-3 in CCR2-mediated recruitment of inflammatory monocytes during *Listeria monocytogenes* infection. *J. Immunol. Baltim. Md 1950* **180**, 6846–6853 (2008).
217. Auffray, C., Sieweke, M. H. & Geissmann, F. Blood monocytes: development, heterogeneity, and relationship with dendritic cells. *Annu. Rev. Immunol.* **27**, 669–692 (2009).
218. Fogg, D. K. *et al.* A clonogenic bone marrow progenitor specific for macrophages and dendritic cells. *Science* **311**, 83–87 (2006).
219. Susa, M., Ticac, B., Rukavina, T., Doric, M. & Marre, R. *Legionella pneumophila* infection in intratracheally inoculated T cell-depleted or -nondepleted A/J mice. *J. Immunol. Baltim. Md 1950* **160**, 316–321 (1998).
220. Shim, H. K. *et al.* *Legionella* lipoprotein activates toll-like receptor 2 and induces cytokine production and expression of costimulatory molecules in peritoneal macrophages. *Exp. Mol. Med.* **41**, 687–694 (2009).
221. Hawn, T. R. *et al.* Altered inflammatory responses in TLR5-deficient mice infected with *Legionella pneumophila*. *J. Immunol. Baltim. Md 1950* **179**, 6981–6987 (2007).
222. Archer, K. A. & Roy, C. R. MyD88-dependent responses involving toll-like receptor 2 are important for protection and clearance of *Legionella pneumophila* in a mouse
-

-
- model of Legionnaires' disease. *Infect. Immun.* **74**, 3325–3333 (2006).
223. Fuse, E. T. *et al.* Role of Toll-like receptor 2 in recognition of *Legionella pneumophila* in a murine pneumonia model. *J. Med. Microbiol.* **56**, 305–312 (2007).
224. Hawn, T. R., Smith, K. D., Aderem, A. & Skerrett, S. J. Myeloid differentiation primary response gene (88)- and toll-like receptor 2-deficient mice are susceptible to infection with aerosolized *Legionella pneumophila*. *J. Infect. Dis.* **193**, 1693–1702 (2006).
225. Archer, K. A., Alexopoulou, L., Flavell, R. A. & Roy, C. R. Multiple MyD88-dependent responses contribute to pulmonary clearance of *Legionella pneumophila*. *Cell. Microbiol.* **11**, 21–36 (2009).
226. Hawn, T. R. *et al.* A common dominant TLR5 stop codon polymorphism abolishes flagellin signaling and is associated with susceptibility to legionnaires' disease. *J. Exp. Med.* **198**, 1563–1572 (2003).
227. Newton, C. A., Perkins, I., Widen, R. H., Friedman, H. & Klein, T. W. Role of Toll-like receptor 9 in *Legionella pneumophila*-induced interleukin-12 p40 production in bone marrow-derived dendritic cells and macrophages from permissive and nonpermissive mice. *Infect. Immun.* **75**, 146–151 (2007).
228. Frutoso, M. S. *et al.* The pattern recognition receptors Nod1 and Nod2 account for neutrophil recruitment to the lungs of mice infected with *Legionella pneumophila*. *Microbes Infect.* **12**, 819–827 (2010).
229. Molofsky, A. B. *et al.* Cytosolic recognition of flagellin by mouse macrophages restricts *Legionella pneumophila* infection. *J. Exp. Med.* **203**, 1093–1104 (2006).
230. Lightfield, K. L. *et al.* Differential requirements for NAIP5 in activation of the NLRC4 inflammasome. *Infect. Immun.* **79**, 1606–1614 (2011).
231. Amer, A. *et al.* Regulation of *Legionella* phagosome maturation and infection through flagellin and host Ipaf. *J. Biol. Chem.* **281**, 35217–35223 (2006).
232. Cazalet, C. *et al.* Analysis of the *Legionella longbeachae* Genome and Transcriptome Uncovers Unique Strategies to Cause Legionnaires' Disease. *PLoS Genet.* **6**, e1000851 (2010).
233. Pereira, M. S. F., Marques, G. G., DeLama, J. E. & Zamboni, D. S. The Nlrc4 Inflammasome Contributes to Restriction of Pulmonary Infection by Flagellated *Legionella* spp. that Trigger Pyroptosis. *Front. Microbiol.* **2**, (2011).
234. Case, C. L., Shin, S. & Roy, C. R. Asc and Ipaf Inflammasomes direct distinct pathways for caspase-1 activation in response to *Legionella pneumophila*. *Infect.*
-

-
- Immun.* **77**, 1981–1991 (2009).
235. Casson, C. N. *et al.* Caspase-11 Activation in Response to Bacterial Secretion Systems that Access the Host Cytosol. *PLoS Pathog.* **9**, e1003400 (2013).
236. Aachoui, Y. *et al.* Caspase-11 protects against bacteria that escape the vacuole. *Science* **339**, 975–978 (2013).
237. Akhter, A. *et al.* Caspase-11 promotes the fusion of phagosomes harboring pathogenic bacteria with lysosomes by modulating actin polymerization. *Immunity* **37**, 35–47 (2012).
238. Lippmann, J. *et al.* Dissection of a type I interferon pathway in controlling bacterial intracellular infection in mice: Role of type I IFNs in *L. pneumophila* infection. *Cell. Microbiol.* **13**, 1668–1682 (2011).
239. Lippmann, J. *et al.* IFN β responses induced by intracellular bacteria or cytosolic DNA in different human cells do not require ZBP1 (DLM-1/DAI). *Cell. Microbiol.* **10**, 2579–2588 (2008).
240. Opitz, B. *et al.* Legionella pneumophila Induces IFN β in Lung Epithelial Cells via IPS-1 and IRF3, Which Also Control Bacterial Replication. *J. Biol. Chem.* **281**, 36173–36179 (2006).
241. Ruiz-Moreno, J. S. *et al.* The common HAQ STING variant impairs cGAS-dependent antibacterial responses and is associated with susceptibility to Legionnaires' disease in humans. *PLOS Pathog.* **14**, e1006829 (2018).
242. Monroe, K. M., McWhirter, S. M. & Vance, R. E. Identification of Host Cytosolic Sensors and Bacterial Factors Regulating the Type I Interferon Response to Legionella pneumophila. *PLoS Pathog.* **5**, e1000665 (2009).
243. LeibundGut-Landmann, S., Weidner, K., Hilbi, H. & Oxenius, A. Nonhematopoietic cells are key players in innate control of bacterial airway infection. *J. Immunol. Baltim. Md 1950* **186**, 3130–3137 (2011).
244. Mascarenhas, D. P. A., Pereira, M. S. F., Manin, G. Z., Hori, J. I. & Zamboni, D. S. Interleukin 1 receptor-driven neutrophil recruitment accounts to MyD88-dependent pulmonary clearance of legionella pneumophila infection in vivo. *J. Infect. Dis.* **211**, 322–330 (2015).
245. Spörri, R., Joller, N., Hilbi, H. & Oxenius, A. A Novel Role for Neutrophils As Critical Activators of NK Cells. *J. Immunol.* **181**, 7121–7130 (2008).
246. Brieland, J. K. *et al.* Immunomodulatory role of endogenous interleukin-18 in gamma interferon-mediated resolution of replicative Legionella pneumophila lung infection.
-

-
- Infect. Immun.* **68**, 6567–6573 (2000).
247. Shinozawa, Y. *et al.* Role of interferon-gamma in inflammatory responses in murine respiratory infection with *Legionella pneumophila*. *J. Med. Microbiol.* **51**, 225–230 (2002).
248. González-Navajas, J. M., Lee, J., David, M. & Raz, E. Immunomodulatory functions of type I interferons. *Nat. Rev. Immunol.* **12**, 125–135 (2012).
249. Kessler, D. S., Levy, D. E. & Darnell, J. E. Two interferon-induced nuclear factors bind a single promoter element in interferon-stimulated genes. *Proc. Natl. Acad. Sci. U. S. A.* **85**, 8521–8525 (1988).
250. Pestka, S. *et al.* The interferon gamma (IFN-gamma) receptor: a paradigm for the multichain cytokine receptor. *Cytokine Growth Factor Rev.* **8**, 189–206 (1997).
251. Bach, E. A., Aguet, M. & Schreiber, R. D. The IFN gamma receptor: a paradigm for cytokine receptor signaling. *Annu. Rev. Immunol.* **15**, 563–591 (1997).
252. Takaoka, A. & Yanai, H. Interferon signalling network in innate defence. *Cell. Microbiol.* **8**, 907–922 (2006).
253. MacMicking, J. D. Interferon-inducible effector mechanisms in cell-autonomous immunity. *Nat. Rev. Immunol.* **12**, 367–382 (2012).
254. Naujoks, J., Lippmann, J., Suttorp, N. & Opitz, B. Innate sensing and cell-autonomous resistance pathways in *Legionella pneumophila* infection. *Int. J. Med. Microbiol.* **308**, 161–167 (2018).
255. Ziltener, P., Reinheckel, T. & Oxenius, A. Neutrophil and Alveolar Macrophage-Mediated Innate Immune Control of *Legionella pneumophila* Lung Infection via TNF and ROS. *PLOS Pathog.* **12**, e1005591 (2016).
256. Lanternier, F. *et al.* Incidence and Risk Factors of *Legionella pneumophila* Pneumonia During Anti-Tumor Necrosis Factor Therapy. *Chest* **144**, 990–998 (2013).
257. Fabroni, C., Gori, A., Prignano, F. & Lotti, T. A severe complication of anti-TNF alfa treatment. *G. Ital. Dermatol. E Venereol.* **145**, 775–777 (2010).
258. Fujita, M. *et al.* TNF receptor 1 and 2 contribute in different ways to resistance to *Legionella pneumophila*-induced mortality in mice. *Cytokine* **44**, 298–303 (2008).
259. Coers, J., Vance, R. E., Fontana, M. F. & Dietrich, W. F. Restriction of *Legionella pneumophila* growth in macrophages requires the concerted action of cytokine and Naip5/Ipaf signalling pathways. *Cell. Microbiol.* **9**, 2344–2357 (2007).
260. Kawamoto, Y. *et al.* TNF- α inhibits the growth of *Legionella pneumophila* in airway epithelial cells by inducing apoptosis. *J. Infect. Chemother.* **23**, 51–55 (2017).
-

-
261. Klatt, A.-B. *et al.* CLEC12A Binds to *Legionella pneumophila* but Has No Impact on the Host's Antibacterial Response. *Int. J. Mol. Sci.* **24**, 3891 (2023).
262. Aktories, P. *et al.* An improved organotypic cell culture system to study tissue-resident macrophages *ex vivo*. *Cell Rep. Methods* **2**, 100260 (2022).
263. Fortier, A., Faucher, S. P., Diallo, K. & Gros, P. Global cellular changes induced by *Legionella pneumophila* infection of bone marrow-derived macrophages. *Immunobiology* **216**, 1274–1285 (2011).
264. Yan, L. & Cirillo, J. D. Infection of murine macrophage cell lines by *Legionella pneumophila*. *FEMS Microbiol. Lett.* **230**, 147–152 (2004).
265. Lavin, Y. *et al.* Tissue-Resident Macrophage Enhancer Landscapes Are Shaped by the Local Microenvironment. *Cell* **159**, 1312–1326 (2014).
266. Bain, C. C. & MacDonald, A. S. The impact of the lung environment on macrophage development, activation and function: diversity in the face of adversity. *Mucosal Immunol.* **15**, 223–234 (2022).
267. Gorki, A.-D. *et al.* Murine *Ex Vivo* Cultured Alveolar Macrophages Provide a Novel Tool to Study Tissue-Resident Macrophage Behavior and Function. *Am. J. Respir. Cell Mol. Biol.* **66**, 64–75 (2022).
268. Subramanian, S. *et al.* Long-term culture-expanded alveolar macrophages restore their full epigenetic identity after transfer *in vivo*. *Nat. Immunol.* **23**, 458–468 (2022).
269. Sadosky, A. B., Wiater, L. A. & Shuman, H. A. Identification of *Legionella pneumophila* genes required for growth within and killing of human macrophages. *Infect. Immun.* **61**, 5361–5373 (1993).
270. Mampel, J. *et al.* Planktonic Replication Is Essential for Biofilm Formation by *Legionella pneumophila* in a Complex Medium under Static and Dynamic Flow Conditions. *Appl. Environ. Microbiol.* **72**, 2885–2895 (2006).
271. Berg, J. *et al.* Tyk2 as a target for immune regulation in human viral/bacterial pneumonia. *Eur. Respir. J.* **50**, 1601953 (2017).
272. Zamboni, D. S. *et al.* The Bir1e cytosolic pattern-recognition receptor contributes to the detection and control of *Legionella pneumophila* infection. *Nat. Immunol.* **7**, 318–325 (2006).
273. Rapino, F. *et al.* C/EBP α Induces Highly Efficient Macrophage Transdifferentiation of B Lymphoma and Leukemia Cell Lines and Impairs Their Tumorigenicity. *Cell Rep.* **3**, 1153–1163 (2013).
274. Gaidt, M. M., Rapino, F., Graf, T. & Hornung, V. Modeling Primary Human
-

-
- Monocytes with the Trans-Differentiation Cell Line BLaER1. in *Innate Immune Activation* (eds. De Nardo, D. & De Nardo, C. M.) vol. 1714 57–66 (Springer New York, 2018).
275. Gaidt, M. M. *et al.* Human Monocytes Engage an Alternative Inflammasome Pathway. *Immunity* **44**, 833–846 (2016).
276. Liberzon, A. *et al.* Molecular signatures database (MSigDB) 3.0. *Bioinformatics* **27**, 1739–1740 (2011).
277. Liberzon, A. *et al.* The Molecular Signatures Database Hallmark Gene Set Collection. *Cell Syst.* **1**, 417–425 (2015).
278. Jassal, B. *et al.* The reactome pathway knowledgebase. *Nucleic Acids Res.* **8**, D498–D503 (2020).
279. Weiner 3Rd, J. & Domaszewska, T. tmod: an R package for general and multivariate enrichment analysis. *PeerJ Preprints* 4:e2420v1 (2016).
280. Chaussabel, D. *et al.* A Modular Analysis Framework for Blood Genomics Studies: Application to Systemic Lupus Erythematosus. *Immunity* **29**, 150–164 (2008).
281. Li, S. *et al.* Molecular signatures of antibody responses derived from a systems biology study of five human vaccines. *Nat. Immunol.* **15**, 195–204 (2014).
282. Kim, J. *et al.* I κ B ζ controls NLRP3 inflammasome activation via upregulation of the Nlrp3 gene. *Cytokine* **127**, 154983 (2020).
283. Staal, J., Bekaert, T. & Beyaert, R. Regulation of NF- κ B signaling by caspases and MALT1 paracaspase. *Cell Res.* **21**, 40–54 (2011).
284. Phin, N. *et al.* Epidemiology and clinical management of Legionnaires' disease. *Lancet Infect. Dis.* **14**, 1011–1021 (2014).
285. Sabria, M. & Yu, V. L. Hospital-acquired legionellosis: solutions for a preventable infection. *Lancet Infect. Dis.* **2**, 368–373 (2002).
286. Endeman, H. *et al.* Mannose-Binding Lectin Genotypes in Susceptibility to Community-Acquired Pneumonia. *Chest* **134**, 1135–1140 (2008).
287. Van Kempen, G. *et al.* Mannose-binding lectin and L-ficolin polymorphisms in patients with community-acquired pneumonia caused by intracellular pathogens. *Immunology* **151**, 81–88 (2017).
288. Grigoryeva, L. S. & Cianciotto, N. P. Human macrophages utilize a wide range of pathogen recognition receptors to recognize *Legionella pneumophila*, including Toll-Like Receptor 4 engaging *Legionella* lipopolysaccharide and the Toll-like Receptor 3 nucleic-acid sensor. *PLOS Pathog.* **17**, e1009781 (2021).
-

-
289. Newton, C. *et al.* Induction of interleukin-4 (IL-4) by legionella pneumophila infection in BALB/c mice and regulation of tumor necrosis factor alpha, IL-6, and IL-1beta. *Infect. Immun.* **68**, 5234–5240 (2000).
290. Rabes, A. *et al.* The C-Type Lectin Receptor Mincle Binds to Streptococcus pneumoniae but Plays a Limited Role in the Anti-Pneumococcal Innate Immune Response. *PLOS ONE* **10**, e0117022 (2015).
291. Rothfuchs, A. G. *et al.* Dectin-1 Interaction with *Mycobacterium tuberculosis* Leads to Enhanced IL-12p40 Production by Splenic Dendritic Cells. *J. Immunol.* **179**, 3463–3471 (2007).
292. Court, N. *et al.* Partial Redundancy of the Pattern Recognition Receptors, Scavenger Receptors, and C-Type Lectins for the Long-Term Control of *Mycobacterium tuberculosis* Infection. *J. Immunol.* **184**, 7057–7070 (2010).
293. Marakalala, M. J., Graham, L. M. & Brown, G. D. The Role of Syk/CARD9-Coupled C-Type Lectin Receptors in Immunity to *Mycobacterium tuberculosis* Infections. *Clin. Dev. Immunol.* **2010**, 1–9 (2010).
294. Omotade, T. O. & Roy, C. R. Legionella pneumophila Excludes Autophagy Adaptors from the Ubiquitin-Labeled Vacuole in Which It Resides. *Infect. Immun.* **88**, e00793-19 (2020).
295. Choy, A. *et al.* The Legionella Effector RavZ Inhibits Host Autophagy Through Irreversible Atg8 Deconjugation. *Science* **338**, 1072–1076 (2012).
296. Marion, J. Pattern Recognition Receptors: Evolution, Redundancy, and Cross Talk. in *Molecular Life Sciences* (eds. Wells, R. D., Bond, J. S., Klinman, J., Masters, B. S. S. & Bell, E.) 1–7 (Springer New York, 2014).
297. Kawai, T. & Akira, S. Toll-like Receptors and Their Crosstalk with Other Innate Receptors in Infection and Immunity. *Immunity* **34**, 637–650 (2011).
298. Ginhoux, F. & Guilliams, M. Tissue-Resident Macrophage Ontogeny and Homeostasis. *Immunity* **44**, 439–449 (2016).
299. Rothchild, A. C. *et al.* Alveolar macrophages generate a noncanonical NRF2-driven transcriptional response to *Mycobacterium tuberculosis* in vivo. *Sci. Immunol.* **4**, eaaw6693 (2019).
300. Barry, K. C., Ingolia, N. T. & Vance, R. E. Global analysis of gene expression reveals mRNA superinduction is required for the inducible immune response to a bacterial pathogen. *eLife* **6**, e22707 (2017).
301. Losick, V. P. & Isberg, R. R. NF- κ B translocation prevents host cell death after low-
-

-
- dose challenge by *Legionella pneumophila*. *J. Exp. Med.* **203**, 2177–2189 (2006).
302. Bartfeld, S. *et al.* Temporal resolution of two-tracked NF- κ B activation by *Legionella pneumophila*. *Cell. Microbiol.* **11**, 1638–1651 (2009).
303. Masumoto, J. *et al.* Nod1 acts as an intracellular receptor to stimulate chemokine production and neutrophil recruitment in vivo. *J. Exp. Med.* **203**, 203–213 (2006).
304. Sandor, F. *et al.* Importance of extra- and intracellular domains of TLR1 and TLR2 in NF κ B signaling. *J. Cell Biol.* **162**, 1099–1110 (2003).
305. Skerrett, S. J. & Martin, T. R. Roles for tumor necrosis factor alpha and nitric oxide in resistance of rat alveolar macrophages to *Legionella pneumophila*. *Infect. Immun.* **64**, 3236–3243 (1996).
306. Price, C. T. D. & Abu Kwaik, Y. The Transcriptome of *Legionella pneumophila*-Infected Human Monocyte-Derived Macrophages. *PLoS ONE* **9**, e114914 (2014).
307. Kitamura, H., Kanehira, K., Okita, K., Morimatsu, M. & Saito, M. MAIL, a novel nuclear I kappa B protein that potentiates LPS-induced IL-6 production. *FEBS Lett.* **485**, 53–56 (2000).
308. Yamazaki, S., Muta, T. & Takeshige, K. A novel IkappaB protein, IkappaB-zeta, induced by proinflammatory stimuli, negatively regulates nuclear factor-kappaB in the nuclei. *J. Biol. Chem.* **276**, 27657–27662 (2001).
309. Motoyama, M., Yamazaki, S., Eto-Kimura, A., Takeshige, K. & Muta, T. Positive and negative regulation of nuclear factor-kappaB-mediated transcription by IkappaB-zeta, an inducible nuclear protein. *J. Biol. Chem.* **280**, 7444–7451 (2005).
310. Sundaram, K. *et al.* IkB ζ Regulates Human Monocyte Pro-Inflammatory Responses Induced by *Streptococcus pneumoniae*. *PLOS ONE* **11**, e0161931 (2016).
311. Winn, W. C. & Myerowitz, R. L. The pathology of the legionella pneumonias. *Hum. Pathol.* **12**, 401–422 (1981).
312. Yu, H. *et al.* Lung Abscess Caused by *Legionella* Species: Implication of the Immune Status of Hosts. *Intern. Med.* **48**, 1997–2002 (2009).
313. Kanangat, S. *et al.* Effects of Cytokines and Endotoxin on the Intracellular Growth of Bacteria. *Infect. Immun.* **67**, 2834–2840 (1999).
314. Woo, Y. D., Jeong, D. & Chung, D. H. Development and Functions of Alveolar Macrophages. *Mol. Cells* **44**, 292–300 (2021).
315. Ku, H.-C. & Cheng, C.-F. Master Regulator Activating Transcription Factor 3 (ATF3) in Metabolic Homeostasis and Cancer. *Front. Endocrinol.* **11**, 556 (2020).
316. Gilchrist, M. *et al.* Systems biology approaches identify ATF3 as a negative regulator
-

-
- of Toll-like receptor 4. *Nature* **441**, 173–178 (2006).
317. Whitmore, M. M. *et al.* Negative Regulation of TLR-Signaling Pathways by Activating Transcription Factor-3. *J. Immunol.* **179**, 3622–3630 (2007).
318. Nguyen, C. T., Kim, E.-H., Luong, T. T., Pyo, S. & Rhee, D.-K. ATF3 Confers Resistance to Pneumococcal Infection Through Positive Regulation of Cytokine Production. *J. Infect. Dis.* **210**, 1745–1754 (2014).
319. Nguyen, Cuong Thach, Kim, Eun-Hye, Luong, Truc Thanh, Pyo, Suhkneung, & Rhee, Dong-Kwon. TLR4 Mediates Pneumolysin-Induced ATF3 Expression through the JNK/p38 Pathway in Streptococcus pneumoniae-Infected RAW 264.7 Cells. *Mol. Cells* **38**, 58–64 (2015).
320. Subramanian, A. *et al.* A Legionella toxin exhibits tRNA mimicry and glycosyl transferase activity to target the translation machinery and trigger a ribotoxic stress response. *Nat. Cell Biol.* **25**, 1600–1615 (2023).
321. Baek, S. J. & Eling, T. Growth differentiation factor 15 (GDF15): A survival protein with therapeutic potential in metabolic diseases. *Pharmacol. Ther.* **198**, 46–58 (2019).
322. Luan, H. H. *et al.* GDF15 Is an Inflammation-Induced Central Mediator of Tissue Tolerance. *Cell* **178**, 1231-1244.e11 (2019).
323. Mullican, S. E. *et al.* GFRAL is the receptor for GDF15 and the ligand promotes weight loss in mice and nonhuman primates. *Nat. Med.* **23**, 1150–1157 (2017).
324. Hsu, J.-Y. *et al.* Non-homeostatic body weight regulation through a brainstem-restricted receptor for GDF15. *Nature* **550**, 255–259 (2017).
325. Johann, K., Kleinert, M. & Klaus, S. The Role of GDF15 as a Myomitokine. *Cells* **10**, 2990 (2021).
326. Shembade, N. & Harhaj, E. W. Regulation of NF- κ B signaling by the A20 deubiquitinase. *Cell. Mol. Immunol.* **9**, 123–130 (2012).
327. Lee, E. G. *et al.* Failure to Regulate TNF-Induced NF- κ B and Cell Death Responses in A20-Deficient Mice. *Science* **289**, 2350–2354 (2000).
328. Lademann, U., Kallunki, T. & Jäättelä, M. A20 zinc finger protein inhibits TNF-induced apoptosis and stress response early in the signaling cascades and independently of binding to TRAF2 or 14-3-3 proteins. *Cell Death Differ.* **8**, 265–272 (2001).
329. Tateda, K. *et al.* Chemokine-dependent neutrophil recruitment in a murine model of Legionella pneumonia: potential role of neutrophils as immunoregulatory cells. *Infect. Immun.* **69**, 2017–2024 (2001).
-

-
330. Russell, D. G., Huang, L. & VanderVen, B. C. Immunometabolism at the interface between macrophages and pathogens. *Nat. Rev. Immunol.* **19**, 291–304 (2019).
331. Munder, M., Eichmann, K. & Modolell, M. Alternative Metabolic States in Murine Macrophages Reflected by the Nitric Oxide Synthase/Arginase Balance: Competitive Regulation by CD4⁺ T Cells Correlates with Th1/Th2 Phenotype. *J. Immunol.* **160**, 5347–5354 (1998).
332. Eisenreich, W., Heesemann, J., Rudel, T. & Goebel, W. Metabolic host responses to infection by intracellular bacterial pathogens. *Front. Cell. Infect. Microbiol.* **3**, (2013).
333. Woods, P. S. *et al.* Tissue-Resident Alveolar Macrophages Do Not Rely on Glycolysis for LPS-induced Inflammation. *Am. J. Respir. Cell Mol. Biol.* **62**, 243–255 (2020).
334. Argüello, R. J. *et al.* SCENITH: A Flow Cytometry-Based Method to Functionally Profile Energy Metabolism with Single-Cell Resolution. *Cell Metab.* **32**, 1063-1075.e7 (2020).
335. Lee, M.-S. & Bensinger, S. J. Reprogramming cholesterol metabolism in macrophages and its role in host defense against cholesterol-dependent cytolysins. *Cell. Mol. Immunol.* **19**, 327–336 (2022).
336. Maxfield, F. R. & Van Meer, G. Cholesterol, the central lipid of mammalian cells. *Curr. Opin. Cell Biol.* **22**, 422–429 (2010).
337. Luo, J., Yang, H. & Song, B.-L. Mechanisms and regulation of cholesterol homeostasis. *Nat. Rev. Mol. Cell Biol.* **21**, 225–245 (2020).
338. Lu, H. *et al.* Rapid proteasomal elimination of 3-hydroxy-3-methylglutaryl-CoA reductase by interferon- γ in primary macrophages requires endogenous 25-hydroxycholesterol synthesis. *Steroids* **99**, 219–229 (2015).
339. Li, J., Lee, P. L. & Pfeffer, S. R. Quantitative Measurement of Cholesterol in Cell Populations Using Flow Cytometry and Fluorescent Perfringolysin O*. in *Cholesterol Homeostasis* (eds. Gelissen, I. C. & Brown, A. J.) vol. 1583 85–95 (Springer New York, 2017).
340. Ondari, E., Wilkins, A., Latimer, B., Dragoi, A.-M. & Ivanov, S. S. Cellular cholesterol licenses *Legionella pneumophila* intracellular replication in macrophages. *Microb. Cell* **10**, 1–17 (2023).
341. Ivanov, S. The tug-of-war over MTOR in *Legionella* infections. *Microb. Cell* **4**, 67–68 (2017).
342. Abshire, C. F., Dragoi, A.-M., Roy, C. R. & Ivanov, S. S. MTOR-Driven Metabolic Reprogramming Regulates *Legionella pneumophila* Intracellular Niche Homeostasis.
-

PLOS Pathog. **12**, e1006088 (2016).

Appendix

Publications

Ann-Brit Klatt, Christina Diersing, Juliane Lippmann, Sabine Mayer-Lambertz, Felix Stegmann, Swantje Fischer, Sandra Caesar, et al. ‘CLEC12A Binds to Legionella Pneumophila but Has No Impact on the Host’s Antibacterial Response’. *International Journal of Molecular Sciences* 24, no. 4 (15 February 2023): 3891. <https://doi.org/10.3390/ijms24043891>.

Wee, Bryan A., Joana Alves, Diane S. J. Lindsay, **Ann-Brit Klatt**, Fiona A. Sargison, Ross L. Cameron, Amy Pickering, et al. ‘Population Analysis of Legionella Pneumophila Reveals a Basis for Resistance to Complement-Mediated Killing’. *Nature Communications* 12, no. 1 (9 December 2021): 7165. <https://doi.org/10.1038/s41467-021-27478-z>.